Studies towards the Intrinsic Function of the AVR4 and AVR9 Elicitors of the Fungal Tomato Pathogen *Cladosporium fulvum*

Disulfide bond patterns–Structural markers for protein function

Harrold van den Burg

Promotor:	Prof. dr. ir. P.J.G.M. de Wit Hoogleraar in de Fytopathology Wageningen Universiteit
Co-promotor:	Dr. ir. J. Vervoort Universitair hoofddocent bij het Laboratorium voor Biochemie Wageningen Universiteit
Promotiecommissie:	Prof. dr. B. P. A. Cammue, Katholieke Universiteit Leuven Prof. dr. B. J. C. Cornelissen, Universiteit van Amsterdam Prof. dr. S. C. de Vries, Wageningen Universiteit Dr. G.W. Vuister, Katholieke Universiteit Nijmegen

Harrold Alfred van den Burg

Studies towards the Intrinsic Function of the AVR4 and AVR9 Elicitors of the Fungal Tomato Pathogen *Cladosporium fulvum*

Disulfide bond patterns–Structural markers for protein function

Proefschrift

Ter verkrijging van de graad van doctor
op gezag van de rector magnificus
van Wageningen Universiteit
Prof. dr. ir. L. Speelman
in het openbaar te verdedigen
op maandag 16 juni 2003
des namiddags te vier uur in de Aula

Studies towards the intrinsic function of the AVR4 and AVR9 elicitors of the fungal tomato pathogen *Cladosporium fulvum*: disulfide bonds – structural markers for protein function

Van den Burg, H.A.

PhD Thesis Wageningen University, The Netherlands

With references – With summary in Dutch

ISBN 90-5808-865-0

Science

…I've got a pen in my pocket
does that make me a writer
Standing on the mountain
doesn't make me no higher
Putting on gloves
don't make you a fighter

And all the study in the world doesn't make it science…

Paul Weller, 1997

CONTENTS

	List of Abbreviations	8
Chapter 1	General introduction and outline	11
Chapter 2	Efficient $^{13}C/^{15}N$ double labeling of the avirulence protein AVR4 in a methanol-utilizing strain (Mut^{+}) of *Pichia pastoris*	33
Chapter 3	Disulfide bond structure of the AVR9 elicitor of the fungal tomato pathogen *Cladosporium fulvum*; evidence for a cystine knot	53
Chapter 4	Natural disulfide bond disrupted mutants of AVR4 of the tomato pathogen *Cladosporium fulvum* are sensitive to proteolysis, thereby, circumventing *Cf-4* mediated resistance	75
Chapter 5	Avirulence factor AVR4 of the tomato pathogen *Cladosporium fulvum* is a chitin-binding lectin that protects fungi against plant chitinases	95
Chapter 6	The interaction between the chitin-binding domain of the AVR4 elicitor of *Cladosporium fulvum* and chitin requires three occupied binding subsites	119
Chapter 7	General discussion	147
	Summary	157
	Samenvatting	161
	Dankwoord	163
	List of publications	165
	Curriculum vitae	167

LIST OF ABBREVIATIONS

4VP	4-vinylpyridine
AF	apoplastic fluid
AOX1	methanol-inducible alcohol oxidase 1
Avr	avirulence
AVR4	avirulence protein 4 of the fungus *Cladosporium fulvum*
AVR9^{3SS}/AVR9^{2SS}/../../AVR9^{1SS}/AVR9^{reduced}	AVR9 species with 3/2/1/0 disulfide bridges intact
Cx—Cy	disulfide bond pair
CBM	carbohydrate-binding module
CDAP	1-cyano-4-diethylamino-pyridinium
CDW	cell dry weight
Cf	resistance trait in tomato for *Cladosporium fulvum*
ChBD	chitin-binding domain
CPI	carboxypeptidase inhibitor
CSI	chemical shift index
des-[Cx—Cy]	species lacking a specific disulfide bond (the involved half-cystines are reduced and the sulfhydryl group is cyanylated)
DP	degree-of-polymerization
DO	dissolved oxygen
ECP	extracellular gene product
ELISA	enzyme-linked immunosorbent assay
ESI	electrospray ionization
ΔH^o_{cal}	calorimetric enthalpy
ΔH^o_{vH}	van ‘t Hoff enthalpy
HPLC	high-performance liquid chromatography
HR	hypersensitive response
HSQC	heteronuclear single quantum coherence spectroscopy
GlcNAc	*N*-acetyl-D-glucosamine
IAM	iodoacetamide
inv	invertebrate
ITC	isothermal titration calorimetry

Abbreviations (*continued*)

MALDI-TOF	matrix-assisted laser desorption/ionization time-of-flight
MM-Cf9	tomato genotype Moneymaker carrying the resistance gene *Cf-9*
MS	mass spectrometry
NEM	*N*-ethylmaleimide
Mut^+/ Mut^S	methanol-utilizing strain / methanol-sensitive strain
Mw	molecular mass
NIA	necrosis-inducing activity
NOE	nuclear Overhauser enhancement
NOESY	NOE spectroscopy
PAMP	pathogen-associated molecular pattern
ppm	parts per million
PR	pathogenesis-related
PVX	potato virus X
R	resistance gene
RP-HPLC	reversed-phase high-performance liquid chromatography
SDS-PAGE	sodium dodecyl sulfate-polyacrylamide gelelectrophoresis
τ_c	rotational correlation time
TCEP	tris-(2-carboxyethyl)phosphine
TFA	trifluoroacetic acid
TOCSY	total correlation spectroscopy
t_r	retention time
vvm	volume of gas per volume of medium per minute

1

General introduction and outline

INTRODUCTION

1.1 PERCEPTION OF PATHOGENS BY RESISTANT PLANTS

Plants are constantly challenged by viruses, bacteria, fungi, oomycetes, nematodes, and insects, but in most cases, these attacks are not successful as most plants are resistant (Agrios, 1997). In a few cases, however, a pathogen is successful and a plant species is susceptible (compatible interaction). This means that the invading pathogen is able to infect, colonize, and successfully reproduce on such plant species. Despite this compatibility between pathogen and plant species, individual plants exist within the natural plant population that are resistant, *i.e.* they can recognize the invading pathogen and subsequently arrest its further growth *in planta* (incompatible interaction). This type of resistance is referred to as genotype-specific resistance. Genetic studies have revealed that, in general, genotype-specific resistance of the host plant depends on a monogenic dominant trait (designated as resistance or *R* gene). This trait confers exclusively resistance to a pathogen isolate carrying a matching avirulence (*Avr*) gene encoding an elicitor or avirulence determinant (AVR) that is recognized by the *R* gene containing resistant plant. This concept is known as the gene-for-gene paradigm and was independently proposed by Oort (1944) and Flor (1942, 1946). Over the last decade, numerous *R* genes conferring resistance against various types pathogens have been cloned (*e.g.* Dangl and Jones, 2001; Hulbert et al., 2001; Takken and Joosten, 2000). Only last year, the first *R* gene of potato was cloned that confers resistance against late blight caused by the oomycete *Phytophthora infestans* (Ballvoral et al., 2002). Late blight is worldwide the most destructive disease of potato crop and its control requires such high quantities of chemicals that identification and employment of *R* genes against this pathogen is badly needed. Whereas the identified AVR proteins genes do not share a common denominator, the architecture of the R proteins appears to be fairly similar (Dangl and Jones, 2001). The vast majority of R proteins contain Leucine-Rich Repeats (LRRs) that are combined with one or several of the following domains: Nucleotide-Binding site (NB), Coiled-Coil domain (CC), *Drosophila* Toll and mammalian Interleuking-like Receptor (TIR), and or a Ser/Thr-Kinase domain (Dangl and Jones, 2001) (Figure 1). According to the gene-for-gene model, the *Avr* gene of the pathogen encodes an elicitor protein, which is directly or indirectly perceived by the matching R protein. Evidence for a direct interaction between AVR proteins and R proteins

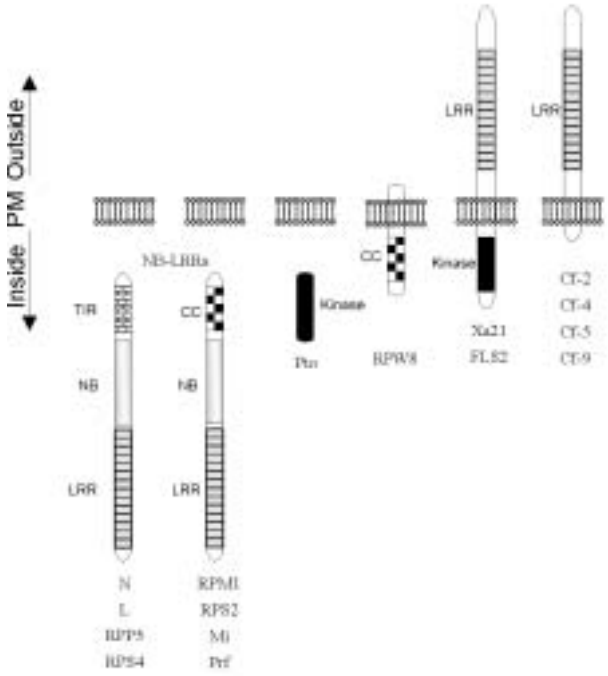

Figure 1. The predicted localization and structure of five main classes of resistance proteins. For references, the reader is referred to *e.g.* Dangl and Jones (2001) and Takken and Joosten (2000). PM, plasma membrane.

has hitherto been shown between AvrPto and Pto (Tang et al., 1996) and between AvrPita and Pita (Jia et al., 2000). Interaction was shown for these cases by using the yeast-two-hybrid (Y2H) assay. The cytoplasmic localization of both Pto and Pita is consistent with the observation that *AvrPto* and *AvrPita* induce both a HR when expressed inside plant cells.

1.2 PLANT DEFENSE RESPONSES IN RESISTANT PLANTS

Recognition of an invading pathogen by a resistant plant is promptly followed by induction of various plant defense responses generally involving a Hypersensitive Response (HR). HR refers to the induction of local cell death around the initial infection site that leads to arrested

growth of the invading pathogen. Active defense is often associated with the accumulation of pathogenesis-related (PR) proteins, which include fungal cell wall hydrolyzing enzymes like β-1,3-glucanases (PR-2) and chitinases (classes PR-3, PR-4 and PR-11) (Stintzi et al., 1993). A few days post-infection or inoculation, PR-proteins may account for ~10% of all soluble proteins present in plant leaves. Physical barriers become also apparent such as callose depositions (β-1.3-glucans), lignin depositions (phenylpropanoids), and the incorporation of hydroxyproline-rich glycoproteins in the cell wall (Stintzi et al., 1993). In addition, antimicrobial secondary metabolites such as phytoalexins accumulate around infection sites (Darvill and Albersheim, 1984; De Wit and Kodde, 1981; Ebel, 1986).

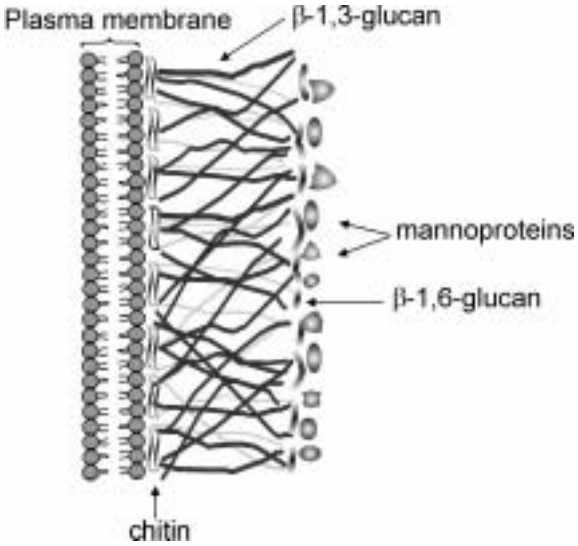

Figure 2 Schematic diagram of the structure of the fungal cell wall

1.3 PLANT CHITINASES HAVE ANTI-FUNGAL ACTIVITY

Chitinases are proposed to play a role in several biological processes in plants including: plant development (de Jong et al., 1992; Kragh et al., 1996; Passarinho and de Vries, 2002) and (active) plant defense against fungal pathogens. Their role in plant defense is supported by the following observations:

(i) All fungal cell walls are largely composed of the polysaccharides chitin, β-1,3-glucan, and β-1,6-glucan, which can be hydrolyzed by plant chitinases and glucanases (Bernard and Latge, 2001; Klis et al., 2001)(Figure 2).

(ii) *In vitro* assays have shown that plant chitinases can indeed cause severe lysis of fungi, in particular when combined with β-1,3-glucanases (Mauch et al., 1988; Roberts and Selitrennikoff, 1988; Sela-Buurlage et al., 1993). The vacuolar class I chitinases (basic chitinases) contain a chitin-binding domain (ChBD), which is linked to a plant specific catalytic domain (Family-19). The presence of this ChBD appears to enhance antifungal activity, but the ChBD is not strictly required for antifungal activity (Iseli et al., 1993; Limon et al., 2001; Sela-Buurlage et al., 1993; Suarez et al., 2001). The presence of carbohydrate-binding domains like ChBDs in chitinases is, in general, explained by arguing that they recruit and mediate a prolonged and intimate contact between enzyme and insoluble chitin (Bolam et al., 1998; Brunner et al., 1998; Iseli et al., 1993).

(iii) Immunocytochemical localization studies performed on plant chitinases and β-1,3-glucanases have shown that they accumulate near fungal structures in infected plants (Benhamou et al., 1990; Wubben et al., 1994).

(iv) Chitinase genes are induced following pathogen infection (Collinge et al., 1993). At early time points after infection, expression levels of chitinase genes are found to be consistently higher in resistant plants than in susceptible plants (Daugrois et al., 1990; Joosten and de Wit, 1989; Rasmussen et al., 1992). Hence, plant chitinases have been used as markers for incompatibility.

(v) In transgenic plants that constitutively express different types of chitinases, disease symptoms caused by many fungal pathogens were often reduced, including those pathogens with a broad host range, such as *Botrytis cinerea* and *Rhizoctonia solani* (Table 1). In addition, a few transgenic crop species constitutively expressing chitinases were evaluated under field conditions, which showed reduced disease incidence in these cases (Grison et al., 1996; Howie et al., 1994; Melchers and Stuiver, 2000).

However, plant chitinases are certainly not effective against all plant pathogenic fungi *in vitro* (Joosten et al., 1995) or in transgenic plants constitutively expressing chitinases (Neuhaus et al., 1991). Some reports suggest that adaptive mechanisms against chitinase activity exist in pathogenic fungi. In the case of *Nectria haematococca* (Ludwig and Boller, 1990) and *Fusarium solani* f.sp. *phaseoli* (Sela-Buurlage, 1996), germlings were less sensitive to normally lethal doses of chitinases/β-1,3-glucanases when they had been pretreated with

Table 1 Plant species genetically engineered to enhance resistance against fungal pathogens using genes encoding microbial and plant chitinases

Plant species	Expressed gene product	Effect on disease development	Reference
Alfalfa (*Medicago sativa*)	Alfalfa glucanase	Reduced symptom development caused by *Phytophthora megasperma*; no effect on *Stemphylium alfalfae*	Masoud et al. (1996)
Apple (Malus ×domestica Auth.)	*Trichoderma harzianum* endochitinase	Reduced lesion number and lesion area caused by *Venturia inaequalis*	Bolar et al. (2000); Wong et al. (1999)
Canola (*Brassica napus)*	Bean chitinase	Reduced infectivity and total seedling mortality caused by *Rhizoctonia solani*	Broglie et al. (1991)
	Tomato chitinase	Lower percentage of diseased plants caused by *Cylindrosporium concentricum* and *Sclerotinia sclerotiorum*	Grison et al. (1996)
Carrot (*Daucus carota* L.)	Tobacco chitinase	Reduced infectivety and disease incidence caused by *Botrytis cinerea*, *Rhizoctonia solani*, and *Sclerotium rolfsii*; no effect on *Thielaviopsis basicola* and *Alternaria radicina*	Punja and Raharjo (1996)
Chrysanthemum (*Dendranthema grandiflorum)*	Rice chitinase	Reduced lesion development caused by *Botrytis cinerea*	Takatsu et al. (1999)
Cucumber (*Cucumis sativus*)	Petunia and tobacco chitinases	No effect on disease development caused by *Colletotrichum lagenarium* and *Rhizoctonia solani*	Punja and Raharjo (1996)
	Rico chitinase	Reduced lesion development caused by *Botrytis cinerea*	Tabei et al. (1998)
Grape (*Vitis vinifera*)	Rice chitinase	Reduced development of *Uncinula necator* and fewer lesions caused by *Elisinoe ampelina*	Yamamoto et al. (2000)

Table 1 (*continued*)

Grape (*Vitis vinifera*)	*Trichoderma harzianum* Endochitinase	Reduction of *Botrytis cinerea* development in preliminary tests	Kikkert et al. (2000)
Peanut (*Arachis hypogaea*)	Tobacco chitinase	Delayed lesion development and smaller lesion size caused by *Cercospora arachidicola*	Rohini and Rao (2001)
Potato (*Solanum tuberosum*)	*Trichoderma harzianum* Endochitinase	Lower lesion numbers and size caused by *Alternaria solani*; reduced mortality caused by *Rhizoctonia solani*	Lorito et al. (1998)
Rice (*Oryza sativa*)	Rice chitinase	Delayed onset and reduced severity of disease symptoms caused by *Magnaporthe grisea*	Nishizawa et al. (1999)
	Rice chitinase	Fewer numbers of lesions and smaller size caused by *Rhizoctonia solani*	Lin et al. (1995); Datta et al. (2000, 2001)
Rose (*Rosa hybrida* L.)	Rice chitinase	Reduced lesion diameter caused by black spot (*Diplocarpon rosae*)	Marchant et al. (1998)
Strawberry (*Fragaria ×ananassa* Duch.)	Rice chitinase	Reduced development of powdery mildew (*Sphaerotheca humuli*)	Asao et al. (1997)
Tobacco (*Nicotiana benthamiana*)	Sugarbeet chitinase	No effect on *Cercospora nicotianae*	Nielsen et al. (1993)
Tobacco (*Nicotiana sylvestris*)	Tobacco chitinase	No effect on *Cercospora nicotianae*	Neuhaus et al. (1991)
	Tobacco chitinase	Reduced colonization by *Rhizoctonia solani*	Vierheilig et al. (1993)
Tobacco (*Nicotiana tabacum*)	Bean chitinase	Lower seedling mortality caused by *Rhizoctonia solani*; no effect on *Pythium aphanidermatum*	Broglie et al. (1991, 1993)
	Serratia marcescens chitinase	Reduced disease incidence caused by *Rhizoctonia solani* on seedlings; no effect on *Pythium ultimum*	Howie et al. (1994)

Table 1 (*continued*)

Plant species	Expressed gene product	Effect on disease development	Reference
Tobacco (*Nicotiana tabacum*)	*Serratia marcescens* chitinase	Reduced development of *Rhizoctonia solani*	Jach et al. (1992)
	Rhizopus oligosporus chitinase	Reduced infectivety, and development and size of lesions on leaves caused by *Botrytis cinerea* and *Sclerotinia sclerotiorum*	Terakawa et al. (1997)
	Trichoderma harzianum endochitinase	Reduced symptoms caused by *Alternaria alternata*, *Botrytis cinerea*, and *Rhizoctonia solani*	Lorito et al. (1998)
	Baculovirus chitinase	Reduced lesion development caused by brown spot (*Alternaria alternata*)	Shi et al. (2000)
Tomato (*Lycopersicon esculentum*)	Wild tomato (*Lycopersicon chilense*) chitinase	Reduced development of *Verticillium dahliae* races 1 and 2	Tabaeizadeh et al. (1999)
	Tobacco chitinase	Reduced development of *Fusarium oxysporum* f.sp. *lycopersici*	Jongedijk et al. (1995)
Wheat (*Triticum aestivum*)	Barley chitinase	Reduced development of colonies of *Blumeria graminis* f. sp. *Tritici*	Bliffeld et al. (1999)
	Barley chitinase	Reduced development of colonies of *Blumeria graminis* and *Puccinia recondita*	Oldach et al. (2001)

Table was revised from Punja (2001)

low doses of these enzymes. As enzymatic activity remained, modifications of the cell wall such as covalent cross-links and depositions of glycoproteins or melanin should not be ruled out. For example, the resistance of the cell wall of *Aspergillus nidulans, Aspergillus fumigatus,* and *Rhizoctonia solani* to digestion by chitinases/β-1,3-glucanases appeared to be dependent on the content of melanin in the cell wall (Kuo and Alexander, 1967; Luther and Lipke, 1980; Potgieter and Alexander, 1966). Other reports have indicated that *Colletotrichum lindemuthianum* and *Phytophthora* species secrete proteinaceous inhibitors of plant endo-β-1,3-glucanases during infection (Albersheim and Valent, 1974; Ham et al., 1997; Rose et al., 2002). To date, proteinaceous inhibitors against chitinases have not yet been identified although indirect support for their occurrence exists. Adaptive evolution was demonstrated for residues found in the active site of plant class I chitinases indicative for the existence of competitive inhibitors of plant chitinases (Bishop et al., 2000), which supports the hypothesis that invading pathogens have acquired defense mechanisms to counteract chitinolytic activity.

1.4 FUNGAL CELL WALL OLIGOSACCHARIDES: GENERAL ELICITORS

Non-host resistance towards most phytopathogenic micro-organisms is the predominant form of plant resistance (Heath, 2000). A variety of microbe-associated general elicitors trigger plant defense responses in a non-cultivar specific manner (Nürnberger and Brunner, 2002). Strikingly, these general elicitors of plant defense responses have characteristics overlapping with pathogen-associated molecular patterns (PAMPs) that trigger innate immune responses in various vertebrates and invertebrates (Medzhitov and Janeway, 1997). Recent evidence suggests that plants may have a similar innate immune system based on Toll-like receptors (Gómez-Gómez and Boller, 2002; Nürnberger and Brunner, 2002). Plant PAMPs that have been identified to date comprise lipopolysaccharides (LPS) of Gram-negative bacteria (Dow et al., 2000), Flg22 – a conserved fragment of bacterial flagellin (Felix et al., 1999), Pep13 – a conserved fragment from Phytophthora transglutaminases (Brunner et al., 2002), Elicitins – sterol-binding proteins of *Phytophthora* and *Pythium* species (Tyler, 2002), RNP-1– a domain of bacterial cold shock proteins (Felix and Boller, 2003), but also oligosaccharide elicitors released from various mycelial walls (Côté and Hahn, 1994; Ebel and Cosio, 1994) (Figure 3). The cell wall hydrolyzing activity presented by glucanolytic and chitinolytic extracellular PR-proteins is, presumably, a source

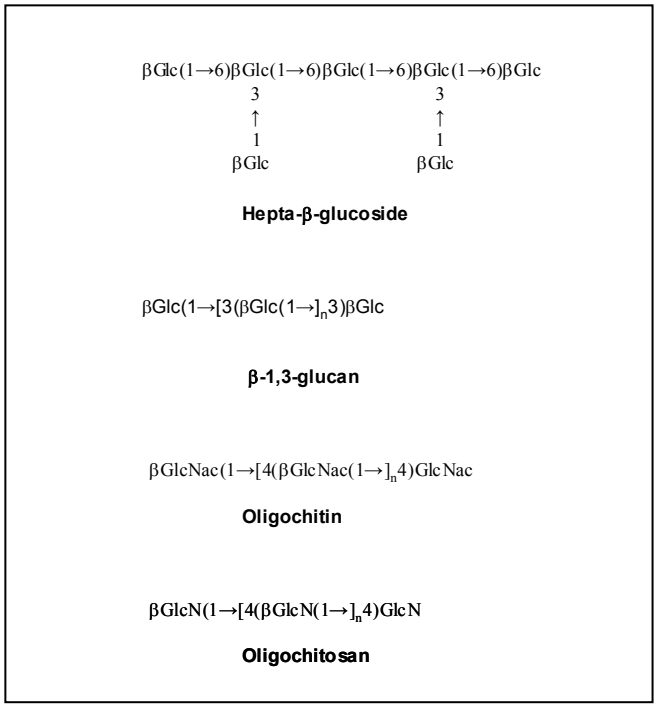

Figure 3. Structures of elicitor-active oligosaccharides

for the release of fungal and oomycete oligosaccharide elicitors. Plasma membrane-derived elicitor-binding sites have been characterized for different elicitors in various plants species, e.g. for the hepta-β-glucoside elicitor from cell walls of *Phytophthora* species (Cheong et al., 1993; Mithöfer et al., 2000; Mithöfer et al., 1996), for oligochitin of fungal cell walls (Felix et al., 1993; Baureithel et al., 1994; Ito et al., 1997), and for a glycopeptide elicitor (Bass et al., 1993). Notably, a chitinase-related receptor-like kinase CHRK1, which exhibits autophosphorylation activity but no chitinase activity (due to a mutation of an essential Glu residue in the active site), has been identified in plasma membranes of tobacco (Kim et al., 2000). The expression of *CHRK1* was strongly induced upon infection. Moreover, the *Arabidopsis* orthologue of CHRK1 (At4g19720) has a motif specific for TonB, a bacterial receptor-associated protein that is involved in active transport of poorly membrane-permeable substrates (Gudmundsdottir et al., 1989; Passarinho, 2002). This motif suggests a receptor-like function for CHRK1.

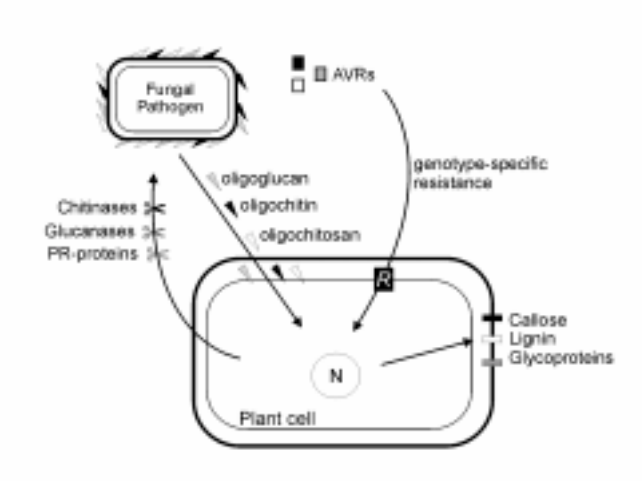

Figure 4. Plant defense responses triggered by genotype-specific AVR elicitors might indirectly enhance defense responses by release of general elicitors from the fungal cell walls.

1.5 PLANT LECTINS AND HOST DEFENSE RESPONSES

In anticipation of attacks by different pathogens, plants accumulate also many types of defense-related proteins in their most vulnerable tissues. A particular class of such defense related proteins is the small cysteine-rich proteins with anti-microbial activity such as thionins, plant defensins, lipid-transfer proteins, and lectins (García-Olmedo et al., 1998; Selitrennikoff, 2001). Lectins have been defined as “carbohydrate-binding proteins or glycoproteins except for enzymes and antibodies” (Goldstein et al., 1980). Lectins have a carbohydrate-binding specificity that can be competed for by simple oligosaccharides (Loris, 2002). In mammals lectins are involved in inflammation, cell-cell adhesion, and activation of the complement system in the absence of specific antibodies. Invertebrate lectins act as clotting factors in the innate immune response against pathogen attacks (Iwanaga et al., 1998; Kawabata, 2002).

In many plants species, the storage of large numbers of vacuolar lectins in seeds has long been recognized (Chrispeels and Raikhel, 1991). Besides a general seed storage function, certain plant lectins appear to have a role in defense (Chrispeels and Raikhel, 1991). Examples of seed-located lectins of Gramineae species are Wheat Germ Agglutinin (WGA) (Raikhel and Wilkins, 1987; Wright, 1980), barley lectin (Lerner and Raikhel, 1989),

and rice lectin (Wilkins and Raikhel, 1989). These three lectins share a homologous domain of approximately 43 amino acids, the “hevein” domain, which is present as a four in-tandem repeat (Figure 5). This domain specifically binds the sugar *N*-actetyl-D-glucosamine (GlcNAc), its oligomers, and its polymer chitin (Wright, 1980). The name “hevein” was derived from a small anti-microbial, chitin-binding protein found in the latex of the rubber tree *Hevea brasiliensis* (Beintema, 1994; Broekaert et al., 1990). One hevein domain contains eight conserved cysteine residues connected by four disulfide bonds. The precursor of hevein resembles members of PR-4 class (chitin-binding) of proteins (Broekaert et al., 1990), which includes the wound-inducible proteins Win1 and Win2 from potato, and CPB20 from tobacco (Ponstein et al., 1994). Hevein is derived from a precursor that contains a signal peptide, a hevein domain, and a carboxy-terminal chitinase domain (Broekaert et al., 1990). Other well-studied examples of plant lectins containing a hevein domain include the stinging nettle lectin UDA (*Urtica dioica* agglutinin; (Broekaert et al., 1989; Harata and Muraki, 2000), and Ac-AMP1/Ac-AMP2 proteins from *Amaranthus caudatus* (Broekaert et al., 1992). UDA is derived from a similar precursor protein as hevein except that UDA has two in-tandem hevein domains of which one only acts as a chitin-binding site (Harata and Muraki, 2000). UDA, Hevein, and Ac-AMP1/Ac-AMP2 were found to have antifungal activity in the micromolar range (Broekaert et al., 1989; Heusing et al., 1991; Van Parijs et al., 1991). The antifungal activity likely results from binding to nascent chitin in the fungal cell wall. By mechanisms not yet understood, the lectins may subsequently disrupt cell polarity with concomitant inhibition of growth (Bormann et al., 1999). The larger lectins, like WGA, have less antifungal activity. Therefore, the smaller size (carrying only one or two ChBDs) of the hevein-like lectins might render them more accessible to nascent chitin and disrupt cell wall morphology (de Nobel et al., 1990; Money and Webster, 1990; Schoffelmeer et al., 1999).

1.6 THE TOMATO-*CLADOSPORIUM FULVUM* INTERACTION

Cladosporium fulvum (syn. *Fulvia fulva*) is a biotrophic pathogenic fungus causing leaf mold of tomato (*Lycopersicon* species). The fungus belongs to the class of Deuteromycetes (Fungi Imperfecti) and has a morphology that resembles that of filamentous ascomycetes. The cell wall of *C. fulvum* contains glucans and chitin as major polysaccharides (Joosten and de Wit, 1999). Chitin is evenly distributed in the inner layer of the fungal cell wall of

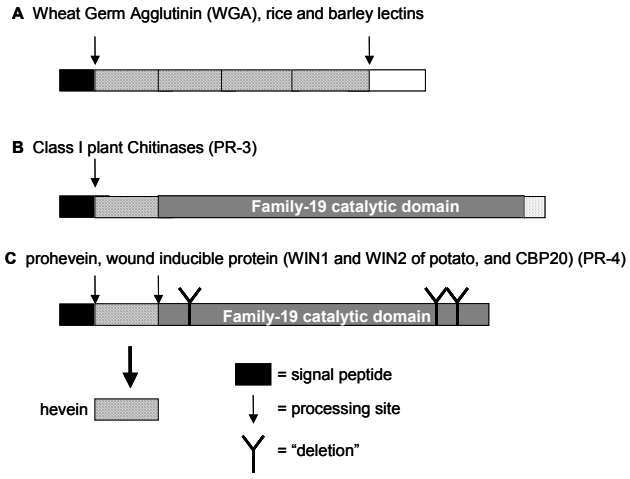

Figure 5. Schematic representation of types of plant proteins containing a hevein domain. (A) The Gramineae lectins Wheat Germ Agglutinin (WGA), barley lectin, and rice lectin contain four hevein domains. (B) Class I plant chitinases contain an N-terminal hevein domain linked by a hinge region to a plant-specific family-19 catalytic domain. (C) The precursor of hevein of *Hevea brasiliensis* is an inactive PR-4 chitinases. The wound-inducible proteins CPB20 of tobacco, Win1 and Win2 of potato also exemplify PR-4 proteins.

C. fulvum, whereas glucans and glycoproteins presumably form the electron-dense outer layer (Wubben, 1994). Infection of tomato by *C. fulvum* occurs under humid conditions when conidia of *C. fulvum* germinate, form runner hyphae across the leaf surface, and eventually penetrate the leaf through stomata without forming penetration structures such as appresoria. In a compatible interaction the fungus subsequently colonizes the entire intercellular (apoplastic) space around leaf mesophyll cells without entering them (de Wit, 1977; Lazarovtis and Higgins, 1976). In an incompatible interaction, fungal growth is, however, limited as tomato recognizes race-specific AVR proteins originating from the fungus, and subsequently mounts a HR (de Wit et al., 1985; de Wit and Spikman, 1982).

Recognition of these race-specific elicitors strictly complies with the gene-for-gene concept (Joosten and de Wit, 1999). In the last decade, a large number of *Cf* (for *Cladosporium fulvum) R* genes mediating recognition of race-specific elicitors of *C. fulvum*

have been cloned (Parniske et al., 1999 and references therein). These *Cf* genes belong to a subclass of *R* genes encoding putative membrane anchored proteins with a predicted extracellular Leucine-Rich Repeat (LRR) domain and a short C-terminal cytoplasmic tail lacking any known signaling domains (Fig 1). The largest difference between the various Cf proteins is their number of LRRs. For example, Cf-4 and Cf-9 share more than 91% sequence identity, but Cf-9 contains 27 LRRs whereas Cf-4 contains 25 LRRs (Thomas et al., 1997). Of the 67 amino acids differences between Cf-4 and Cf-9 only three amino acids residing in three central LRRs appeared essential for a Cf-4-mediated HR (van der Hoorn et al., 2001; Wulff et al., 2001). Both Cf-4 and Cf-9 are apparently part of a protein complex (when isolated) with a molecular mass of ~420 kDa that appears to accommodate only one Cf molecule as determined by size-exclusion chromatogrophy (Rivas et al., 2002a; Rivas et al., 2002b). However, the apparent size of this isolated Cf-9 complex is unaltered by harsh treatments, such as boiling in SDS detergent, incubation in 6 M Urea, or when Cf-9 is expressed and isolated from insect cells (van der Hoorn et al., in preparation). Thus, the apparent size seems to be an intrinsic feature of Cf-9, rather than due to association of Cf-9 with other high molecular-weight proteins.

So far, evidence is lacking for a direct interaction between Cf-4 and Cf-9 proteins and AVR4 and AVR9 elicitors, respectively (Luderer et al., 2001). It remains, therefore, a challenge to dissect the biochemical mechanism of perception of AVR proteins by Cf proteins. Some evidence hints to a role for scaffolding proteins that could bring the two together. In the case of the Cf-2/AVR2 system, a secreted papain-like cysteine endoprotease Rcr3 was shown to be required for the recognition of AVR2 by Cf-2 (Dixon et al., 2000; Krüger et al., 2002). Most interestingly, Rcr3 suppresses the *Cf-2*–dependent autonecrosis conditioned by its *L. esculentum* allele suggesting a role for Cf-2 as a guardee for Rcr3 (Krüger et al., 2002).

1.7 ELICITORS FROM *CLADOSPORIUM FULVUM*

The largest number of fungal elicitors has hitherto been isolated and identified from *C. fulvum* (de Wit and Joosten, 1999; Joosten and de Wit, 1999). The race-specific (AVRs) and none race-specific (ECPs) elicitors of *C. fulvum* are all secreted, small, and cysteine-rich (Joosten and de Wit, 1999; Laugé et al., 2000; Luderer et al., 2002). The only difference between the AVR and the ECP elicitors is that polymorphisms are only observed in the

genes encoding AVR elicitors. These polymorphisms form the basis for the loss-of-recognition by the corresponding Cf proteins. The absence of polymorphism in the genes encoding the ECPs might relate to the fact that *R* genes mediating recognition of ECPs (the so-called *Cf-ECP R* genes) have not yet been introduced in commercial tomato cultivars. Therefore, the *Ecp* genes have not yet encountered a strong selection pressure (Laugé et al., 2000; Laugé et al., 1998). In addition, the ECP1 and ECP2 elicitors were shown to be required for full virulence and mutations in the corresponding genes could, therefore, be associated with a serious virulence penalty (Laugé et al., 1997). Nonetheless, the function at the molecular level of ECP1 and ECP2 elicitors remains unknown.

The ways in which recognition is overcome varies between the different AVRs. The *Avr9* gene was found to be absent in virulent strains of *C. fulvum* (van Kan et al., 1991). The *Avr4* alleles encoded transcripts with point mutations or a frame-shift mutation leading to mutant proteins (Joosten et al., 1994) Besides point mutations, some virulent strains of *C. fulvum* have shown to lack expression of an *Avr* gene as is the case for the *Avr4E* gene (Westerink et al., in preparation). The modifications found in the *Avr2* gene involved frame-shift mutations (either by base-pair deletions/insertions or the presence of a transponson) resulting in a truncated protein (Luderer et al., 2002). The allelic variation in the *Avr* genes appears to have no deleterious effect on the virulence of *C. fulvum* strains, at least not under laboratory conditions (Joosten et al., 1994, 1997; Luderer et al., 2002; van Kan et al., 1991). Nevertheless, It is generally anticipated that fungal AVRs contribute to virulence or fitness of the pathogen, as has now been established for several bacterial AVRs (Bonas and Lahaye, 2002; Kjemtrup et al., 2000; White et al., 2000).

1.8 OUTLINE OF THIS THESIS

The research described in this thesis focuses on the characterization of intrinsic functions for the AVR4 and AVR9 elicitors of *C. fulvum*. At the start of the research project, homologous sequences for AVR4 and AVR9 had not been identified. Therefore, an approach was chosen that would enable us to identify homologous structures in protein databases, rather than searching for homologies at the nucleotide level or primary sequence level. The elucidation of the disulfide bond patterns could possibly provide clues on protein structure (Harrison and Stenberg, 1996; Mas et al., 1998). For this reason, the disulfide bonds were elucidated by partial reduction of the disulfide bonds (Gray, 1993; Wu and Watson, 1997).

This technique was possible due to the “rediscovery” of tris-(-2-carboxy-ethyl)-phosphine (TCEP), as a potent disulfide bond reducing agent (Burns et al., 1991).

The method required larger quantities of proteins than there were available at the time. Chemical synthesis followed by oxidative folding was established as a method to obtain sufficient quantities of AVR9 (Mahé et al., 1998; van den Hooven et al., 1999). For AVR4, a heterologous expression system based on the methylotrophic yeast *Pichia pastoris* was set-up (**Chapter 2**). This system is particularly suitable for high-level expressions of disulfide bond-containing proteins. Fermentation protocols designed for *P. pastoris* were amended in order to improve protein yields with the idea to reduce costs for the incorporation of stable isotopes required for studies involving Nuclear Magnetic Resonance (NMR).

In **Chapter 3,** the disulfide bond pattern and the secondary structure of AVR9 is described. Based on peptide length and cysteine spacing, it was previously suggested that AVR9 is a cystine-knotted peptide. Here NMR data confirmed that AVR9 is structurally related to the cystine-knotted carboxypeptidase inhibitor (CPI). However, although structurally related, in functional assays AVR9 did not show carboxypeptidase inhibitor activity.

In **Chapter 4**, the disulfide bridge pattern of AVR4 is elucidated and homology with a novel chitin-binding domain (ChBD) (Shen and Jacobs-Lorena, 1999) was discovered based on the spacing between six cysteine residues involved in three disulfide bonds. The role of each of the disulfide bridges is correlated to protein (in)stability, Cf-4-dependent recognition, and chitin-binding abilities. The findings described in this chapter give a possible explanation for the virulence of strains of *C. fulvum* carrying a point mutation in *avr4* resulting in a Cys-to-Tyr substitution.

In **Chapter 5,** the possible roles of the ChBD in AVR4 were further examined with regard to virulence. Effects of AVR4 on the activities of plant chitinases were tested *in vitro.* Furthermore, the localization of AVR4 was examined in tomato plants inoculated with *C. fulvum.* Data presented in this chapter support that AVR4 acts as an integral cell wall protein. Strikingly, a passive virulence function for AVR4 would differ from the role of bacterial effector proteins that appear to suppress basal host defense responses.

In **Chapter 6**, the association of AVR4 with oligomers of N-acetyl-D-glucosamine is examined in detail using several techniques. AVR4 interacts with chitin through three subsites. NMR data provide a detailed view of the residues important for the interaction with

chitin. The binding thermodynamics of AVR4 are compared to those of plant chitin-binding lectins and a model for binding is presented.

In **Chapter 7**, the findings presented in the previous chapters are discussed in light of the prevailing 'guard hypothesis' that has been proposed for the indirect interaction between pathogen avirulence factors and plant R proteins. This guard model implies that avirulence factors suppress basal defense of plants by manipulating virulence targets that are sensed by the R proteins, the guards. While this model could hold for various Avrs, the primary function of AVR4 does not seem to fit this model as it protects the fungus against chitinases induced during active defense rather than suppressing active defense responses.

REFERENCES

Agrios, G.N. (1997) *Plant Pathology* (London, Academic Press).

Albersheim, P., and Valent, B. (1974) *Plant Physiol* ***53***, 684-687.

Baureithel, K., Felix, G., and Boller, T. (1994) *J Biol Chem* ***269***, 17931-17938.

Beintema, J.J. (1994). *FEBS Lett* ***350***, 159-163.

Benhamou, N., Joosten, M.H.A.J., and de Wit, P.J.G.M. (1990) *Plant Physiol* ***92***, 1108-1120.

Bernard, M., and Latge, J.P. (2001). *Med Mycol* ***39***, suppl 75-86.

Bishop, J.G., Dean, A.M., and Mitchell-Olds, T. (2000) *Proc Natl Acad Sci USA* ***97***, 5322-5327.

Bolam, D.N., Ciruela, A., McQueen-Mason, S., Simpson, P., Williamson, M.P., Rixon, J.E., Boraston, A., Hazlewood, G.P., and Gilbert, H.J. (1998) *Biochem J* ***331***, 775-781.

Bonas, U., and Lahaye, T. (2002) *Curr Opin Microbiol* ***5***, 44-50.

Bormann, C., Baier, D., Horr, I., Raps, C., Berger, J., Jung, G., and Schwarz, H. (1999) *J Bacteriol* ***181***, 7421-7429.

Broekaert, W.F., Lee, H., Kush, A., Chua, N.-H., and Raikhel, N. (1990) *Proc Natl Acad Sci USA* ***87***, 7633-7637.

Broekaert, W.F., Marien, W., Terras, F.R., de Bolle, M.F., Proost, P., van Damme, J., Dillen, L., Claeys, M., Rees, S.B., Vanderleyden, J., and Cammue, B.P.A. (1992) *Biochemistry* ***31***, 4308-4314.

Broekaert, W.F., van Parijs, J., Leyns, F., Joos, W., and Peumans, W.J. (1989) *Science* ***245***, 1100-1102.

Brunner, F., Rosahl, S., Lee, J., Rudd, J.J., Geiler, C., Kauppinen, S., Rasmussen, G., Scheel, D., and Nürnberger, T. (2002) *EMBO J* ***21***, 6681-6688.

Brunner, F., Stintzi, A., Fritig, B., and Legrand, M. (1998) *Plant J* ***14***, 225-234.

Burns, J.A., Butler, J.C., Moran, J., and Whitesides, G.M. (1991) *J Org Chem* ***56***, 2648-2650.

Cheong, J.J., ALba, R., Côté, H.C., Enkerli, J., and Hahn, M.G. (1993) *Plant Physiol **103***, 1173-1182.

Chrispeels, M.J., and Raikhel, N.V. (1991). *Plant Cell **3***, 1-9.

Collinge, D.B., Kragh, K.M., Mikkelsen, J.D., Nielsen, K.K., Rasmussen, U., and Vad, K. (1993).*Plant J **3***, 31-40.

Côté, F., and Hahn, M.G. (1994) *Plant Mol Biol **26***, 1379-1411.

Dangl, J.L., and Jones, J.D.G. (2001). *Nature **411***, 826-833.

Darvill, A.G., and Albersheim, P. (1984) *Annu Rev Plant Physiol **35***, 243-275.

Daugrois, J.H., Lafitte, C., Barthe, J.P., and Touze, A. (1990). *J Phytopath **130***, 225-234.

de Jong, A.J., Cordewener, J., Lo Schiavo, F., Terzi, M., Vandekerckhove, J., van Kammen, A., and de Vries, S.C. (1992) *Plant Cell **4***, 425-433.

de Nobel, J.G., Klis, F.M., Priem, J., Munnik, T., and van den Ende, H. (1990) *Yeast **6***, 491-499.

de Wit, P.J.G.M. (1977) *Neth J Plant Pathol **83***, 109-122.

de Wit, P.J.G.M., Hofman, A.E., Velthuis, G.C.M., and Kuc, J.A. (1985) *Plant Physiol **77***, 642-647.

de Wit, P.J.G.M., and Joosten, M.H.A.J. (1999). *Curr Opin Microbiol **2***, 368-373.

De Wit, P.J.G.M., and Kodde, E. (1981) *Physiol Mol Plant Pathol **18***, 143-148.

de Wit, P.J.G.M., and Spikman, G. (1982) *Physiol Plant Pathol **21***, 1-11.

Dixon, M.S., Golstein, C., Thomas, C.M., Van der Biezen, E.A., and Jones, J.D.G. (2000) *Proc Natl Acad Sci USA **97***, 8807.

Dow, M., Newman, M.-A., and von Roepenack, E. (2000) *Annu Rev Phytopathol **2000***, 241-261.

Ebel, J. (1986). *Annu Rev Plant Physiol **24***, 235-264.

Ebel, J., and Cosio, E.G. (1994) *Int Rev Cytol **148***, 1-36.

Felix, G., and Boller, T. (2003) *J Biol Chem **278***, 6201-6208.

Felix, G., Duran, J.D., Volko, S., and Boller, T. (1999) *Plant J **18***, 265-276.

Felix, G., Regenass, M., and Boller, T. (1993). *Plant J **4***, 307-316.

Flor, H.H. (1942) *Phytopathology **32***, 653-669.

Flor, H.H. (1946) *J Agric Res **73***, 335-357.

García-Olmedo, F., Molina, A., Alamillo, J.M., and Rodrígues-Palenzuéla, P. (1998) *Biopolymers **47***, 479-491.

Goldstein, I.J., Hughes, R.C., Monsigny, M., Osawa, T., and Sharon, N. (1980) *Nature **285***, 66.

Gómez-Gómez, L., and Boller, T. (2002) *Trends Plant Sci **7***, 251.

Gray, W.R. (1993). *Protein Sci **2***, 1732-1748.

Grison, R., Grezes-Besset, B., Schneider, M., Lucante, N., Olsen, L., Leguay, J.J., and Toppan, A. (1996) *Nat Biotech **14***, 643-646.

Ham, K.S., Wu, S.C., Darvill, A.G., and Albersheim, P. (1997). *Plant J **11***, 169-179.

Harata, K., and Muraki, M. (2000) *J Mol Biol **297***, 673-681.

Heath, M. (2000) *Curr Opin Plant Bio. **3***, 315-319.

Heusing, J.E., Murdock, L.L., and Shade, R.E. (1991) *Phytochemistry **30***, 3565-3568.

Howie, W., Joe, L., Newbigin, E., Suslow, T., and Dunsmuir, P. (1994) *Transgenic Res **3***, 90-98.

Hulbert, S.H., Webb, C.A., Smith, S.M., and Sun, Q. (2001) *Annu Rev Phytopathol **39***, 285-312.

Iseli, B., Boller, T., and Neuhaus, J.M. (1993) *Plant Physiol **103***, 221-6.

Ito, Y., Kaku, H., and Shibuya, N. (1997) *Plant J **12***, 347-356.

Iwanaga, S., Kawabata, S., and Muta, T. (1998) *J Biochem **123***, 1-15.

Jia, Y., McAdams, S.A., Bryan, G.T., Hershey, H.P., and Valent, B. (2000) *EMBO J **19***, 4004-4014.

Joosten, M.H.A.J., Cozijnsen, T.J., and de Wit, P.J.G.M. (1994) *Nature **367***, 384-386.

Joosten, M.H.A.J., and de Wit, P.J.G.M. (1989). *Plant Physiol **89***, 945-951.

Joosten, M.H.A.J., and de Wit, P.J.G.M. (1999). *Annu Rev Phytopathol **37***, 335-367.

Joosten, M.H.A.J., Verbakel, H.M., Nettekoven, M.E., van Leeuwen, J., Vossen, R.T.M., and de Wit, P.J.G.M. (1995) *Physiol Mol Plant Pathol **46***, 45-59.

Joosten, M.H.A.J., Vogelsang, R., Cozijnsen, T.J., Verberne, M.C., and de Wit, P.J.G.M. (1997) *Plant Cell **9***, 367-379.

Kawabata, S. (2002). *Biochimt Biophys Acta **1572***, 414-421.

Kim, Y.S., Lee, Y.H., Yoon, G.M., Cho, H.S., Park, S.-W., Suh, M.C., Choi, D., Ha, H.J., Liu, J.R., and Pai, H.-S. (2000) *Plant Physiol **123***, 1162-1173.

Kjemtrup, S., Nimchuk, Z., and Dangl, J.L. (2000) *Curr Opin Microbiol **3***, 73-78.

Klis, F.M., de Groot, P., and Hellingwerf, K. (2001) *Med Mycol **39***, Suppl. 1-8.

Kragh, K.M., Hendricks, T., de Jong, A.J., Lo Schiavo, F., Bucherna, N., Horjup, P., Mikkelsen, J.D., and de Vries, S.C. (1996) *Plant Mol Biol **31***, 631-645.

Krüger, J., Thomas, C.M., Golstein, C., Dixon, M.S., Smoker, M., Tang, S., Mulder, L., and Jones, J.D.G. (2002) *Science **296***, 744-747.

Kuo, M.-J., and Alexander, M. (1967). *J Bacteriol **94***, 624-629.

Laugé, R., Goodwin, P.H., de Wit, P.J.G.M., and Joosten, M.H.A.J. (2000). *Plant J **23***, 735-745.

Laugé, R., Joosten, M.H.A.J., Haanstra, J.P.W., Goodwin, P.H., Lindhout, P., and de Wit, P.J.G.M. (1998). *Proc Natl Acad Sci USA **95***, 9014-9018.

Laugé, R., Joosten, M.H.A.J., van den Ackerveken, G.F.J.M., van den Broek, H.W.J., and de Wit, P.J.G.M. (1997) *Mol Plant-Microbe Interact **10***, 725-734.

Lazarovtis, G., and Higgins, V.J. (1976) *Can J Bot **54***, 224-234.

Lerner, D.R., and Raikhel, N.V. (1989) *Plant Physiol **91,*** 124-129.

Limon, M.C., MArgolles-Clark, E., Benitez, T., and Penttila, M. (2001) *FEMS Microbiol let **198***, 57-63.

Loris, R. (2002) *Biochimt Biophys Acta **1572***, 198-208.

Luderer, R., Rivas, S., Nurnberger, T., Mattei, B., van den Hooven, H.W., van der Hoorn, R.A.L., Romeis, T., Wehrfritz, J.M., Blume, B., Nennstiel, D., Zuidema, D., Vervoort, J., De Lorenzo, G., Jones, J.D.G., de Wit, P.J.G.M., and Joosten, M.H.A.J. (2001) *Mol Plant-Microbe Interact **14***, 867-876.

Luderer, R., Takken, F.L., de Wit, P.J.G.M., and Joosten, M.H.A.J. (2002). *Mol Microbiol **45***, 875-884.

Ludwig, A., and Boller, T. (1990) *FEMS Microbiol Lett **69***, 61-66.

Luther, J.P., and Lipke, H. (1980) *Appl Environ Microbiol **40***, 145-155.

Mahé, E., Vossen, P., van den Hooven, H.W., Le-Nguyen, D., Vervoort, J., and de Wit, P.J.G.M. (1998) *J Pept Res **52***, 482-494.

Mauch, F., Mauch-Mani, B., and Boller, T. (1988) *Plant Physiol **88***, 936-942.

Medzhitov, R., and Janeway, C. (1997) *Cell **91***, 295-298.

Melchers, L.S., and Stuiver, M. (2000) *Curr Opin Plant Biol **3***, 147-152.

Mithöfer, A., Fliegmann, J., Neuhaus-Url, G., Scharwz, H., and Ebel, J. (2000) *Biol Chem **381***, 705-713.

Mithöfer, A., Lottspeich, F., and Ebel, J. (1996) *FEBS Lett **381***, 203-207.

Money, N.P., and Webster, J. (1990) *Exp Mycol*, 234-242.

Neuhaus, J.M., Ahl-Goy, P., Hinz, U., Flores, S., and Meins, F. (1991) *Plant Mol Biol **16***, 141-151.

Nürnberger, T., and Brunner, F. (2002) *Curr Opin Plant Biol **5***, 318-324.

Oort, A.J.P. (1944). *Planteziekten **50***, 73-106.

Parniske, M., Wulff, B.B.H., Bonnema, G., Thomas, C.M., Jones, D.A., and Jones, J.D.G. (1999). *Mol Plant-Microbe Interact **12***, 93-102.

Passarinho, P., and de Vries, S.C. (2002). *Arabidopsis book*, C. R. Sommerville, and E. M. Meyerowitz, eds. (Rockville, MD, http://www.aspb.org/publications/arabidopsis, American Society of Plant Biologists), pp. 25.

Ponstein, A.S., Bres-Vloemans, S.A., Sela-Buurlage, M.B., van den Elzen, P.J.M., Melchers, L.S., and Cornelissen, B.J.C. (1994) *Plant Physiol **104***, 109-118.

Potgieter, H.J., and Alexander, M. (1966) *J Bacteriol **91***, 1526-1532.

Punja, Z.K. (2001) *Can J Plant Pathol **23***, 216–235.

Raikhel, N.V., and Wilkins, T.A. (1987) *Proc Natl Acad Sci USA **84***, 6745-6749.

Rasmussen, U., Giese, H., and Mikkelsen, J.D. (1992) *Planta **187***, 328-334.

Rivas, S., Mucyn, T., van den Burg, H.A., Vervoort, J., and Jones, J.D.G. (2002a) *Plant J **29***, 783-796.

Rivas, S., Romeis, T., and Jones, J.D. (2002b) *Plant Cell **14***, 689-702.

Roberts, W.K., and Selitrennikoff, C.P. (1988) *J Gen Microbiol **134***, 169-176.

Rose, J.K.C., Ham, K.S., Darvill, A.G., and Albersheim, P. (2002) *Plant Cell **14***, 1329-1345.

Schoffelmeer, E.A.M., Klis, F.M., Sietsma, J.H., and Cornelissen, B.J.C. (1999) *Fungal Genet Biol **27***, 275-282.

Sela-Buurlage, M.B. (1996) *In vitro* sensitivity and tolerance of *Fusarium solani* towards chitinases and β-1,3-glucanases, Wageningen Agricultural University, Wageningen.

Sela-Buurlage, M.B., Ponstein, A.S., Bres-Vloemans, S.A., Melchers, L.S., van den Elzen, P.J.M., and Cornelissen, B.J.C. (1993) *Plant Physiol* ***101***, 857-863.

Selitrennikoff, C.P. (2001) *Appl Eviron Microbiol* ***67***, 2883-2894.

Shen, Z., and Jacobs-Lorena, M. (1999) *J Mol Evol* ***48***, 341-347.

Stintzi, A., Heitz, T., Prasad, V., Wiedemann-Merdinoglu, S., Kauffmann, S., Geoffroy, P., Legrand, M., and Fritig, B. (1993) *Biochimie* ***75***, 687-706.

Suarez, V., Staehelin, C., Arango, R., Holtorf, H., Hofsteenge, J., and Meins, F. (2001) *Plant Mol Biol* ***45***, 609-618.

Takken, F.L.W., and Joosten, M.H.A.J. (2000) *Eur J Plant Pathol* ***106***, 699-713.

Tang, X., Frederick, R.D., Zhou, J., Halterman, D.A., Jia, Y., and Martin, G.B. (1996) *Science* ***274***, 2060-2063.

Thomas, C.M., Jones, D.J., Parniske, M., Harrison, K., Balint-Kurti, P.J., Hatzixanthis, K., and Jones, J.D.G. (1997) *Plant Cell* ***9***, 2209-2224.

Tyler, B.M. (2002) *Annu Rev Phytopathol* ***220***, 137.

van den Hooven, H.W., Appelman, A.W.J., Zey, T., de Wit, P.J.G.M., and Vervoort, J. (1999) *Eur J Biochem* ***264***, 9-18.

van der Hoorn, R.A.L., Roth, R., and Joosten, M.H.A.J. (2001) *Plant Cell* ***13***, 273-285.

van Kan, J.A.L., van den Ackerveken, G.F.J.M., and de Wit, P.J.G.M. (1991) *Mol Plant-Microbe Interact* ***4***, 52-59.

Van Parijs, J., Broekaert, W.F., Goldstein, I.J., and Peumans, W.J. (1991) *Planta* ***183***, 258-264.

White, F.F., Yang, B., and Johnson, L.B. (2000) ***3***, 291-298.

Wilkins, T.A., and Raikhel, N.V. (1989) *Plant Cell* ***1***, 541-549.

Wright, C.S. (1980) *J Mol Biol* ***141***, 267-291.

Wu, J., and Watson, J.T. (1997) *Protein Sci* ***6***, 391-398.

Wubben, J.P. (1994) Subcellular localization of fungal and plant proteins in the *Cladosporium fulvum*-tomato interaction, Wageningen Agricultural university, Wageningen.

Wubben, J.P., Joosten, M.H.A.J., and de Wit, P.J.G.M. (1994) *Mol Plant-Microbe Interact* ***7***, 516-524.

Wulff, B.B.H., Thomas, C.M., Smoker, M., Grant, M., and Jones, J.D.G. (2001) *Plant Cell* ***13***, 255-272.

Yamamoto, T., Iketani, H., Ieki, H., Nishizawa, Y., Notsuka, K., Hibi, T., Hayashi, T., and Matsuta, N. (2000). *Plant Cell Rep* ***19***, 639–646.

2

Efficient $^{13}C/^{15}N$ double labeling of the avirulence protein AVR4 in a methanol-utilizing strain (Mut^+) of *Pichia pastoris*

Harrold A. van den Burg, Pierre J.G.M. de Wit, and Jacques Vervoort

(Published in Journal of Biomolecular NMR)

ABSTRACT

Cost effective $^{13}C/^{15}N$-isotope labeling of the avirulence protein AVR4 (10 kDa) of the fungal tomato pathogen *Cladosporium fulvum* was achieved with the methylotrophic yeast *Pichia pastoris* in a fermentor. The $^{13}C/^{15}N$-labeled AVR4 protein accumulated to 30 mg/L within 48 h in an initial fermentation volume of only 300 mL, while prolonged optimized overexpressions yielded 126 mg/L. These protein yields were 24 fold higher in a fermentor than in flask cultures. In order to achieve these protein expression levels, we used the methanol-utilizing strain (Mut^+) of *Pichia pastoris,* which has a high growth rate while growing on methanol as only carbon source. In contrast, the methanol-sensitive strain (Mut^S) could intrinsically yield comparable protein expression levels, but at dispense of additional carbon sources. Although both strains are generally used for heterologous protein expression, we show that the costs for ^{13}C-isotope labeling can be substantially reduced using the Mut^+ strain compared to the Mut^S strain, as no $^{13}C_3$-glycerol is required during the methanol-induction phase. Finally, nitrogen limitations were precluded for ^{15}N-labeling by an optimal supply of 10 g/L $(^{15}NH_4)_2SO_4$ every 24 h.

INTRODUCTION

For the detailed analysis of proteins, structural biologists often require advanced eukaryotic heterologous expression systems as many of the proteins under study require extensive posttranslational modifications for correct folding to the native state. The methylotrophic yeast *Pichia pastoris* has been refined into a host in which protein secretion and posttranslational modifications are easily accomplished and has, therefore, gained much attention as a heterologous expression system recently (Cregg et al., 1987; Tschopp et al., 1987; Cregg et al., 1993; Romanos, 1995; Sreekrishna et al., 1997).

For heteronuclear NMR experiments proteins need to be enriched with ^{15}N- or $^{13}C/^{15}N$-isotopes. To a large extent, *Escherichia coli* has been the host-of-choice for isotope labeling of proteins, as simple media for flask cultures are well-defined and rather inexpensive. However, the yeast *P. pastoris* has scarcely been used for $^{13}C/^{15}N$-isotope labeling of proteins as no cost-effective protocol for routine isotope labeling has been available so far. $^{13}C/^{15}N$-isotope labeling in *P. pastoris* has exclusively been carried out in

flask cultures for highly expressed proteins (Laroche et al., 1994; Abbate et al., 1999; Morgan et al., 1999). Even ^{15}N-labeling has almost exclusively been obtained in flask cultures (Denton et al., 1998; McAlister et al., 1998; Mine et al., 1999). Yet, the advantages of *P. pastoris* are best exploited in fermentation with its intrinsically high growth rate and high cell density by which protein yields increase 20-100 fold (Stratton et al., 1998; Wood and Komives, 1999).

Optimized fermentation protocols resulting in high cell densities for *P. pastoris* have been well documented (Stratton et al., 1998; Wood and Komives, 1999). Briefly, a fermentation consists of three growth phases i.e. a glycerol batch phase, a glycerol fed-batch phase, and a methanol-induction phase. In the first phase, the methanol inducible alcohol oxidase 1 (*AOX1)* promoter controlling the heterologous gene is completely repressed by an excess of glycerol. After this initial glycerol supply has been depleted, a minimal glycerol feed for a few hours ensures the derepression of the *AOX1* promoter and a smooth transition to the third phase in which methanol is added as inducer. In the first two phases the biomass accumulates rapidly, while in the last phase the heterologous protein is expressed at high levels.

The growth characteristics in the methanol-induction phase depend on the phenotype of the *P. pastoris* transformants. When the *AOX1* gene is intact (Mut$^+$ strain), the transformant will grow at wild-type rate on methanol. However, when the *AOX1* gene is disrupted (Mut^S strain), the methanol metabolism will rely on the less active *AOX2* gene (Clare et al., 1991; Digan et al., 1989). Consequently, the Mut^S strain has an intrinsic lower growth rate on methanol than the Mut$^+$ strain. The fermentation run with the Mut^S strain needs, therefore, to be extended for comparable protein expression levels. The growth rate of the Mut^S strain will, however, increase if a combined feed of glycerol and methanol is applied in the methanol-induction phase. In conclusion, comparable expression levels can be obtained with the two strains if the proper fermentation protocol is used (Brierley et al., 1990; Clare et al., 1991).

A fermentor offers the best options to reduce the costs for ^{13}C-labeling of proteins in *P. pastoris* as high expression levels combined with the tight control of biomass accumulation allow the volume of the fermentor to be small compared to flask cultures without concessions to the yield. We used the Mut$^+$ strain rather than the Mut^S strain for the fermentation for a few reasons. Firstly, the growth rate, which influences the protein expression levels, is significantly reduced for the Mut^S strain while growing on methanol alone. Secondly, addition of $^{13}C_3$-glycerol is relative expensive as $^{13}C_3$-glycerol is 3.5 times

more expensive than ^{13}C-methanol. Thirdly, the glycerol fed-batch phase could be shorter as the biomass continues to accumulate during the methanol-induction phase of the Mut^{+} strain. This glycerol fed-batch phase normally ensures the derepression of the AOX1 promoter and high biomass accumulation. The latter is of less importance as yields can be optimized for NMR purposes. And finally, when both grow on methanol alone, the total fermentation time is significantly shorter for the Mut^{+} strain than for the Mut^{S} strain.

Here we successfully labeled the avirulence protein AVR4 of the fungus *Cladosporium fulvum* with the ^{13}C-carbon and ^{15}N-nitrogen isotopes in an initial volume of only 300 mL. To achieve ^{15}N-labeling, we had to optimize the $(^{15}NH_4)_2SO_4$ supply. At the expense of only a minimal amount ^{13}C-carbon being consumed, the fermentation still yielded 30 mg/L of AVR4 protein. This general applicable protocol yielded enough AVR4 protein for at least two samples of 2 mM each for NMR measurements.

MATERIALS AND METHODS

Materials. Chemicals of the highest grade available were obtained from Merck. Yeast Nitrogen Base, and Maxisorp Nunc immuno plates were obtained via Life Technologies. Isotope enriched +98% ^{15}N-ammonium sulfate was from Cambridge Isotope Laboratories Inc. (Andover, MA); +99% ^{13}C-methanol and +99% ^{13}C-glycerol were acquired via Cortec (Paris, France).

Methods. Expression levels of AVR4 were visualized by tricine SDS-PAGE (Schägger and Von Jagow, 1987). Necrosis-inducing activity of AVR4 in samples was routinely tested on Moneymaker Cf4 using Moneymaker Cf0 tomato plants as control (Joosten et al., 1994). Heterologous AVR4 was identified on Western blots with a polyclonal antibody raised in Rabbit against the AVR4 protein purified from apoplastic fluid of a compatible interaction between race 5 of *C. fulvum* and tomato genotype Cf5 (Joosten et al., 1997). Final purity of heterologous AVR4 was determined on an analytical C_{18}-RP-HPLC column (25 x 4.6 mm, 300 Å pore, Delta Pak, Waters). AVR4 concentrations were determined in a direct ELISA assay with an anti AVR4 polyclonal antibody raised in Chicken (IgY). Samples were coated in 100 mM sodium acetate buffer (pH 4.0), overnight at 8^{o}C and wells were blocked with 0.5 % (w/v) Bovine Serum Albumine in 100 mM potassium phosphate buffer (pH 7.0), 150 mM sodium chloride at 37^{o}C for 2 h. The primary antibody was detected with alkaline phosphatase conjugated to a secondary Rabbit anti-Chicken IgG (Sigma). Total protein

contents were determined using Bradford reagent (Sigma), and referenced to Bovine Serum Albumine. Mass determinations were performed with a delayed extraction MALDI-TOF mass spectrometer (Perseptive Biosystems, Framingham MA). The MALDI-TOF samples were applied in α-cyano-4-hydroxycinnamic acid (Sigma) as matrix using the dried droplet method (Karas and Hillenkamp, 1988; Kussmann et al., 1997). Spectra were averages of 100-256 consecutive laser pulses. The instrument is generally operated at an acceleration voltage of 22 kV combined with delayed extraction. Spectra were calibrated using bovine Cytochrome C (12,230.9 m/z), Bovine Insulin (5,734.6 m/z) and Microperoxidase 8 (MP8, 1,506.5 m/z; Primus et al., 1998).

Growth media. The media BMGY, BMMY, MD, and YPD were as described in the Invitrogen manual (URL: http://www.invitrogen.com/manuals.html, version L). One liter of FM22 fermentation medium contained 42.9 g KH_2PO_4, 10.0 g $(NH_4)_2SO_4$, 1.0 g $CaSO_4 \cdot 2H_2O$, 14.3 g K_2SO_4, 11.7 g $MgSO_4 \cdot 7H_2O$, and 40 g glycerol (Laroche et al., 1994). The amount of $(NH_4)_2SO_4$ was increased compared to the original paper (see Results section for more details). The 42.9 g KH_2PO_4 and the 10.0 g $(NH_4)_2SO_4$ were both substituted by 26.7 mL 85% H_3PO_4 and 4.13 g KOH in the FM22 medium when NH_4OH was used for the pH control in the fermentor. Trace salt solution PMT4 consisted of 2.0 g $CuSO_4 \cdot 5H_2O$, 0.08 g NaI, 3.0 g $MnSO_4 \cdot H_2O$, 0.2 g $Na_2Mo_2O_4 \cdot 2H_2O$, 0.02 g H_3BO_3, 0.5 g $CaSO_4 \cdot 2H_2O$, 0.5 g $CoCl_2$, 7.0 g $ZnCl_2$, 22 g $FeSO_4 \cdot 7H_2O$, 0.2 g biotin, and 1 mL concentrated H_2SO_4 per liter. To one liter FM22 medium 2.5 mL of PMT4 is added prior to inoculation. To the methanol supply 4 mL PMT4/L was added.

Shake flask culture. P. pastoris GS115 His^+/mut^+ transformants transgenic for *Avr4* were selected for production of the AVR4 protein in BMMY as described in the Invitrogen manual. A mutation coding for a Ser-to-Ala amino acid substitution was introduced in the *Avr4* gene at the position of the potential N-glycosylation site. Growth of *P. pastoris* was performed in two liter baffled flasks containing 200 mL BMGY shaken at 250 rpm for 2 days at 30°C. After 24 h, medium was exchanged by centrifugation at 3,000*g* for 5 min and subsequently, the heterologous gene was induced by resuspending the cells in BMMY medium. Growth continued for another 96 h with additional pulses of 1% (v/v) methanol every 24 h. Supernatant was collected by centrifugation at 3,000*g* followed by 10,000*g* (both for 15 min), and was stored at -70°C till further purification.

High cell density fermentation of P. pastoris *(used for large-scale AVR4 production)* Fermentation was performed according to the procedure described by Stratton et al. (1998). Starter cultures of 50 mL were grown for 2 days at 30°C (OD_{600} >10), and were used to

inoculate a 2 L vessel containing 900 mL FM22 medium. Starter cultures originated from a fresh colony grown on a MD or YPD plate. After autoclaving the pH was adjusted to 4.9 with 5.0 M KOH or 25% (w/v) NH_4OH. Agitation was kept at 1200 rpm, and the airflow was maintained at 1-2 vvm to keep the dissolved oxygen (DO) levels at least above 30%. If needed, excessive foaming was prevented by adding a few droplets of Antifoam 289 (Sigma). Approximately 20 h after inoculation, glycerol depletion was observed by a sharp increase of the DO. At this stage the glycerol-feed was started at a rate of 10 $mL \cdot L^{-1} \cdot h^{-1}$ (glycerol fed-batch phase), and properly adjusted to maintain a steady DO reading (near 35%). After 4 h, the methanol feed was started at a rate of 3.4 $mL \cdot L^{-1} \cdot h^{-1}$. The methanol feed rate was step-wise increased to 6 $mL \cdot L^{-1} \cdot h^{-1}$ as soon as the culture had fully adapted to growth on methanol (4-6 h). To prevent methanol accumulation a DO spike was performed (a sharp increase in the DO levels will occur when the methanol supply is halted; Stratton et al., 1998).

Isotope labeling in the fermentor with ^{15}N-ammonium sulfate, ^{13}C-glycerol, and ^{13}C-methanol. All media contained isotope enriched substrate. A small culture of 300 mL FM22 medium was optimized for double labeling. The glycerol fed-batch phase lasted only for 30 min in the $^{13}C/^{15}N$-labeling experiment. During this phase, a 50% (w/v) $^{13}C_3$-glycerol supply was fed at a rate of 0.2 mL/min (a total of 3 g $^{13}C_3$-glycerol was added). The ^{13}C-methanol was diluted to 25% (w/v) to maintain a continuous methanol supply without toxic effects. The methanol-induction phase lasted 48 h (A total of 50 g of ^{13}C-methanol was added). Aliquots of 10 g $(^{15}NH_4)_2SO_4$ /L were supplied every 24 h. After purification $^{13}C/^{15}N$-isotope enrichment of AVR4 was determined by MALDI-TOF mass spectrometry and NMR spectroscopy.

Purification of AVR4 protein. Cell free culture filtrate containing the AVR4 protein was brought to 45% $(NH_4)_2SO_4$ saturation and was stirred for 30 min at 4^{o}C followed by centrifugation at 13.000*g* for 20 min The supernatant was applied at a rate of 5.0 mL/min to an equilibrated Phenyl Sepharose (high sub) Fast Flow column (26x200 mm, Amersham-Pharmacia). Prior to use the column had been equilibrated with 5 column volumes buffer A (10 mM Tris-HCl, pH 8.6, and 1 mM EDTA) and 2 column volumes buffer B (10 mM Tris-HCl, pH 8.6, 1 mM EDTA, and 45% saturated $(NH_4)_2SO_4$). The column was extensively washed with buffer B before eluting the AVR4 protein with a linear gradient of 300 mL going from buffer B to buffer A. Fractions were checked for AVR4 content by SDS-PAGE. The AVR4 containing fractions were pooled and were exhaustively dialyzed against buffer A. The desalted fractions were loaded at a flow rate of 2.0 mL/min on a Q-Sepharose Fast Flow

column (16x240 mm, Amersham-Pharmacia). Prior to use the Q-Sepharose column had been equilibrated with buffer C (1.0 M NaCl, 10 mM Tris-HCl, pH 8.6, and 1 mM EDTA) followed by 5 volumes of buffer A. The flow through, which contained the AVR4 protein, was acidified with TFA and injected on a C4 RP-HPLC column (25x200 mm, 300 Å, Waters). The AVR4 protein eluted at 30% Acetonitril, 0.1% TFA. The collected AVR4 protein fraction was lyophilized prior to storage.

NMR spectroscopy. The NMR samples in a Shigemi tube (Tokyo, Japan) contained 2.3 mM AVR4 protein dissolved in 90% H_2O/10% D_2O (v/v), 20 mM Acetate-d_4, and 50 mM NaCl at pH 4 in a total volume of 250 µl. NMR experiments were performed on a Bruker Avance 600Mhz spectrometer equipped with a triple-resonance, pulsed-field gradient probe operating at a temperature of 25°C. Residual TFA was removed from the sample by extensive dialysis. ^{1}H chemical shifts were referenced to sodium 2,2-dimethyl-2-silapentane-5-sulfonate (DSS), ^{15}N and ^{13}C chemical shifts were indirectly referenced (Wishart et al., 1995; Markley et al., 1998). Heteronuclear sensitivity enhanced ^{1}H-^{15}N HSQC spectra with pulsed-field gradients and WATERGATE (Kay et al., 1992; Piotto et al., 1992; Stonehouse et al., 1995), as well as HNCO spectra (Peelen et al., 1996) were recorded. The spectral widths of the indirect ^{15}N and ^{13}CO dimensions were both 2000 Hz; the spectral width of ^{1}H dimension was 9259.2 Hz. HNCO and HSQC data sets contained 128 (t_1) x 1024 (t_2) and 192 (t_1) x 1024 (t_2) complex data points, respectively. NMR data sets were processed with Felix 98.0 software.

RESULTS

We adapted the fermentation procedure of the yeast *Pichia pastoris* to grow it on ^{13}C/^{15}N-isotope enriched medium for labeling of the AVR4 protein, as fermentors offer the highest yield due to an optimal growth rate. So far, ^{15}N-labeling in *P. pastoris* has largely been restricted to shake flask cultures and for a large number of overexpressed proteins ^{13}C-labeling is prohibitively expensive in shake flask cultures due to the protein yields. Wood and Komives (1999) showed that ^{15}N-labeling in a fermentor is more cost effective than in shake flask cultures but that ^{13}C-labeling in a fermentor using a Mut^S strain is expensive, mainly due to the large minimal volume needed in their fermentation vessel (see also below). Here we show that it is economically feasible to perform a double ^{13}C/^{15}N-labeling of proteins in a fermentor using the Mut^+ strain of *P. pastoris*.

Ammonium Sulfate as ^{15}N-nitrogen source and pH control with Potassium Hydroxide

^{15}N-isotope incorporation was achieved by replacing NH_4OH by $(^{15}NH_4)_2SO_4$ as nitrogen source. The constant acidification of the medium is normally compensated with NH_4OH. Instead of NH_4OH we used KOH to control the pH in the case of ^{15}N-labeling. For *P. pastoris* the supplied amount of $(NH_4)_2SO_4$ had been shown to influence protein expression levels substantially (Wood and Komives, 1999), while nitrogen limitations have been reported to increase protease activity (McAlister et al., 1998). Therefore, we ascertained that $(NH_4)_2SO_4$ concentrations would be optimal. The effects of different $(NH_4)_2SO_4$ supplies on AVR4 secretion and Cell Dry Weight (CDW) were examined (Figure 1).

In addition, the combination of KOH and $(NH_4)_2SO_4$ can cause K_2SO_4 to precipitate as salt concentrations steadily increase by the KOH supplies needed to compensate for the acidification, which eventually leads to an arrested growth. As a way to circumvent the effects of increased salt concentrations, a medium exchange was recommended prior to the methanol-induction phase for the Mut^S strain (Wood and Komives, 1999). In our approach no medium exchange was applied. The effects of increased salt concentrations were examined over the time course of the experiment for the different $(NH_4)_2SO_4$ supply regimes. For comparison the general set-up of the fermentation contained a glycerol batch phase of 20 h over which the CDW increased to ~24 g/L, which is in agreement with the expected

Figure 1. Secretion of AVR4 (**A** and **D**), total secreted protein (**B** and **E**) and biomass (**C** and **F**), as determined by ELISA, Bradford assay, and CDW, respectively, are shown for the methanol induction phase. The amount of $(NH_4)_2SO_4$ supplied during the fermentations was optimized, as $(NH_4)_2SO_4$ limitations strongly affect the protein secretion levels. Different aliquots, i.e. 5 g (◊), 10 g (□) en 20 g $(NH_4)_2SO_4$ (Δ), were added every 24 h after the start of the fermentation. The fermentation proceeded for at least 96 h to observe the effect of increased salt concentration on the growth of the yeast. The fermentations using $(NH_4)_2SO_4$ are compared to the optimal fermentation using NH_4OH (○). The ^{13}C/^{15}N-labeling was performed in an initial volume of only 300 mL medium with 10 g of $(NH_4)_2SO_4$ supplied every 24 h (■; **D**-**F**) and is compared to the original 1 liter fermentation (□; **A**-**F**) The glycerol fed-batch phase (second phase) was only 30 min in the ^{13}C/^{15}N labeling experiment, which explains the decreased CDW at the start of the induction. The third phase for the ^{13}C/^{15}N labeling experiment only lasted for 48 h, during which 30 mg/L AVR4 had accumulated over this relatively short period. ⟶

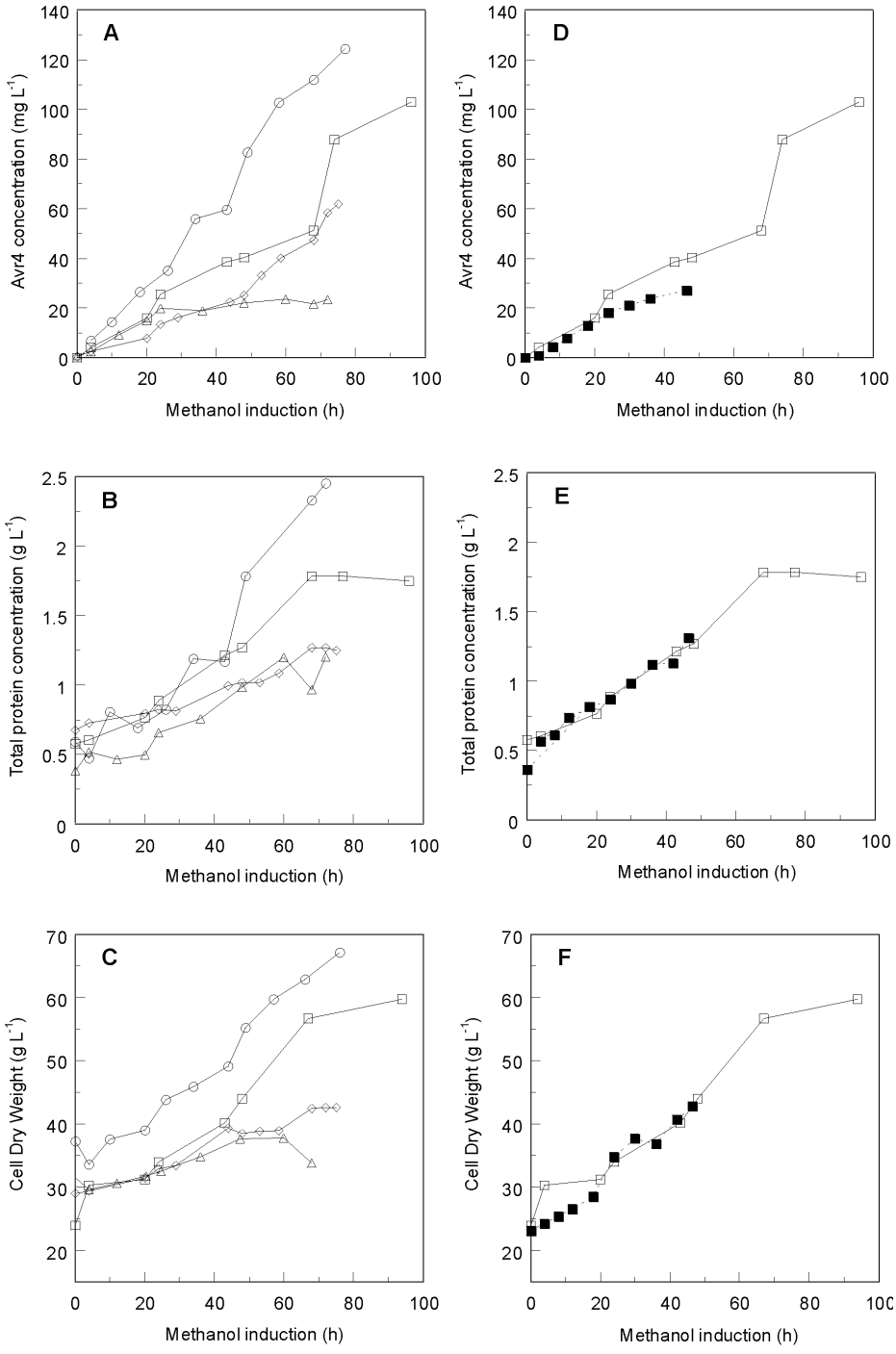
A
Avr4 concentration (mg L-1)
Methanol induction (h)
D
Avr4 concentration (mg L-1)
Methanol induction (h)
B
Total protein concentration (g L-1)
Methanol induction (h)
E
Total protein concentration (g L-1)
Methanol induction (h)
C
Cell Dry Weight (g L-1)
Methanol induction (h)
F
Cell Dry Weight (g L-1)
Methanol induction (h)

growth yield on glycerol. During the glycerol fed-batch phase DO levels were kept steady at 35% for 4 h and CDW increased to ~34 g/L.

We achieved expression levels with $(NH_4)_2SO_4$ that reached the levels obtained with NH_4OH if aliquots of 10 g $(NH_4)_2SO_4$ per liter medium were applied every 24 h (resulting in more than 100 mg AVR4 protein per liter). These levels were 83% of the levels obtained in a NH_4OH controlled fermentor (Figure 1A), which may be classified as an intermediate yield for *P. pastoris* when compared to the reported yields by Cregg et al. (1993). Under these conditions AVR4 concentrations became 24 times higher in a fermentor than in flask cultures, which is in good agreement with other reports (Cregg et al., 1993). After 24 h, the initial supply of 10 g/L $(NH_4)_2SO_4$ had been completely consumed as noticed by the fact that the yeast had stopped acidifying the medium. After adding 10 g/L $(NH_4)_2SO_4$ acidification restored again. DO levels were not seriously effected by this addition. This cycle of $(NH_4)_2SO_4$ supplies was repeated over the next 48 h. As CDW and the total protein content evolved comparably in both 10 g/L $(NH_4)_2SO_4$ and in the NH_4OH controlled fermentations, we concluded that the growth was never under nitrogen starvation conditions if 10 g/L $(NH_4)_2SO_4$ was supplied every 24 h (Figure 1B and 1C).

Nitrogen limitations became evident as growth retarded as soon as less than 10 g/L $(NH_4)_2SO_4$ was applied every 24 h (diamond; Figure 1C). Additionally, with a supply of 5.0 g/L the yeast stopped acidifying within 12 h after the start of the glycerol batch phase. With the addition of 5.0 g/L $(NH_4)_2SO_4$ after 24 h the DO levels dropped to such an extent that the methanol supply was not started until the DO levels had restored again. Proteolytic degradation of AVR4 was not observed under these conditions on SDS-PAGE. On the other hand, higher concentrations of $(NH_4)_2SO_4$ inhibited protein secretion (triangle, Figure 1A). Growth lagged seriously when 20 g/L $(NH_4)_2SO_4$ was applied every 24 h (Figure 1C). Also K_2SO_4 had precipitated at the end of the methanol-induction phase. However, only half the amount of nitrogen is supplied at the optimum of 10 g/L of $(NH_4)_2SO_4$ per 24 h compared to the NH_4OH controlled fermentor.

Based on the results obtained with the supply of 10 g/L $(NH_4)_2SO_4$ every 24 h, we concluded that no medium exchange was needed. The absence of salt effects on the growth could be explained by the fact that the first two phases only lasted for 24 h. In the approach with a medium exchange the first two phases lasted for 60 h prior to the medium exchange (Wood an Komives, 1999). Therefore, elevated salt concentrations could only affect growth at the end of the methanol-induction phase in our case. Indeed, 72 h after the start of the methanol-induction phase growth lagged in our approach and other proteins

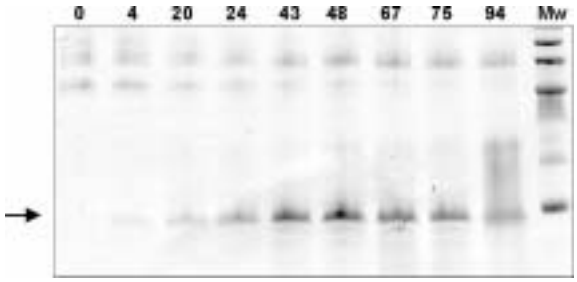

Figure 2. *S*ecretion of the AVR4 protein in the medium is shown on Coomassie-brilliant-blue stained tricine SDS-PAGE gel. The numbers above each lane correspond to consecutive time points in the methanol induction phase. Samples were taken from the fermentation experiment in which 10 g $(NH_4)_2SO_4$ per liter was added every 24 h (Figure 1;□). The AVR4 protein indicated by an arrow is the most abundant protein. Few other proteins are secreted. Molecular weight marker was loaded in the most right lane. 20 μL culture medium was loaded in each lane.

showed up in the medium as seen by SDS-PAGE (Figure 2*).* The acidification did not resume after the third $(NH_4)_2SO_4$ pulse at 72 h. The fermentation was stopped at 96 h (Figure 1).

$^{13}C/^{15}N$ labeling of the AVR4 protein

The optimized $(NH_4)_2SO_4$ conditions guaranteed AVR4 levels to reach 40 mg/L within 48 h of the methanol-induction phase, which was sufficient for cost effective ^{13}C-labeling. We, therefore, decided to reduce the fermentation volume to save on costs for ^{13}C-labeling. A volume of 300 mL would provide enough $^{13}C/^{15}N$-labeled AVR4. A yield of 30 mg/L of AVR4 was obtained in this small vessel (Figure 1D). CDW reached 43.5 g/L, which is slightly less than in the larger vessel (Figure 1F). This small decrease in CDW was partially caused by a shorter glycerol fed-batch phase from 4 h to only 30 min, which was sufficient to derepress the *AOX1* promoter. The total amount $^{13}C_3$-glycerol used was hereby reduced with 50%. Only 15 g $^{13}C_3$-glycerol and 50 g ^{13}C-methanol were needed (Table 1). Additionally, we diluted the methanol supply to circumvent toxicity. At the end of the fermentation the total fermentation volume had increased by 200 mL, which prevented serious salt accumulation, but also decreased CDW.

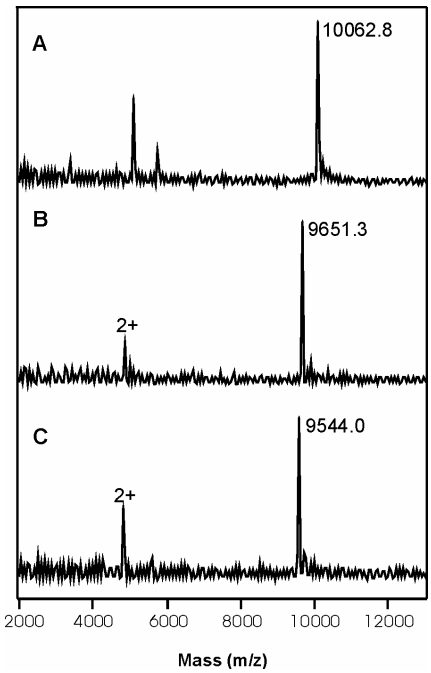

Figure 3. Mass determination of the (**A**) $^{13}C/^{15}N$-, (**B**) ^{15}N-labeled and (**C**) unlabeled AVR4 protein as determined by MALDI-TOF mass spectrometry. The theoretical mass of AVR4 with 4 disulfide bonds is 9544.1 m/z. The mature AVR4 protein contains 110 nitrogen and 421 carbons atoms. The labeling efficiency is +98% for both ^{15}N- and $^{13}C/^{15}N$-labeled AVR4. Relative intensities are shown on the *y*-axis. The masses of the singly charged ions are indicated by their mass-over-charge (m/z) values. Masses of doubly charged ions are indicated by $[M+2H]^{2+}$.

The AVR4 protein was labeled with an efficiency of +98% in ^{13}C- and^{15}N-isotopes as shown by mass spectrometry (Figure 3). All eight Cys residues were shown to be involved in disulfide bonds and no glycosylation had occurred as expected. The heterologous AVR4 protein behaved similar to the native AVR4 produced by *C. fulvum.* A hypersensitive response was specifically induced on Moneymaker Cf4 tomato plants upon injection of the heterologous AVR4 protein into the leaves and an antibody raised against native AVR4 recognized the heterologous AVR4 protein (results not shown). Structural integrity was accessed by a ^{1}H-^{15}N HSQC spectrum on both ^{15}N- and $^{13}C/^{15}N$-labeled AVR4 samples (Figure 4A and 4B). Both line width and chemical shift dispersion were consistent with a

substantially folded protein. The sample has been highly stable for months now and triple resonance experiments like a HNCO experiment (Figure 4C) were performed. Detailed structural analysis and dynamic studies are in progress and shall be reported elsewhere.

DISCUSSION

Overexpression and efficient $^{13}C/^{15}N$-labeling of any protein is essential in order to study its structure-function relationship by NMR. However, overexpression turned out not to be easy for the avirulence protein AVR4 of *Cladosporium fulvum* as *Escherichia coli*, the fungus *Aspergillus niger*, and the fungus *C. fulvum* itself failed to overexpress AVR4 in spite of serious attempts. To overexpress AVR4, we, therefore, employed the methylotrophic yeast *Pichia pastoris* as it handles disulfide bonds very well, it does not hyperglycosylate heterologous proteins which frequently occurs with the yeast *Saccharomyces cerevisiae* (Montesino et al., 1998), and secretion required for proper folding of the AVR4 protein is easily achieved at high protein yields. Using *P. pastoris* we achieved yields of 126 mg/L of AVR4 protein in a fermentor, while in batch flask culture yields remained below 5 mg/L. These expression levels are not excessively high as more than 10 g heterologous protein per liter has been reported for *P. pastoris* fermentations (Cregg et al, 1993; Laroche et al, 1993). In spite of this limited expression level of AVR4 we succeeded in $^{13}C/^{15}N$-labeling of AVR4 at relatively low costs. We expect that this report will advertise a wider use of *P. pastoris* for overexpression of $^{13}C/^{15}N$-labeled proteins.

From our studies we conclude that three factors are important for efficient $^{13}C/^{15}N$ labeling in *P. pastoris:* (1) the use of a small fermentor vessel, (2) the length of the glycerol fed-batch, and most importantly (3) the use of the Mut^+ strain in combination with the first two factors.

Choice of the strain: Mut^+ or Mut^S . The choice of the strain was determined by the optimal feed rates, glycerol consumption in the glycerol fed-batch phase and methanol-induction phase (i.e. the second and third phase), and the prices of the carbon sources. The growth rate in the methanol-induction phase positively influences the protein secretion levels (d'Anjou and Daugulis, 1997). On methanol the Mut^+ strain grows at a rate of 0.14 h^{-1} , while the Mut^S strain only grows at a rate of 0.035 h^{-1} (Brierley et al., 1990). Therefore, the methanol-induction phase will take longer for the Mut^S strain (175 h) than for the Mut^+ strain (45 h) to reach the same expression levels. And although the methanol feed rate of the Mut^S

strain will be half the rate of the Mut^+ strain, more ^{13}C-methanol will still be needed for the Mut^S strain. The growth rate of the Mut^S strain can be increased to 0.14 h^{-1} by a combined feed of glycerol and methanol with an optimal glycerol feed rate of 2.0 $g \cdot L^{-1}$ h^{-1} and a glycerol:methanol ratio of 2:1 (v/v) (Egli et al., 1986; Brierley et al., 1990). The current market price of $^{13}C_3$-glycerol, which is 3.5 times more expensive than ^{13}C-methanol (per gram), lets us concluded that ^{13}C-incorperation is two to four times more expensive with the Mut^S strain than with the Mut^+ strain. In table 1, we compare our fermentation protocol using the Mut^+ strain with previous reports in which also $(NH_4)_2SO_4$ is applied for ^{15}N-labeling in a fermentor. As can be seen from table 1 our efforts result in a cost reduction for ^{13}C-labeling. ^{13}C-Labeling using the Mut^S strain would be at least two times more expensive than with the Mut^+ strain (per volume). In particular this difference can be ascribed to a more efficient biomass accumulation with Mut^+ strain. Another major factor in the cost reduction is the decreased fermentation volume. Hitherto, ^{13}C-labeling had been restricted to flasks cultures although the yields are limited in flasks. The lower limit of the fermentation volume (~1 L up to now) has largely restricted its use for ^{13}C-labeling. It is emphasized that the efficiency of the fermentations presented in table 1 can not be estimated by their respective protein yields, as those have been largely influenced by the heterologous gene itself and the copy number of the heterologous gene (Clare et al, 1991; Cregg et al., 1993). However, carbon and nitrogen consumption may be compared for the different protocols as the total consumption is independent for the method by which the strain was obtained i.e. site of chromosomal integration of the gene (i.e. *AOX1* or *HIS4* loci) or type of integration (insertion or transplacement) (Clare et al., 1991).

Length of the glycerol fed-batch phase (second phase). By shortening the glycerol fed-batch phase from 4 h to only 30 min, costs for ^{13}C-labeling were substantially reduced. In most cases this short period in combination with a methanol-induction phase of 48 h will be sufficient as the heterologous protein will have accumulated to the desired levels. If necessary, the methanol-induction phase can be extended for another 24 h without negative effects (during this period AVR4 levels increased to almost 50 mg/L). On the other hand, the role of this second phase is considered twofold, (1) the *AOX1* promoter is derepressed and (2) the biomass is substantially increased over 4 h. Wood and Komives (1999) suggested even an extension of the glycerol fed-batch phase from 4 to more than 24 h for the Mut^S strain which guaranteed cell densities at the start of the induction which reached the level normally obtained at the end of fermentation, but this extension required 100 g/L of glycerol which would raise costs for ^{13}C-labeling excessively (Table 1).

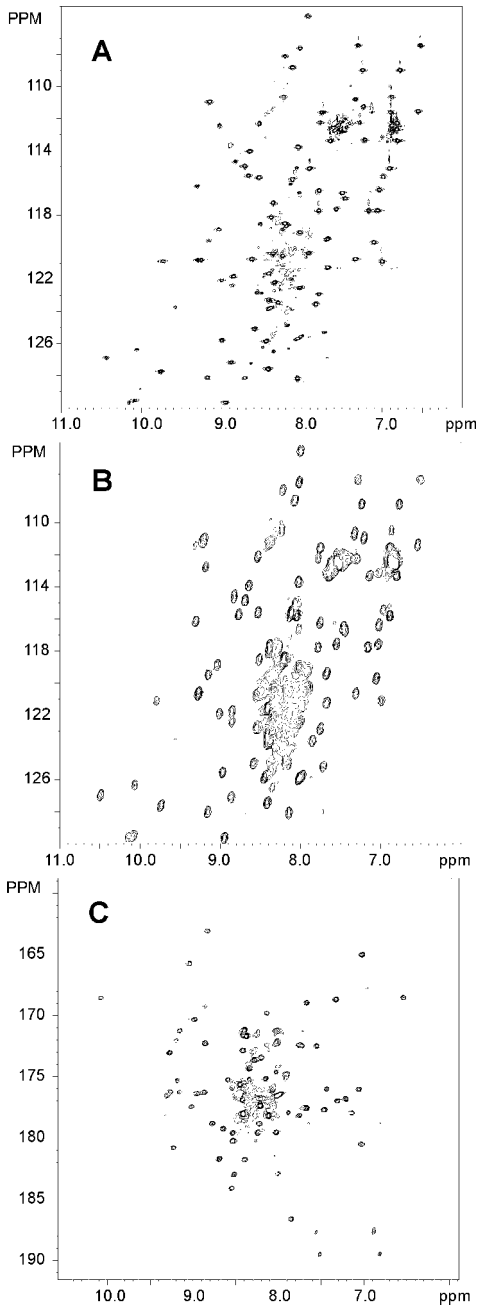

Figure 4. NMR spectra of labeled AVR4: (**A**) ^{1}H-^{15}N HSQC of the ^{15}N-labeled AVR4 sample, (**B**) a ^{13}C-decoupled ^{1}H-^{15}N HSQC of the $^{13}C/^{15}N$ labeled AVR4 sample, and (**C**) a H(N)CO experiment of $^{13}C/^{15}N$ labeled AVR4. Conditions were as described in materials and methods.

Table 1. Comparison of the costs of ^{13}C-labeling for the different fermentation protocols in which $(^{15}NH_4)_2SO_4$ was used. Each protocol was described in relation to ^{13}C-labeling and its efficiency towards the utilization of its carbon sources. ^{13}C-Labeling was exclusively performed in this present study.

	Strain	Volume (L)	Glycerol[a] (g)	Methanol[a] (g)	$(NH_4)_2SO_4$[b] (g L^{-1})	Yield[c] (mg L^{-1})	Cost[d]	Cost per Volume[e]
This study $^{13}C/^{15}N$)[1]	Mut^+	0.3	15	50	30	29	1	1
Loewen et al.[2]	Mut^+	1.0	58.7	309.6	20	30	5.0	1.5
	Mut^S	1.0	158	nd[f]	20	37	>7[g]	>2.1[g]
Wood & Komives[3]	Mut^S	0.8	143	200	57.5	90	6.8	2.6

SHORT DESCRIPTION OF THE FERMENTATION PROTOCOLS**:**

(1) Double labeling method as described in this paper.

(2) Mut^+: Prolonged methanol induction phase due to nitrogen depletion (see text).

Mut^S: A combined feed of glycerol and methanol during the induction phase (Method described as mixed fed-batch for Mut^S by Brierley et al. (1990)).

(3) Prolonged glycerol fed-batch phase ensuring a rapid increase in cell mass before induction started. The medium was exchanged prior to the induction phase.

(**a**)Total consumption; (**b**) In (**1**) and (**3**) aliquots of $(NH_4)_2SO_4$ were applied, while for (**2**) one batch addition occurred at the start of the experiment; (**c**) Total yield of the overexpressed protein per 1 L medium; (**d**) Cost for ^{13}C-labeling indexed to our labeling (**1**) as described in this present study. Our costs were slightly less than $10,000. Used prices for ^{13}C-glycerol and ^{13}C-methanol were $350 and $100 per gram, respectively. (**e**) Cost per volume calculated like **d**. (**f**) Not determined. (**g**) Estimation based on a methanol rate starting at $1 \cdot g \cdot L^{-1} \cdot h^{-1}$ and increased to $2.6 \cdot g \cdot L^{-1} \cdot h^{-1}$ at the end of the fermentation over approximately 100 hours.

The optimal $(NH_4)_2SO_4$ supply. We determined an optimal $(NH_4)_2SO_4$ supply for the Mut^+ strain of 10 gram per liter every 24 h. The nitrogen limitations affected the protein yields clearly as the yield of AVR4 improved with 30% as the $(NH_4)_2SO_4$ supply increased from 5 g to 10 g/L every 24 h. This increase is less pronounced than reported by Wood and Komives (1999). If one corrects for the different $(NH_4)_2SO_4$ regimes the total amount consumed is quite comparable over time for both regimes. In the regime of Wood and Komives, the discontinuous $(NH_4)_2SO_4$ supplies could have caused a more pronounced temporary nitrogen starvation when too little $(NH_4)_2SO_4$ was applied. Considering this negative effect on the protein yields, we conclude that the addition of $(NH_4)_2SO_4$ every 24 h is preferred.

Besides an arrested acidification, a steady increase of the DO levels in time also indicates growth retardation. The adaptation to the growth on methanol takes ~4 h after which the DO levels are kept constant by a slight increase of the methanol feed rate. Even at the end of the methanol-induction phase, DO levels had never become higher than 60%. Loewen *et al.* (1997) described that the DO levels had reached almost 100% at the end of their fermentation (Table 1). With a rate of 10 g/L of $(NH_4)_2SO_4$ being consumed every 24 h as here described, the total supply of 20 g/L $(NH_4)_2SO_4$ would have been consumed within 48 h with its consequences. The nitrogen limitation in this case was not only reflected in the increased DO readings, but also the increase of CDW lagged in the second half of the fermentation run. Again, these data strongly suggest that balancing the nitrogen supply is crucial for ^{15}N-labeling in fermentation.

Although a few alternatives for ^{13}C-labeling could be appealing, most probably they will not be as successful as the protocol described here. $^{13}C_6$-Glucose as replacement of $^{13}C_3$-glycerol looks attractive, as the growth rate remains the same (Brierley et al., 1990). However, glucose is a strong repressor of the *AOX1* promoter, and the glycerol fed-batch phase would, therefore, take longer than with $^{13}C_3$-glycerol. The current market prices are virtually identical for $^{13}C_6$-glucose and $^{13}C_3$-glycerol, although in the past $^{13}C_3$-glycerol was relatively more expensive than $^{13}C_6$-glucose. Therefore, the use of $^{13}C_6$-glucose is less cost effective for ^{13}C-labeling of proteins than the use of $^{13}C_3$-glycerol.

Although the replacement of glycerol for methanol seems to separate two different phases, namely biomass accumulation and induction of the heterologous gene, Wood and Komives (1999) showed that 70% of the carbon incorporated in the heterologous protein comes from the cell mass which was present at the start of the methanol-induction phase,

which excludes the isotopic enrichment of only one of the two carbon sources. Enriched yeast extract media (which are often used with *E. coli)* used in batch flask cultures are not expected to improve protein yields substantially as growth of *P. pastoris* is limited by the aeration in the flasks. Moreover, protein purification is found to be easy form the salt-based medium, as the heterologous protein is the most predominantly secreted protein (Penheiter et al., 1998) (Figure 2).

In conclusion, cost-effective $^{13}C/^{15}N$-labeling for triple resonance experiments with our protocol may be useful for the production of many other proteins with difficult folding pathways. Interestingly, deuterium labeling was achieved using *P. pastoris* without deuterated carbon sources, but solely with D_2O (Massou et al., 1999; Morgan et al., 2000). Deuterium labeling could also be performed with our approach using the Mut^+ strain. Thus, we have shown that, *P. pastoris* is an attractive alternative whenever *E. coli* is unsuitable.

REFERENCES

Brierley, R.A., Bussineau, C., Kosson, R., Melton, A. and Siegel, R.S. (1990), *Ann. New York Acad. Sci.,* **589***,* 350-362.

Clare, J.J., Rayment, F.B., Ballantine, S.P., Sreekrishna, K. and Romanos, M.A. (1991), *Bio/Technology,* **9***,* 455-460.

Cregg, J.M., Tschopp, J.F., Stillman, C., Siegel, R., Akong, M., Craig, W.S., Buckholz, R.G., Madden, K.R., Kellaris, P.A., Davis, G.R., Smiley, B.L., Cruze, J., Torregrossa, R., Velicelebi, G., Thill, G.P. (1987), *Bio/Technology,* **5***,* 479-485.

Cregg, J.M., Vedvick, T.S. and Raschke, W.C. (1993), *Bio/Technology,* **11***,* 905-910.

d'Anjou, M.C. and Daugulis, A.J. (1997), *Biotechnol. Techniq.,* **11***,* 865-868.

Denton, H., Smith, M., Husi, H., Uhrin, D., Barlow, P.N., Batt, C.A. and Sawyer, L. (1998), *Protein Expr. Purif.,* **14***,* 97-103.

Digan, M.E., Lair, S.V., Brierley, R.A., Siegel, R.S., Williams, M.E., Ellis, S.B., Kellaris, P.A., Provow, S.A., Craig, W.S., Veliçelebi, G., Harpold, M.M. and Thill, G.P. (1989), *Bio/Technology*, **7** 160-164.

Egli, T., Bosshard, C. and Hamer, G. (1986), *Biotechnol. Bioeng.,* **18***,* 1735-1741.

Joosten, M.H.A.J., Cozijnsen, T.J. and De Wit, P.J.G.M. (1994), *Nature,* **367***,* 384-386.

Joosten, M.H.A.J., Vogelsang, R., Cozijnsen, T.J., Verberne, M.C. and De Wit, P.J.G.M. (1997), *Plant Cell,* **9**, 367-379.

Karas, M. and Hillenkamp, F. (1988), *Anal. Chem.,* **60**, 2299-301.

Kay, L.E., Keifer, P. and Saarinen, T. (1992), *J. Am. Chem. Soc.,* **114**, 10663-10665.

Kussmann, M., Nordhoff, E., Rahbek-Nielsen, H., Haebel, S., Rossel-Larsen, M., Jakobsen,

L., Gobom, J., Mirgorodskaya, E., Kroll-Kristensen, A., Palm, L. and Roepstorff, P. (1997), *J. Mass Spec.,* **32**, 593-601.

Laroche, Y., Storme, V., De Meutter, J., Messens, J. and Lauwereys, M. (1994), *Bio/Technology,* **12**, 1119-1124.

Loewen, M.C., Liu, X., Davies, P.L. and Daugulis, A.J. (1997), *Appl. Microbiol. Biotech.,* **48**, 480-486.

Markley, J.L., Bax, A., Arata, Y., Hilbers, C.W., Kaptein, R., Sykes, B.D., Wright, P.E. and Wuethrich, K. (1998), *Eur. J. Biochem.,* **256**, 1-15.

Massou, S., Puech, V., Talmont, F., Demange, P., Lindley, N.D., Tropis, M. and Milon, A. (1999), *J. Biomol. NMR,* **14**, 231-239.

McAlister, M.S.B., Davis, B., Pfuhl, M. and Driscoll, P.C. (1998), *Protein Eng.,* **11**, 847-853.

Mine, S., Ueda, T., Hashimoto, Y., Tanaka, Y., Imoto, T. (1999), *FEBS Lett.,* **448**, 33-37.

Montesino, R., Garcia, R., Quintero, O. and Cremata, J.A. (1998), *Protein Exp. Purif.,* **14**, 197-207.

Morgan, W.D., Birdsall, B., Frenkiel, T.A., Gradwell, M.G., Burghaus, P.A., Syed, S.E.H., Uthaipibull, C., Holder, A.A. and Feeney, J. (1999), *J. Mol. Biol.,* **289**, 113-122.

Morgan, W.D., Kragt, A., and Feeney, J. (2000), *J. Biol. NMR,* **17**, 337-347.

Peelen, S., Wijmenga, S.S., Erbel, P.J.A., Robson, R.L., Eady, R.R. and Vervoort, J. (1996), *J. Biomol. NMR,* **7**, 315-330.

Penheiter, A.R., Klucas, R.V. and Sarath, G. (1998), *Protein Exp. Purif.*, **14**, 125-130.

Piotto, M., Saudek, V. and Sklenar, V. (1992), *J. Biomol NMR,* **2**, 661-665.

Primus, J.L., Boersma, M.G., Mandon, D., Boeren, S., Veeger, C., Weiss, R, Rietjens, I.M. (1999), *J. Biol. Inorg. Chem.*; **4**, 274-83

Romanos, M. (1995), *Curr. Opin. Biotechnol.,* **6**, 527-533.

Schägger, H. and Von Jagow, G. (1987), *Anal. Biochem.,* **166**, 368-379.

Sreekrishna, K., Brankamp, R.G., Kropp, K.E., Blankenship, D.T., Tsay, J.T., Smith, P.L., Wierschke, J.D., Subramaniam, A. and Birkenberger, L.A. (1997), *Gene,* **190**, 55-62.

Stonehouse, J., Clowes, R.T., Shaw, G.L., Keller, J. and Laue, E.D. (1995), *J. Biomol. NMR,* **5**, 226-232.

Stratton, J., Chiruvolu, V. and Meagher, M. (1998), In *Pichia Protocols* (Eds., Higgins, D. R. and Cregg, J. M.), Humana Press, Totowa, New Jersey, pp. 107-120.

Tschopp, J.J., Sverlow, G., Kosson, R., Craig, W. and Grinna, L. (1987), *Bio/Technology*, **5**, 1305-1308.

Wishart, D.S., Bigam, C.G., Yao, J., Abildgaard, F., Dyson, H.J., Oldfield, E., Markley, J.L. and Sykes, B.D. (1995), *J. Biomol. NMR*, **6**, 135-140.

Wood, M.J. and Komives, E.A. (1999), *J. Biomol. NMR*, **13**, 149-159.

3

Disulfide bond structure of the AVR9 elicitor of the fungal tomato pathogen *Cladosporium fulvum*; evidence for a cystine knot

Henno W. van den Hooven, Harrold A. van den Burg, Paul Vossen, Sjef Boeren, Pierre J. G. M. de Wit, Jacques Vervoort

(Published in Biochemistry)

ABSTRACT

Disease resistance in plants is commonly activated by the product of an avirulence (*Avr*) gene of a pathogen after interaction with the product of a matching resistance (*R*) gene in the host. In susceptible plants *Avr* products might function as virulence or pathogenicity factors. The AVR9 elicitor from the fungus *Cladosporium fulvum* induces defense responses in tomato plants carrying the *Cf-9* resistance gene. This 28-residue β-sheet AVR9 peptide contains 3 disulfide bridges, which were identified in this study as Cys2-Cys16, Cys6-Cys19, and Cys12-Cys26. For this purpose, AVR9 was partially reduced and the thiol groups of newly formed cysteines were modified to prevent reactions with disulfides. After HPLC purification the partially reduced peptides were sequenced to determine the positions of the modified cysteines, originating from the reduced disulfide bridge(s). All steps involving molecules with free thiol groups were performed at low pH to suppress disulfide scrambling. For that reason cysteine modification by *N*-ethylmaleimide was preferred over iodoacetamide. Upon (partial) reduction of native AVR9 the Cys2-Cys16 bridge opened selectively. The resulting molecule was further reduced to two one-bridge intermediates, which were subsequently completely reduced. The (partially) reduced cysteine-modified AVR9 species showed little or no necrosis-inducing activity, demonstrating the importance of the disulfide bridges for biological activity. Based on peptide length and cysteine spacing AVR9 was previously suggested to be a cystine-knotted peptide. Now, we have proven that the bridging pattern of AVR9 is indeed identical to that of cystine-knotted peptides. Moreover, NMR data obtained for AVR9 show that it is structurally very much related to the cystine-knotted carboxypeptidase inhibitor (CPI). However, AVR9 does not show any carboxypeptidase inhibiting activity, indicating that the cystine-knot fold is a commonly occurring motif with varying biological functions.

INTRODUCTION

Surfaces and intercellular spaces of plants are continuously threatened by potential pathogens. However, only few pathogens do cause diseases of plants. In compatible interactions a plant becomes diseased upon attack by a virulent pathogen, whereas in incompatible interactions a plant is resistant to attack by avirulent pathogens. Disease resistance in plants commonly requires two complementary genes (gene-for-gene

relationship) (*1*): an avirulence (*Avr*) gene in the pathogen and a matching resistance (*R*) gene in the host. An elicitor-receptor model has been proposed in which the pathogen-derived *Avr* products activate plant defense mechanisms upon *R*-protein-mediated recognition (e.g. *2, 3*). Pathogens secrete various proteins during interaction with plants. These proteins function as virulence or pathogenicity factors by modifying host metabolism or suppressing resistance mechanisms. It is suggested that plants produce R-proteins that detect proteinaceous molecules from invaders. The majority of the R-proteins contain leucine-rich-repeats, which are expected to be involved in the detection of invading pathogens, either directly or indirectly (*4*). So far, little is known about possible virulence or pathogenicity functions of AVR proteins.

A well studied example of a fungal avirulence protein is AVR9 (*5*), which is produced by particular races of *Cladosporium fulvum* when infecting its only natural host, tomato. This 28-residue peptide induces a hypersensitive response in tomato plants carrying the resistance gene *Cf-9* (*6, 7*). This response is the most common plant resistance response to viruses, bacteria, fungi, and nematodes (*2, 3, 8, 9*). AVR9 is a β-sheet peptide and contains three disulfide bridges (*10*). Mutagenesis studies revealed sites in AVR9 that are important for its necrosis-inducing activity (*10, 11*). All three disulfide bridges are required for this activity ((*11*) and this study).

The intrinsic function of AVR9 for the producing fungus is not known yet. The recognition of AVR9 by races of *C. fulvum* is clearly not the intrinsic function. Sequence homology could give a clue to this function, but no close homologues were found in the sequence databases. It was noted that the length and the cysteine spacing of AVR9 is related to that of small cystine-knotted peptides (*10, 12*), which function as proteinase inhibitors or ion-channel blockers. Our NMR studies on AVR9 also suggested this relatedness (*10*). However, in that study the determination of a high-resolution 3D structure of AVR9 was hampered by the low amount of material, and lack of information on the disulfide connectivities. Our recent folding studies on synthetic AVR9 (*13*) solved the first problem. Here, we report on the determination of the disulfide bridges of AVR9 to fully establish its relatedness to cystine-knotted peptides, and to obtain significant input for NMR structure calculations to get insight into the molecular mechanism mounting plant defense responses. In addition, a search for the intrinsic function of AVR9 was started with a comparison of AVR9 to the most closely related cystine-knotted peptide, the carboxypeptidase inhibitor (CPI) (*14*). However, AVR9 did not show any carboxypeptidase inhibiting activity.

Disulfide bridges play important structural roles in proteins. The determination of the correct bridging pattern is not straightforward. A serious problem is disulfide scrambling: exchange of partners between thiols and disulfides. This occurs at neutral or alkaline pH, but it can be suppressed at low pH (*15*). Different approaches have been applied to assign disulfide bridges. Classically, proteins are digested proteolytically, followed by characterization of the resulting fragments. Alternatively, partial hydrolysis can be used rather than proteolysis (e.g. (*16*)). Another method that is frequently used at the moment is partial reduction of disulfide bonds using tris-(2-carboxyethyl)phosphine (TCEP) (*17*). Advantages of this approach are its independence of accessible cleavage sites, and minimization of disulfide scrambling using low-pH solutions. Using this reduction approach we elucidated the bridging pattern of the cysteine-rich AVR9 (six cysteines out of 28 residues).

MATERIALS AND METHODS

Materials. Folded synthetic AVR9, proven to be identical to native fungal AVR9, was obtained as described previously (*13*). TCEP was from Sigma. *N*-ethylmaleimide (NEM) and 4-vinylpyridine (4VP) were purchased from Fluka. Iodoacetamide (IAM), potato carboxypeptidase inhibitor, bovine pancreas carboxypeptidase A, and benzoylglycyl-*L*-phenylalanine were obtained from ICN Biomedicals Inc. All solvents were HPLC grade. 4VP was vacuum-distilled, and kept under nitrogen at -70 ºC.

Partial reduction. Native AVR9 (36 μg; mw 3189.6) was dissolved in 10 μL of 0.1 M citrate buffer pH 3 containing 6 M of guanidine hydrochloride in water. Reduction was started by adding the appropriate amount of an aqueous solution containing 0.1 M TCEP, 0.1 M citrate pH 3, and 6 M guanidine-HCl. In most cases 240 equivalents of TCEP (mole TCEP to mole AVR9) were added (27.2 μL of TCEP solution). This partial-reduction mixture was incubated at room temperature for 15 min (unless stated otherwise), directly followed by alkylation or HPLC analysis. HPLC fractions containing partially-reduced peptides were collected manually, and the masses of the corresponding peptides were determined by MALDI-TOF MS.

Alkylation with iodoacetamide. Partially reduced AVR9 (see above) in 37.2 μL 0.1 M citrate pH 3, 6 M guanidine-HCl in water with 240 equivalents of TCEP was alkylated with iodoacetamide as described previously (*17*). For one reaction 20-40 mg of IAM was used.

Incubation was for 30 sec at room temperature, after which the reaction was quickly acidified with phosphoric acid (85%) to prevent disulfide scrambling. This mixture was immediately applied to the HPLC column.

Alkylation with N-ethylmaleimide. To the mixture after partial reduction of AVR9 (240 equivalents of TCEP, 15 min) was added 68 μL of 0.1 M *N*-ethylmaleimide (600 equivalents), 0.1 M citrate pH 3, and 6 M guanidine-HCl in water. After incubation for 30 min at room temperature the mixture was directly applied to the HPLC column.

Alkylation with 4-vinylpyridine. Only fully reduced peptides were alkylated with 4-vinylpyridine (*17*). Complete reduction was obtained by incubation of freeze-dried HPLC-purified peptides in 200 μL of an aqueous solution containing 20 mM TCEP and 250 mM Tris-acetate, pH 8 for 30 min at 50 °C. After cooling to room temperature 4 μL of neat colorless 4VP was added. The mixture was incubated for 15 min in the dark at room temperature, immediately followed by addition of 20 μL 85% phosphoric acid and HPLC purification.

Reversed-phase high-performance liquid chromatography. Different disulfide forms of AVR9 were separated by analytical RP-HPLC. The elution solvents consisted of 5% acetonitrile (v/v) and 0.1% trifluoroacetic acid (TFA) in water (solvent A); and 10% water and 0.1% TFA in acetonitrile (solvent B). A 150 × 3.9 mm Delta-Pak C_{18} column (300 Å, 5 μm) (Waters Corporation, Milford, U.S.A.) was used. The separation was monitored at 215 nm. The flow rate was 1 mL/min. The gradient to analyze reaction mixtures was: 0%B to 12%B in 7 min (percentage solvent B in solvent A), 12%B to 37%B in 33 min giving a total time of 40 min. Relative amounts of different disulfide forms of AVR9 were determined by integrating the appropriate peaks in the analytical HPLC profiles using standard Waters software.

Peptide sequence analysis. Automated Edman degradation using a Perkin Elmer/Applied Biosystems model 476A was performed at the Sequence Center Utrecht (University of Utrecht, The Netherlands). The sequencer was on-line connected to an RP-HPLC for the identification of the phenylthiohydantoin derivatives of the released amino acids.

Assay of necrosis-inducing activity. Injections of peptides (20 μL) into the intercellular space of leaves of tomato cultivars MM-Cf9 (containing the *Cf-9* resistance gene) and MM-Cf0 (lacking the *Cf-9* gene) were carried out as described previously (*11, 18*).

Assay of carboxypeptidase inhibitor activity. The K_i values of the carboxypeptidase inhibitor and of AVR9 were determined according to Henderson (*19*). Benzoylglycyl-*L*-

phenylalanine was used as substrate at different concentrations as reported previously (*20*). The concentration of carboxypeptidase A was 67 nM in all cases.

Mass spectrometry. Average molecular masses were determined by MALDI-TOF MS on a Perseptive Biosystems Voyager DE-RP. A saturated matrix solution (α-cyano-4-hydroxycinnamic acid, Aldrich) was freshly prepared in acetonitrile/water/TFA (50/50/1, v/v/v). One μL of each protein sample (freeze-dried HPLC fractions; dissolved in 10 μL water) was mixed with 1 μL matrix solution on the MALDI target. Data were acquired in the positive reflector mode. External calibration was performed with a tryptic digest of the C116S mutant of para-hydroxybenzoate hydroxylase (EC 1.14.13.2) using fragments with calculated $[M+H]^+$ of 1099.6 and 2086.2.

NMR spectrometry. The sample contained 5 mg of native AVR9 in 0.2 mL $H_2O/^2H_2O$ (9:1 v/v) at pH 5.0 (pH meter reading), and was transferred to a Shigemi tube (Shigemi Inc., Allison Park, U.S.A.). Experiments were conducted at 35 °C. 1D-NMR spectra, a clean MLEV17-TOCSY spectrum with a mixing time of 50 ms, and a NOESY spectrum with a mixing time of 300 ms were recorded at 500 MHz on a Bruker AMX500 NMR spectrometer. Acquisition and processing parameters were essentially the same as those described previously (*10*). The spectra were referenced to sodium 3-(trimethylsilyl)-1-propanesulfonate (DSS).

RESULTS

The determination of the disulfide bridge structure of AVR9 involved four steps: 1) partial reduction, 2) alkylation of free thiol groups of newly formed cysteines, 3) separation of different peptides by HPLC, and 4) Edman degradation of peptides to locate the positions of the alkylated cysteines.

Partial reduction of AVR9. Native AVR9 was reduced by TCEP. This water-soluble reagent has proven to be an excellent reducing agent for disulfides (*21*), and can be used at acidic pH to suppress disulfide scrambling (*17, 22*). The reduction reactions (at pH 3) were performed in 6 M of guanidine-HCl to facilitate equal TCEP-accessibility to the three disulfide bridges of AVR9. A partial reduction typically yielded five different AVR9 species as can be seen in the HPLC profile presented in Figure 1a. MALDI-TOF MS demonstrated that one of these species contained 3 bridges ($AVR9^{3SS}$), one contained 2 bridges ($AVR9^{2SS}$), two contained 1 bridge ($AVR9^{1SS}$), and one contained no bridges ($AVR9^{reduced}$) (Figure 1a).

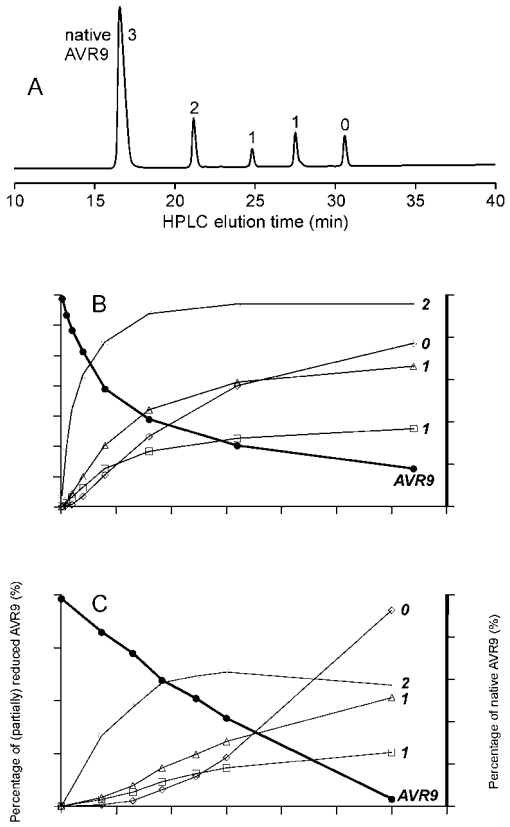

Figure 1. Partial reduction of AVR9. (**A**) HPLC profile (monitored at 215 nm) of a partial reduction reaction of native AVR9 in 6 M of guanidine-HCl, pH 3, with a 240-fold molar excess of TCEP, at room temperature for 15 min. For every peak the number of disulfide bridges present in the corresponding AVR9-derived species is indicated. The peak at 17 min represents native AVR9. (**B**) Relative amounts of native AVR9 and (partially) reduced AVR9 species as a function of the molar excess of TCEP (other conditions as stated above; reaction time 15 min). The percentages were determined by integration of the corresponding HPLC profiles. (**C**) Partial reduction as function of time (other conditions as stated above; 240-fold excess of TCEP).

The retention time on HPLC and the biological activity of the $AVR9^{3SS}$ species are identical to those of native AVR9. Thus, next to native and fully reduced AVR9, three partially reduced AVR9 species were obtained. The three disulfide bridges of AVR9 could be assigned based on the three partially-reduced species obtained, as demonstrated below. The amount of TCEP in the reaction mixture (Figure 1B), and the incubation time (Figure 1C) affect the reduction rate and the yields of the different disulfide forms. Relatively high concentrations of TCEP are required to obtain significant quantities of the partially-reduced AVR9 molecules (Figure 1B). The presence of guanidine-HCl in the TCEP solution decreased the yields of $AVR9^{2SS}$, $AVR9^{1SS}$, and $AVR9^{reduced}$ somewhat. In time, as expected, an $AVR9^{2SS}$ species appeared first, followed after a short lag time by two $AVR9^{1SS}$ species, and finally the $AVR9^{reduced}$ species appeared (Figure 1c). The amount of $AVR9^{reduced}$ increased slowly in the first 10 min, but increased strongly after 15 min, when significant amounts of $AVR9^{1SS}$ became available. This phenomenon can also be observed in the TCEP titration experiment (Figure 1B). The data presented in Figure 1 suggest that AVR9 is sequentially reduced as follows: $AVR9^{3SS} \rightarrow AVR9^{2SS} \rightarrow AVR9^{1SS} \rightarrow AVR9^{reduced}$. In the subsequent alkylation reactions partial-reduction mixtures were used that were obtained after 15 min of incubation with 240 equivalents of TCEP.

Iodoacetamide labeling of partially reduced AVR9. In the originally proposed strategy (*17*) IAM was used to irreversibly block the thiol groups of cysteines formed during partial reduction. This reagent alkylates at pH 8. The partial-reduction mixture, containing 6 M of guanidine-HCl, was squirted into a concentrated IAM solution, and was quenched after 30 s by acidification. The resulting mixture was directly applied to the HPLC column. The number of peaks in the resulting HPLC profile (Figure 2) exceeded that observed after partial reduction without alkylation (Figure 1a). The peak with a retention time of 31 min in Figure 2 (TCEP/IAM) was also seen in a control experiment with TCEP/IAM without the peptide. Native AVR9 was not modified by IAM and showed the expected retention time on HPLC of 17 min. MS demonstrated that all other peaks contained AVR9 species alkylated on all free cysteines (AVR9[IAM]), depending on the number of disulfide bridges left in the molecule. The additional peaks formed during treatment with IAM contain AVR9-related species with 1 or 2 bridges and 4 or 2 *S*-carboxamidomethylcysteine residues, respectively. These species were caused by disulfide scrambling during alkylation. The three most-intense peaks eluting between 20 and 25 min (numbered in Figure 2; TCEP/IAM) correspond to peaks observed after partial reduction without alkylation ($AVR9^{2SS}$, most-abundant $AVR9^{1SS}$, and $AVR9^{reduced}$; Figure 1a). The less-abundant $AVR9^{1SS}$ peak observed after partial reduction

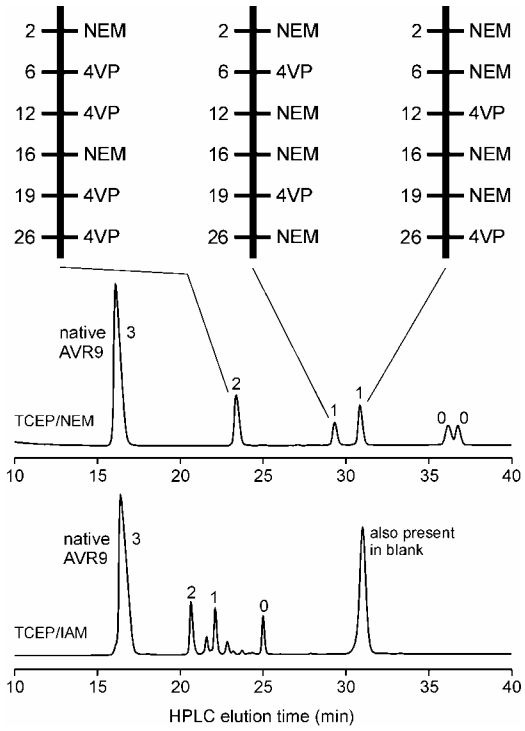

Figure 2. HPLC profiles of partially-reduced and cysteine-modified AVR9, and the positions of those cysteine modifications. Native AVR9 was partially reduced for 15 min by a 240-fold molar excess of TCEP, at room temperature, pH 3, and 6 M of guanidine-HCl. The reaction mixture was analyzed by HPLC after treatment with IAM (*bottom HPLC profile*) or with NEM (*top HPLC profile*). The numbers of disulfide bridges present in AVR9 derivatives in various peaks are indicated. In the profile of the TCEP/IAM reaction a peak was observed at 31 min that was not related to AVR9. This peak was the only one present in a control reaction without AVR9. The partially-reduced NEM-modified peptides were collected, lyophilized, and fully reduced by TCEP followed by modification of free cysteines by 4-vinylpyridine. The positions of the modifications, as determined by Edman degradation, are shown in the top panel.

(Figure 1a) could not be recognized with certainty after alkylation. AVR9^{2SS}[IAM] and the most abundant AVR9^{1SS}[IAM] peptide were sequenced.

Partial reduction of the small cysteine-rich AVR9 peptide results in free thiol groups, which are always in the vicinity of the remaining disulfides, thereby favoring scrambling. The presence of 6 M guanidine-HCl in the TCEP solution reduced the level of scrambling somewhat. Attempts to alkylate the partially-reduced AVR9 species after HPLC purification did not further reduce the level of scrambling.

N-ethylmaleimide labeling of partially reduced AVR9. Alkylation with NEM was carried out for 30 min at pH 3 by adding 600 molar equivalents of NEM, directly after partial reduction. This reaction was complete as evidenced by mass spectrometry, whereas lower amounts of NEM resulted in incomplete alkylation. HPLC analysis of the reaction mixture (Figure 2; TCEP/NEM) showed the absence of disulfide scrambling. The AVR9 species present after partial reduction (Figure 1a) are all recognized after alkylation with NEM (Figure 2). The AVR9[NEM] derivatives showed increased retention times on HPLC in comparison with the corresponding (partially) reduced AVR9 species. However, AVR9^{reduced}[NEM] shows two HPLC peaks (both marked '0'). MALDI-TOF MS showed that the AVR9-related species in the latter two peaks have identical masses. The peaks of AVR9^{reduced}[NEM] were collected separately, freeze-dried, and analyzed again by HPLC. No redistribution in two peaks was observed, indicating that the two AVR9 derivatives are not in a conformational equilibrium. Multiple peaks after NEM labeling have been observed before (*23*, *24*), and probably represent diastereoisomers, caused by the attack of a thiol group to the maleimide introducing a new chiral center, or ring opening of the *N*-ethylsuccinimidocysteines.

Sequencing of AVR9 peptides with labeled cysteines. The two partially-reduced IAM-labeled peptides (Figure 2; TCEP/IAM, labeled '1' and '2') still contain one or two disulfide bridges. Cysteine residues involved in these bridges do not give a signal during peptide sequencing, whereas *S*-carboxamidomethylcysteines give clear identifiable signals. As the sequence of AVR9 is known, only the cycles concerning cysteine-derived residues give relevant information. In all cases the signals of the non-cysteine-derived residues were in perfect agreement with the known sequence. Edman degradation of the AVR9^{2SS}[IAM] peptide revealed signals of *S*-carboxamidomethylcysteines in the cycles 2 and 16, and absence of signals in the cycles 6, 12, 19, and 26. Thus, the first-opened disulfide bridge connects residues Cys2 and Cys16. The AVR9^{1SS}[IAM] peptide, unfortunately, did not show two cycles where signals were clearly absent, although the signals observed in the cycles 12

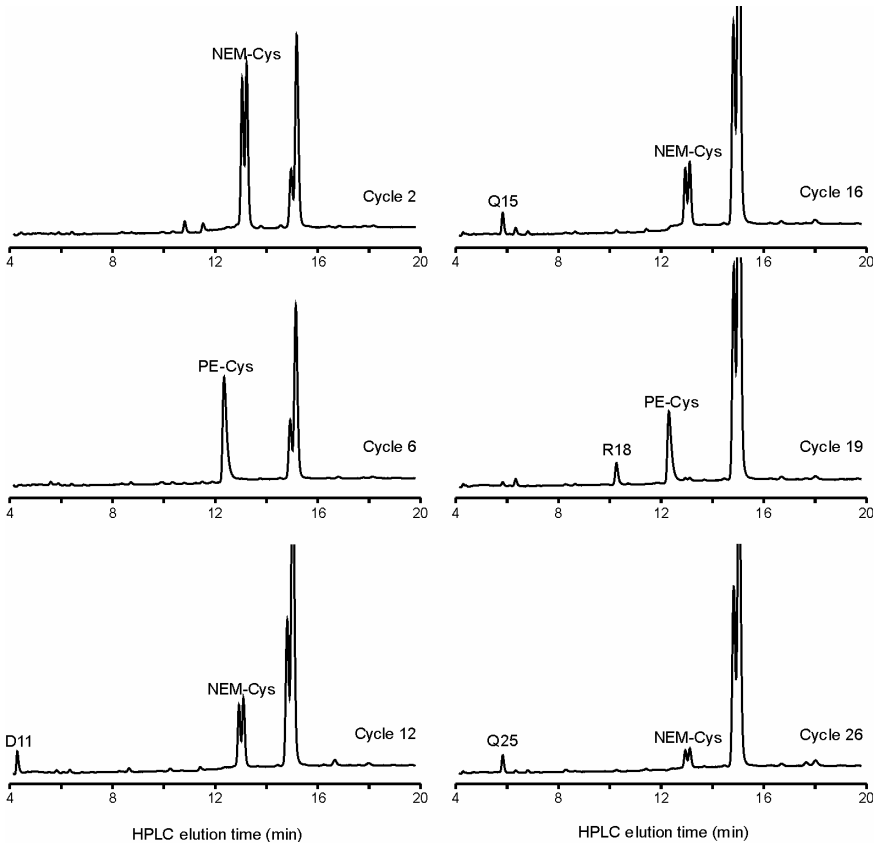

Figure 3. HPLC profiles of Edman-sequencing cycles corresponding to the release of modified cysteines from the first-eluting AVR9^{1SS}[NEM,4VP] peptide. Native AVR9 was partially reduced to AVR9^{1SS} (HPLC peak at 25 min in Figure 1). The 4 newly-formed cysteines were modified by NEM (AVR9^{1SS}[NEM]; HPLC peak at 29 min in Figure 2). Subsequently, the remaining bridge was reduced, and those 2 cysteines were modified by 4VP. The resulting peptide was sequenced, and the signals of the phenylthiohydantoin derivatives of the released modified cysteines in the cycles 2, 6, 12, 16, 19, and 26 are shown. Signals of cysteines modified by *N*-ethylmaleimide are indicated by 'NEM-Cys', and those of pyridylethylated cysteines (4VP) by 'PE-Cys'. A disulfide bridge between the residues Cys6 and Cys19 is deduced from these data. The signals of the preceding amino acid in the sequence observed in the cycles 12, 16, 19, and 26 are indicated by the one-letter code of those residues (D11, Q15, R18, and Q25, respectively). Two chemical by-products elute in the HPLC chromatograms at about 15 min.

and 26 were the lowest. No disulfide connectivity could be deduced with certainty from this experiment. Possibly, the HPLC-purified peptide was contaminated with disulfide-scrambled AVR9 species, blurring the difference between absence and presence of *S*-carboxamidomethylcysteine signals. Discrimination will be easier when the remaining bridge(s) is/are reduced, and the newly formed cysteines are modified by another label. The IAM modified peptides were more difficult to purify than the NEM-modified ones (Figure 2).

The three partially-reduced NEM-labeled AVR9 peptides were purified by HPLC (Figure 2), freeze-dried, completely reduced, and treated with 4VP. The resulting linear peptides contained NEM- and 4VP-labeled cysteines, which were easily observed and identified during sequencing. The phenylthiohydantoin derivative of NEM-labeled cysteine eluted as two peaks (Figure 3). Multiple peaks for this residue have been observed before (*23, 24, 25*). This may be related to hydrolysis of the maleimide ring, or to the introduction of a chiral center upon NEM labeling. Sequencing of the 4VP-treated fully-reduced AVR9^{2SS}[NEM] peptide (AVR9^{2SS}[NEM,4VP]) yielded signals corresponding to NEM-Cys in the cycles 2 and 16, and signals of pyridylethylcysteine (PE-CYS) in the cycles 6, 12, 19, and 26 (results summarized in Figure 2). These data confirm the existence of a disulfide bridge between the residues Cys2 and Cys16 in native AVR9, as was deduced from the sequencing of the AVR9^{2SS}[IAM] peptide. The first-eluting AVR9^{1SS}[NEM,4VP] peptide showed PE-CYS signals in cycles 6 and 19 (Figure 3), whereas the last-eluting AVR9^{1SS}[NEM,4VP] peptide displayed these signals in cycles 12 and 26. The other four cysteines of both peptides appeared all modified by NEM. In summary, disulfide bridges connect the residues 2 and 16, 6 and 19, and 12 and 26. The primary structure of native AVR9 including the bridging pattern is shown in Figure 4.

Necrosis-inducing activities of partially-reduced NEM-labeled AVR9 species. The NEM-modified peptides, at various concentrations, were injected in leaves of MM-Cf9 tomato plants to determine the necrosis-inducing activities (shown in Table 1). Native AVR9 showed full activity, AVR9^{2SS}[NEM] displayed strongly reduced activity, and peptides with one or no bridges were not active at all. Reduced AVR9 with free thiol groups showed a very low necrosis-inducing activity at the highest concentration. This is likely due to some refolding in the intercellular space of tomato leaves. None of the injections in MM-Cf0 plants showed necrosis-inducing activity (result not shown).

Table 1. Necrosis-inducing activities[a] of native AVR9, (partially) reduced NEM-modified AVR9 species, and fully reduced AVR9 as observed upon injection in leaves of MM-Cf9 tomato plants.

AVR9 species[b]	Concentration		
	30 μM	3 μM	0.3 μM
native AVR9	+ + + + + +	+ + + +	+ +
$AVR9^{2SS}$[NEM](6-19,12-26)	+	-	-
$AVR9^{1SS}$[NEM](6-19)[c]	-	-	-
$AVR9^{1SS}$[NEM](12-26)[d]	-	-	-
$AVR9^{0SS}$[NEM][e]	-	-	-
$AVR9^{0SS}$[NEM][f]	-	-	-
$AVR9^{0SS}$	+	-	-

[a] Necrosis-inducing activities are qualified as reported previously (*11*). [b] The numbers of disulfide bridges in the molecules are indicated. Cysteine thiol modifications by *N*-ethylmaleimide (NEM), and the remaining disulfide bridges (SS) in the partially-reduced AVR9 species are also indicated. [c] RP-HPLC peak at 29 min (Figure 2, top chromatogram). [d] RP-HPLC peak at 31 min (Figure 2, top chromatogram). [e] First-eluting on RP-HPLC at 36 min (Figure 2, top chromatogram). [f] Last-eluting on RP-HPLC at 37 min (Figure 2, top chromatogram).

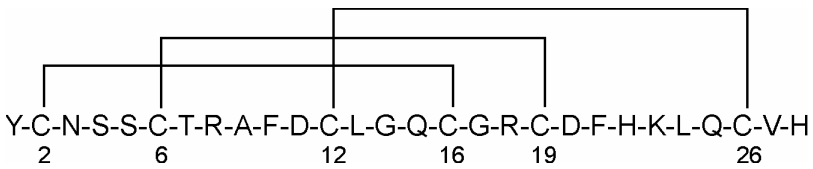

Figure 4. Primary structure and disulfide bonding pattern of AVR9. The disulfide bridges are indicated, and the cysteine residues are numbered.

NMR analysis of AVR9. Based on length, cysteine spacing, and disulfide connectivities AVR9 belongs to the family of cystine-knotted peptides, such as the ω-conotoxins (Figure 5). A strong homology is observed to carboxypeptidase inhibitor (CPI). To prove structural homology, NMR spectra were recorded for AVR9 at the temperature at which NMR spectra of CPI had been obtained (*26*). The resonances of AVR9 at 35 °C were assigned on the basis of those obtained for the peptide at room temperature and 5 °C (*10, 13*). No significant differences were observed between these three data sets. The backbone H^{α}-proton chemical shifts of AVR9 at 35 °C and pH 5 are depicted in Figure 6, together with those obtained for CPI (35 °C and pH 3.8, (*26*)). Strong similarities are observed between the shifts of AVR9 and CPI, despite the large differences in the amino-acid sequence, indicating a comparable fold.

Testing possible carboxypeptidase-inhibiting activity of AVR9. To determine whether common fold would still lead to common functions and to study the intrinsic function of AVR9 for the producing fungus, the possibility was investigated whether AVR9 would have biological activities similar to its most related peptide. First, the competitive inhibitory activity of the carboxypeptidase inhibitor towards carboxypeptidase A was determined. The inhibition constant K_i of 2.1 nM is in perfect agreement with previously reported values of 1.5-2.7 nM (*27*) and 0.9-2.1 nM (*20*). However, inhibition of carboxypeptidase was not observed with AVR9. Even a concentration of AVR9 1000-fold higher than that of CPI did not inhibit carboxypeptidase A.

AVR9	Y**C**---NSS**C**TRAF-D**C**--LGQ**C**GR**C**DFHKLQ**C**VH
CPI IIb	<EEHADPI**C**---NKP**C**KTHD-D**C**SGAWF**C**QA**C**WNSART**C**GPYVG
Kalata B1	NGLPV**C**---GET**C**VGGT--**C**NTPG-**C**-T**C**SWP--V**C**TR
CMTI I	RV**C**PRILME**C**KKDS-D**C**--LAE**C**-V**C**LEH-GY**C**G
ω-GVIA	**C**KSOGSS**C**SOTSYN**C**-----**C**RS**C**NOYTKR**C**Y

Figure 5. Alignment of amino-acid sequences of the cystine-knotted peptides AVR9, carboxypeptidase inhibitor IIb (CPI IIb) (*27*), Kalata B1 (*12, 30*), trypsin inhibitor CMTI I (*40*), and ω-conotoxin GVIA (*41*). Cysteines involved in disulfide bridges are indicated in bold. The bridging patterns in these molecules are identical. The residue hydroxyproline in the ω-conotoxin GVIA is indicated by O. The N-terminal residue in CPI IIb is a pyroglutamate, which is indicated by <E.

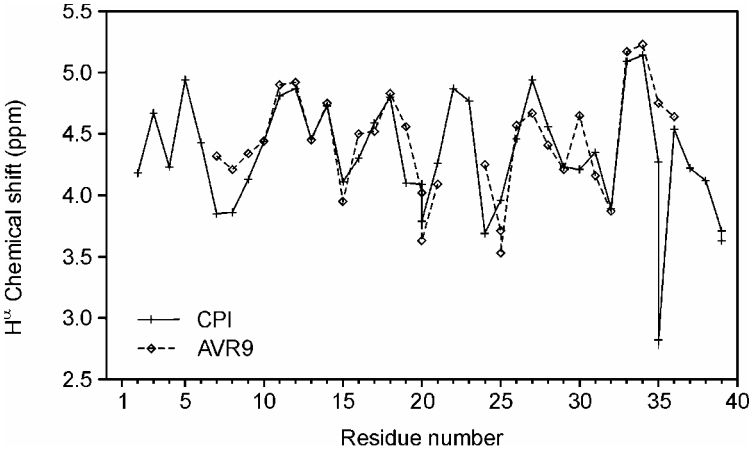

Figure 6. Comparison of H^{α}-proton chemical shifts of AVR9 and carboxypeptidase inhibitor. H^{α} Chemical shifts (ppm) are shown versus the residue number for CPI (+, solid line), and for AVR9 (◊, dashed line). The data for CPI were derived from NMR spectra recorded at 35 ºC and pH 3.8 (*26*), and the data for AVR9 from spectra taken at 35 ºC and pH 5. The residues of AVR9 are superimposed (and numbered) onto the corresponding ones of CPI (Figure 5).

DISCUSSION

The fungal AVR9 elicitor is secreted in the intercellular space of tomato leaves, and is likely to require additional stability, for which purpose disulfide bridges are ideally suited. The disulfide connectivities have now been identified as Cys2-Cys16, Cys6-Cys19, and Cys12-Cys26 (Figure 4). These overlapping disulfide bridges are envisioned to increase the stability of the peptide.

The applied 'partial-reduction procedure' worked out well for AVR9, despite the high cysteine content (6 'half-cystines' out of 28 residues). For this procedure sufficient accessibility of the sulfur atoms of at least one bridge is required. In this respect, it is noted that the bridging rendered AVR9 insensitive towards trypsin and chymotrypsin (*6*), complicating a determination of disulfide connectivities via proteolytic digestions. In general, these digestions are performed at a pH that does not suppress disulfide scrambling. The high cystine content also complicated an NMR spectroscopic approach to determine the

bridging pattern, as also observed for some related (*vide infra*) cystine-rich peptides (*28, 29, 30*). This suggests that the partial reduction procedure is an attractive approach for highly bridged peptides.

In the course of reduction of AVR9 only the bridge between Cys2 and Cys16 opened. This intermediate was further reduced to two $AVR9^{1SS}$ species (Figure 1), which subsequently were reduced completely. The reduction pathway is depicted in Figure 7. In general, multiple intermediates with one opened bridge are used to deduce the bridging. However, intermediates with one bridge left can be used equally well as demonstrated for AVR9. Though reduction was performed in the presence of 6 M of guanidine-HCl to lessen possible differences in the accessibility of TCEP to each disulfide bond, only the Cys2-Cys16 bridge in the intact molecule is sufficiently accessible to TCEP. A relatively high TCEP concentration was required for partial reduction of AVR9 when compared to other

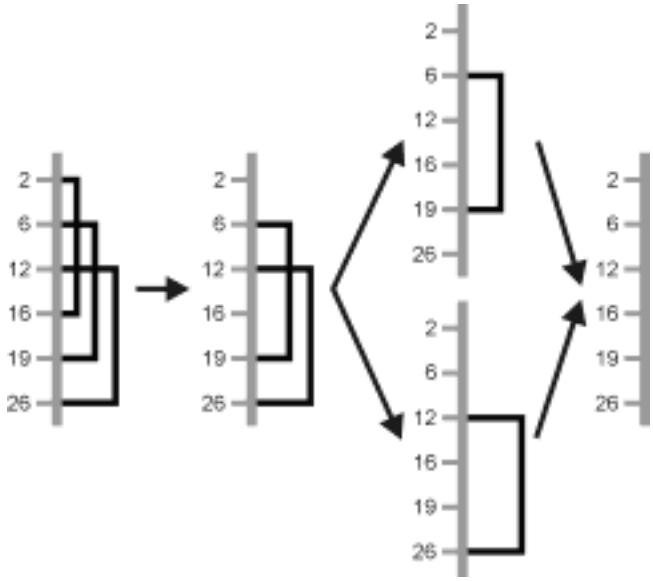

Figure 7. Scheme of the reduction of AVR9 by TCEP. The peptide sequence is represented by a gray line. Only the positions of the six cysteines are indicated. The disulfide bridges in the different molecules are shown by connections between the cysteines involved. If not connected, cysteines have free sylfhydryl groups.

proteins (*17, 22*). From these data qualitative information on the spatial structure of AVR9 is obtained. The sulfur atoms of two bridges are buried in AVR9, and those of the bridge Cys2-Cys16 are partially shielded within the molecule. The molecule is rather stable under denaturing conditions.

Iodoacetamide was used first for the labeling of the cysteines formed during partial reduction, as originally proposed (*17*). Unfortunately, disulfide scrambling, also reported by Gray (*17*), was significant during this modification. As a result the low-intensity $AVR9^{1SS}$[IAM] intermediate got lost (Figures 1 and 2). One of the two remaining partially-reduced IAM-modified peptides gave clear results after sequencing, whereas the other peptide gave hardly differential signals for IAM-modified cysteines and 'blank' half-cystines. One way to improve this is to reduce the remaining bridges and label the resulting cysteines with a different agent. Contrary to the case when using iodoacetamide, no scrambling was observed during modification with *N*-ethylmaleimide at the low pH at which the partial reduction was performed. The remaining bridges of the purified $AVR9^{2SS}$[NEM] and $AVR9^{1SS}$[NEM] intermediates were reduced, followed by modification with 4-vinylpyridine. Sequencing revealed the positions of the modifications, as the signals originating from Cys(NEM) and Cys(4VP) are clearly different (Figure 3). Labeling with NEM rather than with IAM was essential for the elucidation of the bridging of AVR9. The compatibility of the low-pH partial reduction and modification with NEM is probably also useful for the determination of disulfide bridges in other peptides as well, because of substantially less disulfide scrambling. An alternative agent to alkylate cysteines under acid catalysis is (hydroxymethyl)benzamide in TFA (*31*), but this reagent is less compatible with TCEP. For larger proteins the TCEP/NEM approach can be combined with proteolytic digestions (*23*). Alternatively, cysteines, formed by partial reduction, can be cyanylated at low pH allowing cleavage of the N-terminal peptide bond followed by mass mapping (*22*). This cyanylation approach may in case of (poly)peptides yield very small fragments that might escape detection by MALDI-TOF MS because of interference with signals arising from the matrix.

The necrosis-inducing activity of AVR9 strongly decreased upon reduction of the Cys2-Cys16 disulfide bond. Further reduction inactivated the molecules completely. Thus, the bridges are very important for the activity of AVR9, which is in perfect agreement with mutagenesis studies (*11*). Most likely the drop in activity is caused by reduced stability and/or loss of native conformation, suggesting that at least the Cys2-Cys16 bridge is required for a stable native spatial structure. It is noted that in the case of the related cystine-knotted ω-conotoxins each of the three bridges plays an essential role in stabilizing

the structure (*32*). The strongly reduced necrosis-inducing activity of the AVR9^{2SS} molecule, which has the only accessible bridge reduced, does not favor a mechanism involving formation of a disulfide bridge between AVR9 and a (co)receptor in tomato.

The search for an intrinsic function of AVR9 for *C. fulvum* was initiated by examining homologous peptides. No proteins with high sequence identity to AVR9 could be found. However, based on length, cysteine spacing (Figure 5), and β-sheet character, homology to inhibitor cystine-knotted peptides was suggested (*10, 12*). AVR9 is most homologous to the CPI (Figure 5The present study shows that the bridging of AVR9 is identical to that of the cystine-knotted peptides. Also, the backbone H$^{\alpha}$-proton chemical shifts of AVR9 resemble those of CPI, indicating strong structural homology. Amide proton exchange data of AVR9 and CPI are comparable (*10, 26*). Thus, it is firmly established now that AVR9 is a cystine-knotted peptide indeed. Because of the structural homology to CPI, the solvent accessible

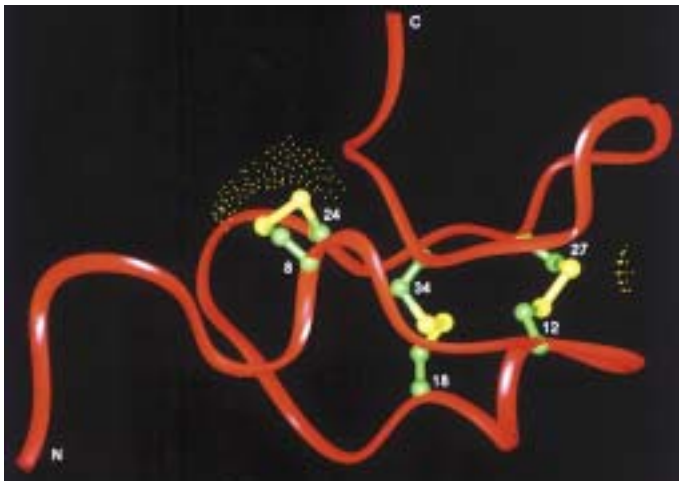

Figure 8. Solvent accessible surface of the sulfur atoms in the carboxypeptidase inhibitor. The coordinates of CPI are taken from the crystal structure of the inhibitor complex of carboxypeptidase A (*42*). The backbone of CPI is indicated as a red solid ribbon with labeled termini. Cysteine side-chains are depicted in ball-and-stick representation with their numbers in the sequence. The solvent accessible surfaces of the sulfur atoms are indicated by yellow dots. Only the bridge Cys8-Cys24 is sufficiently accessible to a molecule of the size of TCEP.

surfaces of the sulfur atoms involved in the bridging of CPI were examined (Figure 8). The sulfur atoms of the bridges Cys12-Cys27 and Cys18-Cys34 are not accessible to a TCEP molecule, whereas those of the bridge Cys8-Cys24 are sufficiently accessible. This perfectly rationalizes that only the bridge Cys2-Cys16 of AVR9 can be opened at relatively high TCEP concentrations. During reduction of the cystine-knotted trypsin inhibitor EETI II only one intermediate was observed, which lacked the bridge between Cys2 and Cys19 (*33, 34*). Also for this cystine knot the bridge between the first and fourth cysteine is the only one accessible to reducing agents. This further supports that AVR9 is a cystine knot. Also, similarities in the folding of CPI (*35*), ω-conotoxins (*36, 37*), and AVR9 (*13*) were observed. Possible relatedness to other proteins comes from a folding motif of CPI that was also identified in the cellulose-binding domain of fungal cellobiohydrolase I, wheat germ agglutinin, the erabutoxin family, and human neurophysin (*38*). A database search for cysteine patterns indicated that also an Amaranth α-amylase inhibitor, gurmarin (sweet taste-suppressing peptide), and antimicrobial peptides from *Amaranthus* are related to cystine-knotted peptides (*39*). Our recent query with the pattern x-C-x(2,6)-C-x(3,6)-C-x(2,5)-C-x(1,2)-C-x(3,6)-C-x (http://motif.genome.ad.jp/MOTIF2.html) resulted in peptide hits for 25 trypsin inhibitors, 8 toxins, 2 carboxypeptidase inhibitors, and Kalata B1, but no new relevant sequences that are related to AVR9 were found.

The absence of obvious sequence identity to other structurally related peptides or proteins complicates the elucidation of the intrinsic function of AVR9. As this peptide is most homologous to CPI, we set out to test whether it possibly contained carboxypeptidase-inhibiting activity. However, AVR9 did not inhibit the carboxypeptidase, even not at very high concentrations. Also no antibacterial or antifungal activity could be detected for AVR9. This peptide was not active in an ω–conotoxin assay (David Craik, personal communication). It is, however, still possible that AVR9 displays an inhibitory or a channel-blocking activity, in common with the related cystine-knotted peptides.

The elucidation of the bridging pattern of AVR9 provides a solid basis for the calculation of the 3D structure to gain insight into the molecular mechanism underlying interaction with its (co)receptor and the subsequent onset of plant defense responses. This work is currently in progress.

REFERENCES

1. Flor, H. H. (1971) *Annu. Rev. Phytopathol. 9*, 275-296.
2. De Wit, P. J. G. M. (1997) *Trends Plant Sci. 2*, 452-458.
3. Joosten, M.H.A.J., and De Wit, P. J. G. M. (1999) *Annu. Rev. Phytopathol.37*, 335-367.
4. Hammond-Kosack, K. E., and Jones, J. D. G. (1997) *Annu. Rev. Plant Physiol. Plant Mol. Biol. 48*, 575-607.
5. Scholtens-Toma, I. M. J., and De Wit, P. J. G. M. (1988) *Physiol. Mol. Plant Pathol. 33*, 59-67.
6. De Wit, P. J. G. M., Hofman, A. E., Velthuis, G. C. M., and Kuc, J. A. (1985) *Plant Physiol. 77*, 642-647.
7. Jones, D. A., Thomas, C. M., Hammond-Kosack, K. E., Balint-Kurti, P. J., and Jones, J. D. G. (1994) *Science 266*, 789-793.
8. De Wit, P. J. G. M. (1995) *Adv. Bot. Res. 21*, 147-185.
9. Crute, I. R., and Pink, D. A. C. (1996) *Plant Cell 8*, 1747-1755.
10. Vervoort, J., Van den Hooven, H. W., Berg, A., Vossen, P., Vogelsang, R., Joosten, M. H. A. J., and De Wit, P. J. G. M. (1997) *FEBS Lett. 404*, 153-158.
11. Kooman-Gersmann, M., Vogelsang, R., Hoogendijk, E. C. M., and De Wit, P. J. G. M. (1997) *Mol. Plant Microbe Interact. 10*, 821-829.
12. Pallaghy, P. K., Nielsen, K. J., Craik, D. J., and Norton, R. S. (1994) *Protein Sci. 3*, 1833-1839.
13. Van den Hooven, H. W., Appelman, A. W. J., Zey, T., De Wit, P. J. G. M., and Vervoort, J. (1999) *Eur. J. Biochem.264*, 9-18.
14. Hass, G. M., Nau, H., Biemann, K., Grahn, D. T., Ericsson, L. H., and Neurath, H. (1975) *Biochemistry 14*, 1334-1342.
15. Ryle, A. P., and Sanger, F. (1955) *Biochem. J. 60*, 535-540.
16. Zhou, Z., and Smith, D. L. (1990) *J. Prot. Chem. 9*, 523-532.
17. Gray, W. R. (1993) *Protein Sci. 2*, 1732-1748.
18. Mahé, E., Vossen, P., Van den Hooven, H. W., Le-Nguyen, D., Vervoort, J., and De Wit, P. J. G. M. (1998) *J. Peptide Res. 52*, 482-494.
19. Henderson, P. J. F. (1972) *Biochem. J. 127*, 321-333.
20. Molina, M. A., Marino, C., Oliva, B., Avilés, F. X., and Querol, E. (1994) *J. Biol. Chem. 269*, 21467-21472.
21. Burns, J. A., Butler, J. C., Moran, J., and Whitesides, G. M. (1991) *J. Org. Chem. 56*, 2648-2650.
22. Wu, J., and Watson, J. T. (1997) *Protein Sci. 6*, 391-398.
23. Bures, E. J., Hui, J. O., Young, Y., Chow, D. T., Katta, V., Rohde, M. F., Zeni, L., Rosenfeld, R. D., Stark, K. L., and Haniu, M. (1998) *Biochemistry 37*, 12172-12177.
24. Young, Y., Zeni, L., Rosenfeld, R. D., Stark, K. L., Rohde, M. F., and Haniu, M. (1999) *J. Peptide Res. 54*, 514-521.

25. Hui, J. O., Le, J., Katta, V., Rohde, M. F., and Haniu, M. (1997) in *Techniques in Protein Chemistry VIII*, pp277-287, Academic Press, San Diego.
26. Clore, G. M., Gronenborn, A. M., Nilges, M., and Ryan, C. A. (1987) *Biochemistry 26*, 8012-8023.
27. Hass, G. M., and Ryan, C. A. (1981) *Methods Enzymol. 80*, 778-791.
28. Heitz, A., Chiche, L., Le-Nguyen, D., and Castro, B. (1989) *Biochemistry 28*, 2392-2398.
29. Arai, K., Ishima, R., Morikawa, S., Miyasaka, A., Imoto, T., Yoshimura, S., Aimoto, S., and Akasaka, K. (1995) *J. Biomol. NMR 5*, 297-305.
30. Saether, O., Craik, D. J., Campbell, I. D., Sletten, K., Juul, J., and Norman, D. G. (1995) *Biochemistry 34*, 4147-4158.
31. Heck, S. D., Kelbaugh, P. R., Kelly, M. E., Thadeio, P. F., Saccomano, N. A., Stroh, J. G., and Volkmann, R. A. (1994) *J. Am. Chem. Soc. 116*, 10426-10436.
32. Price-Carter, M., Salem Hull, M., and Goldenberg, D. P. (1998) *Biochemistry 37*, 9851-9861.
33. Le-Nguyen, D., Heitz, A., Chiche, L., El Hajji, M., and Castro, B. (1993) *Protein Sci. 2*, 165-174.
34. Mahé, E., Le Nguyen, D., Heitz, A., Dafniet, R., Alfazema, L., Castro, B., and El Hajji, M. (1995) in *Proceedings of the 23 rd European Peptide Symposium September 4-10, Braga, Portugal* (Maia, H.L.S., Ed.) pp422-423, ESCOM, Leiden.
35. Chang, J. Y., Canals, F., Schindler, P., Querol, E., and Avilés, F. X. (1994) *J. Biol. Chem. 269*, 22087-22094.
36. Price-Carter, M., Gray, W. R., and Goldenberg, D. P. (1996) *Biochemistry 35*, 15537-15546.
37. Price-Carter, M., Gray, W. R., and Goldenberg, D. P. (1996) *Biochemistry 35*, 15547-15557.
38. Holm, L., and Sander, C. (1993) *J. Mol. Biol. 233*, 123-138.
39. Chagolla-Lopez, A., Blanco-Labra, A., Patthy, A., Sánchez, R., and Pongor, S. (1994) *J. Biol. Chem. 269*, 23675-23680.
40. Wieczorek, M., Otlewski, J., Cook, J., Parks, K., Leluk, J., Wilimowska-Pelc, A., Polanowski, A., Wilusz, T., and Laskowski, M. (1985) *Biochem. Biophys. Res. Commun. 126*, 646-652.
41. Lew, M. J., Flinn, J. P., Pallaghy, P. K., Murphy, R., Whorlow, S. L., Wright, C. E., Norton, R. S., and Angus, J. A. (1997) *J. Biol. Chem. 272*, 12014-12023.
42. Rees, D. C., and Lipscomb, W. N. (1982) *J. Mol. Biol. 160*, 475-498.

4

Natural disulfide bond disrupted mutants of AVR4 of the tomato pathogen *Cladosporium fulvum* are sensitive to proteolysis, thereby, circumventing *Cf-4* mediated resistance

Harrold A. van den Burg, Nienke Westerink, Kees-Jan Francoijs, Ronelle Roth, Esmeralda Woestenenk, Sjef Boeren, Pierre J.G.M. de Wit, Matthieu H.A.J. Joosten, and Jacques Vervoort

(Published in Journal of Biological Chemistry *on line*)

ABSTRACT

The extracellular AVR4 elicitor of the pathogenic fungus *Cladosporium fulvum* induces defense responses in the tomato genotype *Cf-4*. Here, the four disulfide bridges of AVR4 were identified as C11–C41, C21–C27, C35–C80, and C57–C72 by partial reduction with TCEP, subsequent cyanylation, and base-catalyzed chain cleavage. The resulting peptide fragments were analyzed by mass spectrometry. Sequence homology and the disulfide bond pattern revealed that AVR4 contains an invertebrate (inv) Chitin-Binding Domain (ChBD). Binding of AVR4 to chitin was confirmed experimentally. The three disulfide bonds encompassing the inv ChBD motif are also required for protein stability of AVR4. Independent disruption of each of the three conserved disulfide bonds in AVR4 gave a protease sensitive protein, while the fourth disulfide bond was not required for protein stability. Most strains of *C. fulvum* virulent on *Cf-4* tomato contain Cys-to-Tyr mutations in AVR4 involving two (C11–C41, C35–C80) of these three disulfide bonds present in the inv ChBD motif. These natural Cys-to-Tyr mutant AVR4 proteins did retain their chitin-binding ability and when bound to chitin these mutant proteins were less sensitive to proteases. Thus, the widely applied tomato *Cf-4* resistance gene is circumvented by mutations affecting two disulfide bonds in AVR4 resulting in the absence of AVR4 isoforms in apoplastic fluid. Nevertheless, these natural isoforms of AVR4 appear to have retained their intrinsic function, *i.e.* protection of the fungal cell wall against plant chitinases.

INTRODUCTION

Gene-for-gene based disease resistance in plants commonly requires two complementary genes, an avirulence (*Avr*) gene in the pathogen and a matching resistance (*R*) gene in the host (1,2). The *Cf* resistance genes of tomato mediate specific recognition of extracellular elicitor proteins encoded by *Avr* genes of the pathogenic fungus *Cladosporium fulvum* (3). The *Avrs* of *C. fulvum* and their matching *Cf* genes have become valuable instruments to investigate signal transduction pathways leading to plant disease resistance (4-9). To obtain sustainable resistance, the *Cf* resistance genes were introgressed from wild *Lycopersicon* species into commercial tomato cultivars. However, due to selection pressure new strains of *C. fulvum* emerged that had overcome the introgressed resistance traits by modification of the *Avr* genes (10). While some *Avr* genes in these virulent *C. fulvum* strains were found to be absent (11), others contained point mutations (12) or transposon insertions (13). The

natural strains of *C. fulvum* carrying these mutated *Avr* genes did not exhibit significantly reduced virulence under laboratory conditions (11-14), suggesting that AVR proteins are not essential for virulence or that the modified isoform of the AVRs can still contribute to virulence of *C. fulvum.* This genetic variation is so far strictly limited to the race-specific *Avrs* and is absent in genes that encode other extracellular elicitor proteins (*Ecps*) of *C. fulvum* (15).

Although the intrinsic role of the AVR proteins of *C. fulvum* during infection remains obscure, they are anticipated to contribute to virulence in susceptible hosts (16-18). This implies that evasion of *Cf*-mediated resistance by modification of *Avr* genes might be associated with a reduction or loss in virulence unless a functional gene remains. One candidate protein to investigate the latter idea is the race-specific elicitor AVR4 as *Cf-4*-mediated resistance is overcome in all but one case by single amino acid substitutions in the *Avr4* gene (12,14). Moreover, for AVR4 a virulence function is proposed in association with its ability to bind to chitin. AVR4 was found to protect fungi against degradation by plant chitinases by association with their hyphal wall (19). Mutations in the *Avr4* gene, as they are found in strains of *C. fulvum* virulent on the tomato genotype *Cf-4,* encode mostly single Cys-to-Tyr substitutions. In addition, two other mutations were found, i.e. Thr66-to-Ile and Tyr67-to-His. The Cys-to-Tyr substitutions involved the positions 64, 70, or 109 (which corresponds with C35, C41, and C80 in the mature protein, respectively) (14). Some of these *avr4* alleles still exhibit necrosis inducing activity when transiently expressed in *Cf-4* tomato using potato virus X (PVX) (14). However, none of the AVR4 mutant isoforms could be detected in apoplastic fluid isolated from tomato leaves inoculated with *C. fulvum* (14).

Mass spectrometry revealed that all Cys residues in AVR4 are involved in disulfide bonding (20). Together the disulfide bond pattern and the sequential spacing between Cys residues largely define the protein fold of secreted small proteins (21,22). Here, the disulfide bond connectivities of AVR4 are elucidated. The disulfide bond pattern of AVR4 shows homologies which the disulfide bond pattern of the recently identified “invertebrate Chitin-Binding Domain” (inv ChBD) (23), *i.e.* three of the four disulfide bonds of AVR4 (C11—C41, C35—C80, and C57—C72) are represented in the inv ChBD motif. Independent disruption of each of these three disulfide bonds in AVR4 results in a protein that is sensitive to proteases, which suggests that these disulfide bridges are required for conformational stability of AVR4. The Cys-to-Tyr mutations identified in natural strains of *C. fulvum* involve two (C11—C41 and C35—C80) of these three conserved disulfide bonds. AVR4 isoforms with a disruption in one of these two disulfide bonds are still able to bind chitin. Our data

support a model where evasion of *Cf-4*-mediated resistance appears to be based on decreased conformational stability of the AVR4 isoform leading to protein degradation upon release in the tomato apoplast. Noteworthy, the AVR4 isoforms were found to be more resistant to proteases when bound to chitin. These findings argue that mutant AVR4 isoforms are fully functional and can associate with chitin upon release, while excess of secreted (and unbound) protein is degraded before triggering host defense responses.

EXPERIMENTAL PROCEDURES

Construction of PVX derivatives and transcription. Avr4 mutants encoding various Cys-to-Ala substitutions were generated by PCR-based primer-directed mutagenesis on the plasmid pTXΔGC3a, containing the native Avr4 sequence (14). PCR amplification was carried out using mutagenic primers (Table 1) designated to generate two overlapping PCR fragments. PCR was used to combine the overlapping PCR fragments using the primers OX10 and N31 and the PCR product was cloned into the ClaI site of the vector pTXΔGC3a (24) and sequenced. In vitro transcription of the plasmids and subsequent inoculation on *N. clevelandii* and tomato was performed as described (14). *Nicotiana clevelandii* and the tomato (*Lycopersicon esculentum*) cultivars Moneymaker (MM) and the near-isogenic line MM-Cf4 were grown as described (25).

Partial reduction and cyanylation of the AVR4 protein. Expression of heterologous AVR4 was achieved in the methylotrophic yeast *Pichia pastoris*, and AVR4 was purified from culture fluid (20). The disulfide bonds of AVR4 were partially reduced with TCEP (Sigma) (26,27). A 0.1 M TCEP stock solution was prepared in 6 M guanidine-HCl in 0.1 M citrate buffer (pH 3) and stored at –20^{o}C (for at least six months without any deterioration detected). For each reduction reaction, 100 μg of native AVR4 was dissolved in 10 μL of 6 M guanidine-HCl in 0.1 M citrate buffer (pH 3). The reaction was initiated by adding a 6 fold molar excess of TCEP to AVR4, followed by incubation at 20 $^{\circ}$C for 15 min. Subsequently, an 80-fold molar excess of CDAP (Sigma) was added to cyanylate the freed thiol groups (15 min, 20^{0}C, in the dark). The 0.1 M CDAP stock solution in 6M guanidine-HCl in 0.1 M citrate buffer (pH 3) was freshly prepared prior to each reaction.

Reverse-phase high-performance liquid chromatography of the peptide mixture. The TCEP/CDAP reaction mixtures were separated by analytical reverse-phase high performance liquid chromatography (RP-HPLC) using a 150 × 3.9 mm Delta-Pak C18

column (300 Å, 5 μm; Waters). The separation was monitored at 215 nm and predominant peaks were manually collected. HPLC elution solvents consisted of 0.1% (v/v) trifuoroacetic acid (TFA) in water (*solvent A*), and 0.1% (v/v) TFA in acetonitrile (*solvent B*). HPLC was operated at a flow rate of 1 mL/min. The applied gradient was 5%→20%B (percentage B in solvent A) in 2 min, 20%→30% in 40 min, and 30%→60% in 3 min. AVR4 eluted at ~25%B. Integration of the HPLC profile was achieved using standard Waters software. Appropriate fractions (containing the AVR4 *des*-species) were lyophilized for storage. All solvents used were HPLC grade.

Peptide cleavage and full reduction of the disulfide bonds / Peptide mass analysis. Lyophilized HPLC fractions containing the AVR4 *des*-species were dissolved in two consecutive steps: first, 2 μL in 1 M NH_4OH, 6 M guanidine-HCl, and second 5 μL of 1 M NH_4OH, and incubated at 20 °C for 1 hr. The excess of NH_4OH was evaporated in a Speed-Vac system in 30 min (to almost complete dryness). Subsequently, the remaining disulfide bonds were reduced by adding an excess of TCEP (10 μL of 0.1 M TCEP stock) and the mixture was incubated at 37 °C for 30 min. The peptide mixtures were analyzed by mass spectrometry using a MALDI-TOF MS (Perseptive Biosystems Voyager DE-RP). Small aliquots of the peptide samples were applied to a saturated matrix solution that was freshly prepared (α-cyano-4-hydroxycinnamic acid; Sigma; 10 mg/mL in acetonitrile/water/TFA (50/50/1, v/v/v)) and one μL was deposited on a sample plate (28,29). Depicted spectra were averages of 100-256 consecutive laser pulses. The instrument was generally operated in the positive mode at an acceleration voltage of 23 kV combined with delayed extraction.

Table 1 Mutagenic primers of AVR4 used to introduce a Cys-to-Ala mutation in PVX::Avr4

Primer	5'	3'
C11Aa	CTT GGG GCT TGG CTG GGT TGT ATG G	
C11Ab	CCA TAC AAC CCA GCC AAG CCC CAA G	
C21Aa	CCT TGG GAC CCA TGG CCT TGG TGT CG	
C21Ab	CGA CAC CAA GGC CAT GGG TCC CAA GG	
C27Aa	GGG TTC GGG TAG AGG GCA TCC TTG GGA CCC	
C27Ab	GGG TCC CAA GGA TGC CAC TGT CGG GG	
C35Aa	GTA TGT AGG TTG TGG CAC TGT CGG GG	
C35Ab	CCC CGA CAG TGC CAC AAC CTA CAT AC	
C41Aa	CGT CGA GCG GTA CGG CCT GTA TGT AGG	
C41Ab	CCT ACA TAC AGG CCG TAC CGC TCG ACG	
C57Aa	GCA GTC CTT TTG GGG CTG GCT TAA CCA C	
C57Ab	GTG GTT AAG CCA GCC CCA AAA GGA CTG C	
C72Aa	GGT TTG GAT AGT CGG CCC ACT TCT TGC C	
C72Ab	GGC AAG AAG TGG GCC GAC TAT CCA AAC C	
C80Aa	GTC TTT ACC GGG GCC GTA CTC AGG	
C80Ab	CCT GAG TAC GGC CCC GGT AAA GAC	
OX10	CAA TCA CAG TGT TGG CTT GC	
N31	GAC CCT ATG GGC TGT GTT G	

Spectra were externally calibrated with bovine Cytochrome C (12,230.9 Da), Bovine Insulin (5,734.6 Da) (both Sigma) and Microperoxidase 8 (MP8, 1,506.5 Da; Ref. (30)).

Incubation of the AVR4 des-species with apoplastic fluid. Apoplastic fluids (AFs) were isolated from intercellular spaces of near isogenic tomato genotypes *Cf-4* and *Cf-0* (31), which had been inoculated with a *C. fulvum* race 4 (strain #38, a non-AVR4 producing strain) and a race 5, respectively (14). Native AVR4 and AVR4 *des*-species (4 μg) were incubated at 30 °C for 1 hr in the presence of 0.1 μL AF (~0.1 μg total protein). Protease inhibitors used were standard protein inhibitor cocktail with EDTA (Roche; 1 × per ml of AF). Protein samples were separated on tricine SDS-PAGE gels (32).

Polysaccharide substrate binding assay. Native AVR4 and AVR4 des-species (4 μg) were incubated at ambient temperature for 1 hr (unless stated otherwise) with an excess of 5 mg of insoluble chitin beads (New England Biolabs) or chitosan (Sigma) in 50 mM Tris·HCl (pH 8) and 150 mM NaCl (500 μL final volume) as described (19). The insoluble material was precipitated by centrifugation (13.000 g for 3 min). Supernatants were recovered and lyophilized. The pellet fraction was boiled in 200 μL 1% SDS to release bound protein and centrifuged. Both the retrieved supernatant (containing bound AVR4) and the lyophilized supernatant fraction (containing unbound AVR4) were examined for protein content of by tricine SDS-PAGE.

Molecular modeling of AVR4 with the tachycitin NMR structure. The mean NMR structure of tachycitin (ID code PDB databank: 1DQC) was used as template structure to model the structure of AVR4 using Modeler 6.1 (33-35). Additional loop refinement was used to model the two relatively large gaps (12 aa and 6 aa). The disulfide bridges were fixed during the calculations. Thousand models were constructed, of which the ten lowest scoring structures were further examined. The models were found reliable using standard algorithms (36,37).

RESULTS

Four Cys residues in AVR4 are required for induction of Cf-4-specific defense responses. By using transient PVX-mediated expression some AVR4 alleles, *i.e.* C35Y, Y38H and C80Y, were identified that exhibited reduced necrosis inducing activity (NIA) in the tomato genotype *Cf-4*, while the other natural Avr4 alleles induced no necrosis (14). To determine whether other Cys residues, for which no mutations were found in strains of C. fulvum, are also required for NIA of AVR4, we independently replaced all individual Cys

residues by Ala in PVX::*Avr4*. Four-week-old tomato plants were inoculated with these PVX::*Avr4* derivatives and NIA was scored (Fig 1) as described (14). The introduction of an Ala residue at the positions 35, 41, and 80 gave similar results as previously reported for the corresponding Tyr mutations (14). Interestingly, the mutations C21A and C27A were found to result in reduced necrosis on *Cf-4* tomato similar to the mutations C35A and C80A. The PVX::*Avr4* constructs carrying a Cys-to-Ala mutation in C11, C41, C57 or C72 induced no NIA on *Cf-4* tomato plants. These finding suggest that the latter four Cys residues have interrelated disulfide bonds in AVR4. For C21, C27, C35, and C80 of which the single mutations showed reduced NIA, double Cys-to-Ala mutations were constructed. Four of the six double mutants did no longer induce HR on *Cf-4* tomato, whereas mutants carrying the mutations C21A+C27A and C35A+C80A were as active as the corresponding single Cys-to-Ala mutants (Table 2). These data suggest that C21 is connected with C27 by a disulfide bond and C35 with C80 by another disulfide bond.

Figure 1. Necrosis-inducing activity of PVX::*Avr4* containing Cys-to-Ala mutations on the tomato cv. MM-Cf4. The first group of four plants were inoculated with PVX::*Avr4* containing a mutation in C11 (*1*), C41 (*5*), C57 (*6*), and C72 (*7*), respectively; note that these plants exhibited no necrosis, but rather mosaic symptoms induced by rival infection. The second group of four plants was inoculated with PVX::*Avr4* containing a mutation in C21 (*2*), C27 (*3*), C35 (*4*), and C80 (*8*), respectively; these plants developed severe necrotic symptoms and stunted growth. Photograph was taken 10 days post inoculation. The Cys residues involved in natural mutants are underlined.

Table 2 Necrosis-inducing activity (NIA) on tomato cv. MM-Cf4 of mutant PVX::*Avr4*

Single Cys-to-Ala mutation	Necrosis-inducing activity	Double Cys-to-Ala mutation	Necrosis-inducing activity
Wild type	+++++	C21A+C27A	++
C11A	-	C21A+C35A	-
C21A	++	C21A+C80A	-
C27A	++	C27A+C35A	-
C35A	++	C27A+C80A	-
C41A	-	C35A+C80A	++
C57A	-		
C72A	-		
C80A	++		

NIA was scored as described (14).

Chemical reduction and cyanylation of the disulfide bonds in AVR4. In order to determine the disulfide bond connectivities in AVR4 by a direct chemical approach, we partially reduced the disulfide bridges with tris-(2-carboxyethyl)-phosphine hydrochloride (TCEP) at pH 3.0. Acidic conditions prevent intramolecular rearrangements of disulfide bridges (38,39). The reduction of the cystines was directly followed by cyanylation of the newly formed thiol groups using 1-cyano-4-diethylamino-pyridinium (CDAP) under similar conditions. The reaction mixture was subsequently separated by reverse-phase HPLC (Fig 2A). In the presence of 6 molar equivalents of TCEP per AVR4, ~50% of native AVR4 was (partially) reduced, as determined from the HPLC profile. The newly formed species eluted at increased acetonitrile concentrations as compared to native AVR4 (Fig 2A). MALDI-TOF mass spectrometry identified subsequently four product peaks containing AVR4 species in which only one disulfide bond had been reduced (hereafter denoted as *des*-species; Fig 2B, 2C). Together these four *des*-species formed ~70% of the reduced AVR4 species. More than one disulfide bridge had undergone a reduction in the other species (as determined by mass spectrometry), which all eluted at even more increased acetonitrile concentrations. The increased retention time seemingly reflects a more unfolded state of these species resulting in increased hydrophobicity of isoform. The peaks, which eluted at 30.8 min and 30.9 min, could not be completely separated in the first HPLC run, but an additional HPLC run resulted in both species being more than 85% pure (Fig 2B).

Assignment of the disulfide bonds with mass mapping. To determine which disulfide bond was reduced in each *des*-species, the HPLC fractions were lyophilized and redissolved in 1 M NH_4OH, which induces base-catalyzed cleavage at the peptide bond that precedes the modified half-cystines (converting the cysteine in an iminothiazolidine derivative; *itz*) (27). After complete reduction, the reaction mixtures were analyzed by MALDI-TOF MS (Fig 3). Theoretically, the reaction should yield five peptide fragments per *des*-species, *i.e.* three peptide fragments originate from a double chain cleavage and two fragments originate from a β-elimination reaction (26,40). The latter is a side-reaction that occurs at either one of the two half-cystines thereby preventing chain cleavage at this half-cystine. Assignment of the disulfide bonds was performed in a two-step approach. Mass

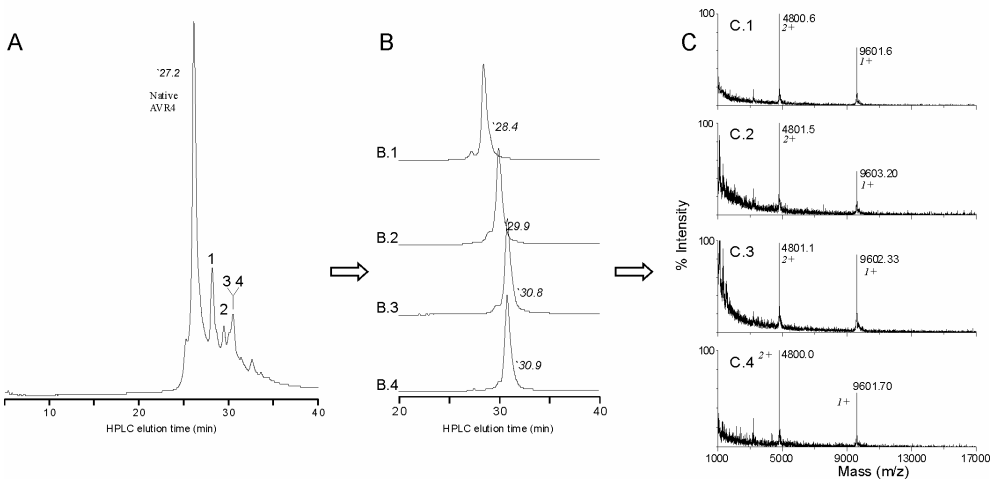

Figure 2. Purification of the partially reduced and cyanylated AVR4 species. (**A**) Peaks corresponding to singly reduced and cyanylated AVR4 species (*des*-species) are numbered 1-4. The collected speaks were repurified across a HPLC column (**B**) and subsequently analyzed by mass spectrometry for identification (**C**). The reaction involved 100 μg of AVR4 that reacted with a 6 fold excess of TCEP. The relative abundance of native AVR4 and the four *des*-species was: 48% (retention time (t_r) 27.2 min; native AVR4), 17% (28.4 min), 6.1% (29.9 min), 4.3%, (30.8 min), 8.2%, (30.9 min).

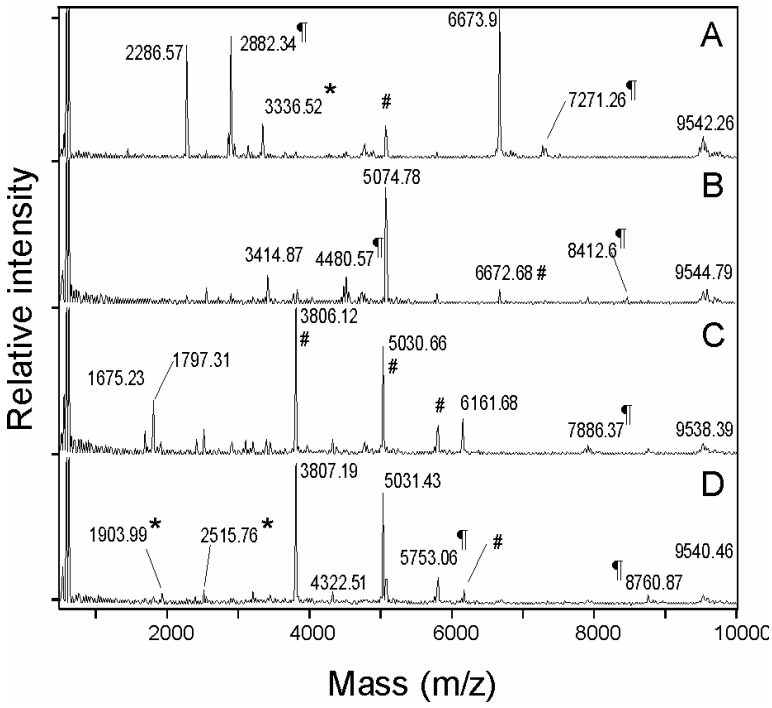

Figure 3. MALDI-TOF mass spectra of the four peptide mixtures obtained after base-induced cleavage of the peptide bond and full reduction of the *des*-species. Using the marked mass peaks (¶) the following disulfide bonds were identified: (A) C21–C27, (B) C11–C41, (C) C57–C72, and (D) C35–C80 (A-D reflects the order of elution from HPLC). Reoccurring mass peaks (#) reflect cross-contamination of some *des*-species, mass peaks corresponding to double charged mass peaks ($[M+2H]^{2+}$) are marked (∗); m/z, mass per charge.

peaks that corresponded to the N- and C-terminal peptide fragments towards the first reduced half-cystines were first identified. In Fig 3A, the mass peaks *m/z* 2286.6 Da and 6673.9 Da correspond such a peptide fragment encompassing the peptide fragments [1-20] and [27-86], respectively (Table 3). C27 is converted to an *itz*-derivative in the latter fragment. This assignment could subsequently be confirmed by other mass peaks that originate from the β-elimination reaction, *i.e. m/z* 2882.3 Da and 7271.3 Da (the peptide fragment [1-26] with a β-elimination at C21 and [21-86] with a β-elimination at C27, respectively). The remaining fragment (*itz*21-26) was too small to be detected due to the

settings of the lower mass detection limit (1000 Da). Together, these data establish the disulfide bond C21—C27. The relative mass deviations between measured and calculated mass were less than 0.05% for the majority of the peptide fragments. Comparable analyses of the other reaction mixtures resulted in the assignment of the other three disulfide bonds, *i.e.* C11—C41, C57—C72, and C35—C80 (Figures 3B, 3C and 3D, respectively). It was noted that some mass peaks reoccurred, *e.g.* the mass peaks 3805.4 and 5031.8 Da in fraction 3 (Fig 3C). Their relative intensity would suggest a substantial overlap between fraction 3 and 4, certainly more than as shown in the HPLC elution profile in Figure 2B. However, these two mass peaks were consistently readily observed in multiple independent replicate experiments, which suggests that these two peptides are easily ionized by MALDI. The intensity of the mass peaks does, therefore, not correspond to the actual concentration in the pooled fraction. In conclusion, this approach confirmed the two 'putative' disulfide bonds as deduced from the PVX data (Figure 1).

Three disulfide bonds are required for conformational stability of AVR4. Joosten et al. (14) showed previously that AVR4 isoforms encoded by natural *avr4* alleles appeared not to accumulate in tomato leaves during a compatible interaction (genotype *Cf-4*), while the expression levels appeared unaltered for these *avr4* genes as compared to the wild type *Avr4* gene. We compared the stability of the four *des*-species and that of native AVR4 in the presence of AF isolated from genotype *Cf-4* infected with a non-AVR4 producing strain of *C. fulvum*. First, in the absence of AF, both native AVR4 and the four *des*-species were found

Table 3 Theoretical mass, [M+H], of the peptide fragments obtained after base-catalyzed cleavage of the peptide bond as calculated for the AVR4 *des*-species[A]

des-[11 41]		*des*-[21-27]		*des*-[35-80]		*des*-[57-72]	
Fragment	*m/z*	Fragment	*m/z*	Fragment	*m/z*	Fragment	*m/z*
1-10	1144.3	1-20	2285.6	1-34	3805.4	1-56	6160.2
itz11-40	3415.9	itz21-26	676.8	itz35-79	5031.8	itz57-71	1800.0
itz41-86	5075.9	itz27-86	6673.7	itz80-86	798.9	itz72-86	1675.9
β-(1-40)	4482.2	β-(1-26)	2884.4	β-(1-79)	8759.2	β-(1-71)	7882.2
β-(11-86)	8413.8	β-(21-86)	7272.4	β-(35-86)	5752.7	β-(57-86)	3397.9

[A], AVR4 *des*-species denotes singly reduced and cyanylated AVR4 species.

β : β-elimination (40)

itz, 2-iminothiazolidine-4-carboxyl group

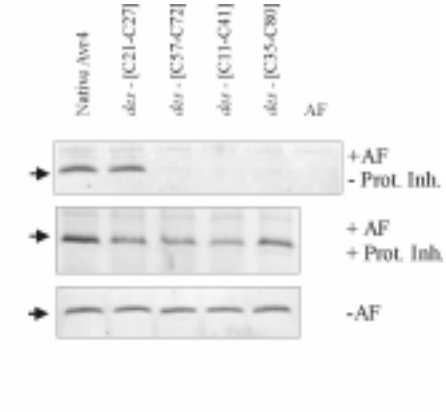

Figure 4. Stability of disulfide mutants of AVR4 in the presence of apoplastic fluid. Protein samples were incubated for one hr at 30°C in the absence (-AF) or presence (+AF) of apoplastic fluid. As control, AF was supplied with protease inhibitors (+Prot. Inh.). The stability was examined by SDS-PAGE. Sample loading order reflects the order of elution from the HPLC (Fig 2). AF was obtained from cv. MM-Cf4 infected with a race 4 *C. fulvum* (frame shift mutant). Experiments with AF form cv. MM infected with race 5 gave similar results (data not shown).

to be stable over the time span of one hr (Fig 4). However, in the presence of low concentrations of AF rapid degradation occurred of three of the four *des*-species, while native AVR4 and *des*-[C21—C27] were not affected by the incubation. On the other hand, in the presence of protease inhibitors, degradation of the three sensitive *des*-species was effectively blocked establishing that proteases were responsible for degradation. These results argue that the disulfide bonds C11—C41, C35—C80, and C57—C72 are important for conformational stability of AVR4.

AVR4 contains a single invertebrate chitin-binding domain. The identified disulfide pattern of AVR4 was further exploited to perform a query (URL:http://motif.genome.ad.jp). This search identified a homologous sequence stretch in genes of the invertebrates *Manduca sexta, Brugia malayi*, and *Penaeus japonicus*. These genes encode for chitinases. The homology is restricted to the C-terminal domain, which contains six conserved Cys residues. This C-terminal domain was recently identified as a chitin-binding domain designated the invertebrate Chitin-Binding Domain (inv ChBD) (23). For one family member, tachycitin of Japanese Horseshoe crab (*Tachypleus tridentatus*) (41), the disulfide bond

pattern has been solved. Unlike AVR4, tachycitin contains five disulfide bonds of which three reflect the conserved disulfide bonds of the inv ChBD motif. Sequence alignment appointed the conserved disulfide bridges in AVR, *i.e.* C11—C41, C35—C80, and C57—C72 (Fig 5). The additional disulfide bond C21—C27 within AVR4 does not share homology with the disulfide bonds in tachycitin. In contrast to tachycitin and AVR4, the other inv ChBD family members do not contain additional disulfide bonds. A three-dimensional model of AVR4 was constructed using the 3D-structure of tachycitin as a template structure (42) (data not shown). The modeled structure of AVR4 contains the secondary structure elements as found in tachycitin, but the sequence insertion encompassing the disulfide bridge C21—C27 was too large to construct a reliable model for this part of the protein.

Disulfide bonds disrupted mutants of AVR4 display affinity for chitin. In chapter 5, it is demonstrated that native AVR4 binds specifically to chitin, but not to other cell wall polysaccharides (19). Moreover, for human chitinase, it has been shown that the six conserved Cys residues that belong to the inv ChBD need to be intact for chitin binding (43). To examine whether AVR4 des-species still exhibited chitin-binding activity, we incubated the *des*-species with chitin (Fig 6). Following incubation, each of the *des*-species was detected the chitin-containing pellet. This suggests that absence of one disulfide bridge in

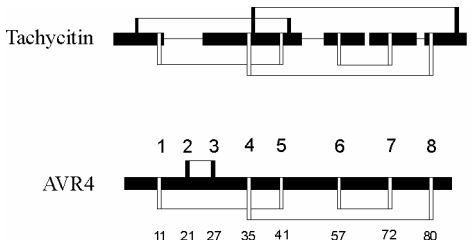

Figure 5. Schematic diagram of the disulfide bond pattern of tachycitin and AVR4. The connected open bars represent three conserved disulfide bonds of the invertebrate chitin-binding domain (inv ChBD). The connected filled bars represent additional disulfide bonds. Gaps in the alignment are represented as a thin line in tachycitin. Residue number and successive number of the Cys residues are indicated at the *bottom* and *top*, respectively. The diagram is based on the alignment of AVR4 with other inv ChBDs using the consensus found in the Pfam database (19,47,48).

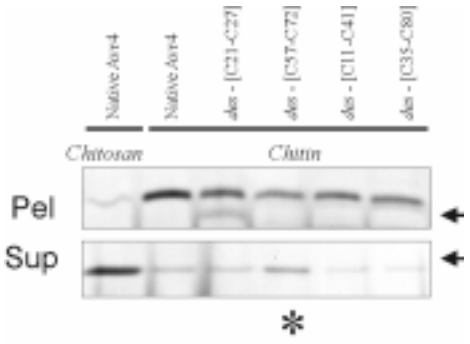

Figure 6. Chitin-binding affinity of the disulfide bond disrupted isoforms of AVR4 (*des*-species). The *des*-species were incubated together with insoluble chitin and the chitin-binding affinity was estimated by SDS-PAGE. Chitosan, to which native AVR4 does not bind, was included as negative control. Note that more *des*-[C57-C72] (∗) remains in solution as compared to the other *des*-species. Pel, chitin pellet; Sup, supernatant.

AVR4 does not abolish the affinity for chitin. However, for *des*-[C57—C72] binding was repeatedly less complete than for the other three *des*-species (as more protein remained in solution) (Fig 6), but after prolonged incubation (from 1 to 4 hrs) all of the *des*-[C57—C72] protein was found in the pellet. This finding suggests a decreased affinity of this AVR4 isoform for chitin. It is noted that *des*-[C57—C72] is potentially contaminated with *des*-[C35—C80], which could have interfered with the chitin-binding assay. As *des*-[C35—C80] has a comparable chitin-binding affinity as native AVR4, the *des*-[C57—C72] might even exhibit a lower affinity than observed in our assay.

Binding to chitin extends the lifetime of the des-*species in the presence of apoplastic fluid.* During growth in tomato *C. fulvum* remains confined to the intercellular spaces of tomato (44). It has been proposed that after release AVR4 associates directly to regions of the hyphal walls of *C. fulvum* where chitin is exposed (19). When chitin is saturated, excess of AVR4 may than locate throughout the apoplast. We investigated whether the various *des*-species were less sensitive to proteolytic degradation after binding to chitin. Therefore, we incubated the *des*-species with chitin for 4 hrs, rather than one, to ensure complete association between these proteins and chitin. After incubation with chitin, the

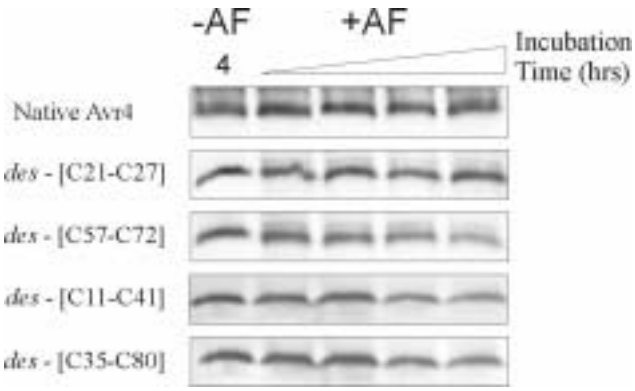

Figure 7. Binding to chitin stabilizes the disulfide bond disrupted isoforms of AVR4 (des-species). AVR4 and the *des*-species were trapped to chitin before incubation with apoplastic fluid Upon addition of AF, the stability of the protein species was followed over the course of four hrs, and analyzed by SDS-PAGE. As control, a parallel experiment was performed without AF. Samples were taken at 30 min, 1 hr, 2 hrs, and 4 hrs. Control is only shown for 4 hrs.

solutions were supplied with AF and stability of the AVR4 isoforms was followed in time. Over the period of four hrs, native AVR4 and *des*-[C21—C27] bound to chitin, remained fully stable in the presence of AF (Fig 7). Moreover, association with chitin resulted in an increased half-life time of *des*-[C11—C41], *des*-[C35—C80] and *des*-[C57—C72] in the presence of AF. Thus, when bound to chitin, normally unstable *des*-species are protected against proteases present in AF.

Discussion

Here, we have elucidated the disulfide bridge pattern of AVR4 by a method known as partial reduction/mass mapping. The method allowed us to selectively disrupt a single disulfide bond in AVR4 and to purify these so-called *des*-species for further research. The following disulfide bonds were found in AVR4: C11—C41, C21—C27, C35—C80, and C57—C72. A query based on this disulfide bond pattern and the spacing between the Cys residues indicated that AVR4 contains the invertebrate chitin-binding domain (inv ChBD) family (23). Except for tachycitin, no disulfide bridge pattern has been solved for any of the family

members (29). For AVR4, we found that three disulfide bonds, excluding C21—C27, are essential for protein stability and the six Cys residues involved in these bonds are conserved amongst the inv ChBD family (23). Although for human chitinase it has been demonstrated that all these six Cys residues are essential for recognition of chitin (43), disruption of one of the conserved disulfide bonds for AVR4 does not result in a complete loss of binding to chitin. However, disruption of the disulfide bond C57—C72 appeared to reduce the affinity for chitin in the case of this particular *des*-species.

Strains of *C. fulvum* were found to evade *Cf-4*-mediated resistance by producing AVR4 mutant proteins. The majority of these modifications involved substitution of Cys residues at positions 35, 41, and 80 by Tyr (14), indicating that disruption of only two of the three conserved disulfide bonds has, so far, contributed to evasion of AVR4 recognition. When AVR4 mutant proteins carrying a disruption in one of these conserved disulfide bonds were exposed to apoplastic fluid (AF) isolated from healthy or *C. fulvum* infected tomato leaves, the isoforms were found to be rapidly degraded as a result of protease activity present in AF. Thus, as suggested by Joosten et al. (14), *C. fulvum* evades *Cf-4* mediated resistance by production of AVR4 isoforms that are degraded due to protease activity present in AF. As fore mentioned, these unstable AVR4 isoforms still exhibited chitin-binding activity.

Supporting data for a role of C57—C72 in chitin-binding comes from the 3D-structure of tachycitin. Part of the structure of tachycitin can be superimposed on the structure of hevein, a plant chitin-binding lectin (42). This part of tachycitin was, therefore, proposed to act as the chitin-binding site. The shared structural motif encompasses the second β-sheet in tachycitin, a short helical turn, and the third conserved disulfide bridge of the inv ChBD motif (C57—C72 in AVR4). In chapter 6, it is described that AVR4 and tachycitin adopt a similar protein fold and that the residues important in AVR4 for the interaction with chitin could be superimposed on the structure of hevein. The findings in this chapter predict that strains of *C. fulvum* will evade *Cf-4*-mediated resistance when they produce an AVR4 isoform that lacks the disulfide bond C57—C72. However, strains of *C. fulvum* producing such a disulfide bond disrupted mutant have not yet been identified. A possible explanation for the absence of such a strain could be that selection pressure exists on the chitin-binding functionality of AVR4. Modification of this disulfide bond C57—C72 could, therefore, come with a virulence penalty for *C. fulvum.*

As opposed to three conserved disulfide bonds, our data indicate that the disulfide bond C21—C27 does not contribute to conformational stability of AVR4. Possibly, this

disulfide bond is required for local conformational stability around the sequence insertion. However, preliminary NMR data indicate that the sequence insertion surrounding C21 adopts a α-helix in AVR4 (chapter 6). As the α-helix apparently increases the stability of this part of the structure, the disulfide bond C21—C27 itself would not be essential for the conformational stability of AVR4. Similar observations for the role of additional disulfide bonds were previously reported for the cystine-knot fold (45).

When the necrosis-inducing activity (NIA) was tested of the AVR4 isoform lacking the disulfide bond C21—C27 in *Cf-4* tomato using PVX, the NIA was found to be similar to the NIA of AVR4 isoforms lacking C35—C80. NIA of both mutant proteins, however, is less than that of native AVR4. However, in contrast to disulfide bond C35—C80, disulfide bond C21—C27 does not contribute to protein stability, suggesting that the mechanisms underlying the reduced NIA of both AVR4 *des*-species are different. In the case that the disulfide bond C35—C80 is disrupted, a certain fraction of the resulting protein will be degraded by proteases present in the intercellular space, while the remaining fraction of protein triggers to some degree the *Cf-4*-mediated defense responses. The reduced NIA of AVR4 mutant carrying a disrupted disulfide bond C21—Cy27 cannot be explained by sensitivity to proteases, but is most likely due to the amino acid substitution itself or due to a conformation change of the protein. The remaining NIA could be a reason why, in spite of the fact that disruption of disulfide bond C21—C27 does not affect chitin-binding activity of AVR4, no natural *C. fulvum* strains have thus far been found that carry such a mutation.

In addition to the three Cys-to-Tyr substitutions found in natural isolates, two other natural amino acid mutations have been found in AVR4 (T37I and Y38H). Both modifications are thought to affect the conformational stability of AVR4, based on a report by Zhu and Braun (46). The latter two mutations affect the strand β2 of the first anti-parallel β-sheet, which is in the core of the protein structure (42). In AVR4, T37 and Y38 are putatively paired with P30 and Y29 in strand β1, respectively. These four residues are well conserved in the inv ChBD (19). The report of Zhu and Braun indicates that Pro-Ile cross-strand contact pairs in β-strands are virtually absent, whereas Pro-Thr cross-strand contact pairs are allowed (46). Similarly, aromatic residues are exclusively found at position 38 (Y/F/W>98%) of the inv ChBD. Hydrophobic residues are found to be the favorite cross-strand contact partners, whereas His residues are disfavored. Based on these statistical analyses, we propose that the mutations T37I and Y38H both will lead to a partially destabilized first anti-parallel β-sheet, which could decrease the overall conformational stability of AVR4 and increase its sensitivity to proteases.

Overall, the natural AVR4 isoforms lacking one disulfide bond appear to show increased sensitivity towards proteases present in the apoplast as compared to native AVR4. However, after binding to chitin in the cell wall of *C. fulvum,* these mutant isoforms seem to escape degradation by proteases present in the apoplast. Thus, while *Cf-4*-mediated recognition is evaded, the chitin-binding activity of natural AVR4 mutants of *C. fulvum* remains, thereby contributing to the protection of *C. fulvum* against plant chitinases.

Table 4 Summary of the observed phenotypes per disrupted disulfide bond in AVR4

Disrupted disulfide bond[1]	Cys residue pair[2]	Necrosis-inducing activity (NIA)[3]	Stability in AF[4]	Binding to Chitin[5]	Stability of the AVR4 chitin complex[6]	Number of strains of race 4[7]
Native	-	+++++	+	+	+	
C21-C27	2-3	+++	+	+	+	0
C57-C72	6-7	–	–	+/–	+ (+/–)	0
C11-C41	1-5	–	–	+	+ (+/–)	2
C35-C80	4-8	+++	–	+	+	6

1) Disruption of one disulfide bond by either a cysteine substitution in PVX::*Avr4* or by partial reduction
2) Successive numbering of the Cys residues as in Fig 5
3) Necrosis inducing activity (NIA) was assayed on tomato cv. MM-Cf4 using PVX::*Avr4* (Fig 1)
4) AVR4 *des*-species is present (+) or absent (-)after incubation with apoplastic fluid (AF) (Fig 4)
5) Affinity of AVR4 *des*-species for chitin; +, binds to chitin; +/- decreased affinity for chitin (Fig 6)
6) Stability of AVR4 *des*-species when bound to chitin in the presence of AF; +, stable ; partially stable in the presence of chitin (Fig 7)
7) Number of strains of *Cladosporium fulvum* identified so far with a single Cys substitution (12,14).

REFERENCES

1. Flor, H. H. (1971) *Annu. Rev. Phytopathol.* **9,** 275-296
2. Dangl, J. L., and Jones, J. D. G. (2001) *Nature* **411,** 826-833
3. Joosten, M. H. A. J., and de Wit, P. J. G. M. (1999) *Annu. Rev. Phytopathol.* **37,** 335-367
4. Romeis, T., Piedras, P., Zhang, S. Q., Klessig, D. F., Hirt, H., and Jones, J. D. G. (1999) *Plant Cell* **11,** 273-287
5. de Jong, C. F., Honée, G., Joosten, M. H. A. J., and de Wit, P. J. G. M. (2000) *Physiol. Mol. Plant Pathol.* **56,** 169-177
6. Durrant, W. E., Rowland, O., Piedras, P., Hammond-Kosack, K. E., and Jones, J. D. G. (2000) *Plant Cell* **12,** 963-977.
7. Romeis, T., Ludwig, A. A., Martin, R., and Jones, J. D. G. (2001) *EMBO J.* **20,** 5556-5567.
8. de Jong, C. F., Laxalt, A. M., Ligterink, W., de Wit, P. J. G. M., Joosten, M. H. A. J., and Munnik, T. (2002) submitted
9. Rivas, S., Mucyn, T., van den Burg, H. A., Vervoort, J., and Jones, J. D. G. (2002) *Plant J.* **29,** 783-796
10. Day, P. R. (1957) *Nature* **179,** 1141
11. van Kan, J. A. L., van den Ackerveken, G. F. J. M., and de Wit, P. J. G. M. (1991) *Mol. Plant-Microbe Interact.* **4,** 52-59
12. Joosten, M. H. A. J., Cozijnsen, T. J., and de Wit, P. J. G. M. (1994) *Nature* **367,** 384-386
13. Luderer, R., Takken, F. L., de Wit, P. J. G. M., and Joosten, M. H. A. J. (2002) *Mol. Microbiol.* **45,** 875-84.
14. Joosten, M. H. A. J., Vogelsang, R., Cozijnsen, T. J., Verberne, M. C., and de Wit, P. J. G. M. (1997) *Plant Cell* **9,** 367-379
15. Luderer, R., de Kock, M. J. D., Dees, R. H. L., de Wit, P. J. G. M., and Joosten, M. H. A. J. (2002) *Mol. Plant Pathol.* **3,** 91-95
16. Kjemtrup, S., Nimchuk, Z., and Dangl, J. L. (2000) *Curr. Opin. Microbiol* **3,** 73-78
17. White, F. F., Yang, B., and Johnson, L. B. (2000) *Curr. Opin. Plant Biol.* **3,** 291-298
18. Bonas, U., and Lahaye, T. (2002) *Curr. Opin. Microbiol.* **5,** 44-50
19. van den Burg, H. A., Harrison, S., Joosten, M. H. A. J., de Wit, P. J. G. M., and Vervoort, J. (2003) submitted
20. van den Burg, H. A., de Wit, P. J. G. M., and Vervoort, J. (2001) *J. Biomol. NMR* **20,** 251-261
21. Harrison, P. M., and Sternberg, M. J. E. (1996) *J. Mol. Biol.* **264,** 603-623
22. Mas, J. M., Aloy, P., Marti, R. M. A., Oliva, B., Blanco, A. C., Molina, M. A., De, L. R., Querol, E., and Aviles, F. X. (1998) *J. Mol. Biol.* **284,** 541-548
23. Shen, Z., and Jacobs-Lorena, M. (1999) *J. Mol. Evol.* **48,** 341-347

24. Chapman, S., Kavanagh, T., and Baulcombe, D. (1992) *Plant J.* **2,** 549-557
25. de Wit, P. J. G. M., and Flach, W. (1979) *Physiol. Plant Pathol.* **15,** 257-267
26. Wu, J., and Watson, J. T. (1997) *Protein Sci.* **6,** 391-398
27. Wu, J., and Watson, J. T. (1998) *Anal. Biochem.* **258,** 268-276
28. Karas, M., and Hillenkamp, F. (1988) *Anal. Chem.* **60,** 2299-2301
29. Kussmann, M., Nordhoff, E., Rahbek-Nielsen, H., Haebel, S., Rossel-Larsen, M., Jakobsen, L., Gobom, J., Mirgorodskaya, E., Kroll-Kristensen, A., Palm, L., and Roepstorff, P. (1997) *J. Mass Spectrom.* **32,** 593-601
30. Primus, J. L., Boersma, M. G., Mandon, D., Boeren, S., Veeger, C., Weiss, R., and Rietjens, I. M. (1999) *J. Biol. Inorg. Chem.* **4,** 274-283.
31. de Wit, P. J. G. M., and Spikman, G. (1982) *Physiol. Plant Pathol.* **21,** 1-11
32. Schägger, H., and Von Jagow, G. (1987) *Anal. Biochem.* **166,** 368-379
33. Sali, A., and Blundell, T. L. (1993) *J. Mol. Biol.* **234,** 779-815
34. Sali, A., Potterton, L., Yuan, F., Van Vlijmen, H., and Karplus, M. (1995) *Proteins* **23,** 318-326
35. Fiser, A., Do, R. K. G., and Sali, A. (2000) *Protein Sci.* **9,** 1753-1773
36. Sippl, M. J. (1993) *Proteins* **17,** 355-362
37. Sanchez, R., and Sali, A. (1998) *Proc. Natl. Acad. Sci. USA* **95,** 13597-13602
38. Gray, W. R. (1993) *Protein Sci.* **2,** 1732-1748
39. van den Hooven, H. W., van den Burg, H. A., Vossen, P., Boeren, S., de Wit, P. J. G. M., and Vervoort, J. (2001) *Biochemistry* **40,** 3458-3466
40. Degani, Y., and Patchornik, A. (1974) *Biochemistry* **13,** 1-11
41. Kawabata, S., Nagayama, R., Hirata, M., Shigenaga, T., Agarwala, K. L., Saito, T., Cho, J., Nakajima, H., Takagi, T., and Iwanaga, S. (1996) *J. Biochem.* **120,** 1253-1260
42. Suetake, T., Tsuda, S., Kawabata, S., Miura, K., Iwanaga, S., Hikichi, K., Nitta, K., and Kawano, K. (2000) *J. Biol. Chem.* **275,** 17929-17932
43. Tjoelker, L. W., Gosting, L., Frey, S., Hunter, C. L., Trong, H. L., Steiner, B., Brammer, H., and Gray, P. W. (2000) *J. Biol. Chem.* **275,** 514-520
44. de Wit, P. J. G. M. (1977) *Neth. J. Plant Pathol.* **83,** 109-122
45. Darling, R. J., Ruddon, R. W., Perini, F., and Bedows, E. (2000) *J. Biol. Chem.* **275,** 15413-15421.
46. Zhu, H., and Braun, W. (1999) *Protein Sci.* **8,** 326-342
47. Schultz, J., Milpetz, F., Bork, P., and Ponting, C. P. (1998) *Proc. Natl. Acad. Sci. USA* **95,** 5857-5864
48. Bateman, A., Birney, W., Cerruti, L., Durbin, R., Etwiller, L., Eddy, S. R., Griffiths-Jones, S., Howe, K. L., Marshall, M., and Sonnhammer, E. L. (2002) *Nuc. Acids Res.* **30,** 281-283

5

Avirulence factor AVR4 of the tomato pathogen *Cladosporium fulvum* is a chitin-binding lectin that protects fungi against plant chitinases

Harrold A. van den Burg, Stuart J. Harrison, Matthieu H.A.J. Joosten, Jacques Vervoort, and Pierre J.G.M. de Wit

(submitted for publication)

ABSTRACT

Recognition of the avirulence protein AVR4 of the pathogenic fungus *Cladosporium fulvum* is mediated by the tomato *Cf-4* resistance gene. So far, no intrinsic functions have been demonstrated for AVR elicitors of *C. fulvum*. Here, AVR4 is discovered to constitute a functional invertebrate chitin-binding domain (inv. ChBD), a domain abundantly present in proteins of eukaryotes, but so far not found in fungi and plants. AVR4 binds to chitin present in cell walls of *Trichoderma viride* and *Fusarium solani* f.sp. *phaseoli*, and protects these fungi against lysis by plant chitinases. Chitin in cell walls of *in vitro*-grown *C. fulvum* is not accessible and the fungus does not produce AVR4 under these conditions. However, during infection of tomato, chitin in cell walls of *C. fulvum* is accessible and production of AVR4 is induced to protect the fungus against tomato chitinases. Thus, in contrast to most bacterial AVR factors that actively suppress host defense responses, AVR4 may have a role in the protection of *C. fulvum* against host defense responses.

INTRODUCTION

In general, plant defense responses are activated upon specific recognition of a pathogen-derived avirulence gene (*Avr*) product (also called elicitor) by plants expressing the matching resistance gene (*R*) (Dangl and Jones, 2001). Apart from their role in triggering defense responses in resistant plants, AVR proteins are anticipated to contribute to virulence in susceptible hosts (Kjemtrup et al., 2000; White et al., 2000; Bonas and Lahaye, 2002). For some bacterial AVR proteins, it has been reported that they are required for full virulence (*e.g.* Casper-Lindley et al., 2002; Guttman et al., 2002). The interaction between these so-called effector proteins and their virulence targets inside the host cytoplasm is also relevant for *R* gene-mediated recognition (Kim et al., 2002; Mackey et al., 2002).

In contrast, very little is known about intrinsic functions of fungal elicitors (Laugé and de Wit, 1998; Idnurm and Howlett, 2001; Van 't Slot and Knogge, 2002). In a few cases a biological function has been suggested. The *AVR-Pita* gene of the rice blast fungus (*Magnaporthe grisea*) encodes a putative secreted metalloprotease (Orbach et al., 2000) and the avirulence protein NIP1 of the barley pathogen *Rhynchosporium secalis* stimulates H^+-ATPases of barley and other plants (Wevelsiep et al., 1993). The largest group of fungal elicitors has been identified in the well-established *Cladosporium fulvum*-tomato system (de

Wit and Joosten, 1999; Joosten and de Wit, 1999). The *C. fulvum* elicitor proteins, including race-specific (AVRs) and non-race-specific (ECPs) elicitors, have in common that they are secreted, small, and cysteine-rich (reviewed in Joosten and de Wit, 1999; Laugé et al., 2000; Luderer et al., 2002). Despite these common features, the genes are all distinct and homologous sequences have not yet been identified in other organisms. For the AVR9 elicitor protein a putative biological function was proposed on the basis of structural homology with carboxy peptidase inhibitor, but this could not be shown experimentally (van den Hooven et al., 2001). Gene replacement studies demonstrated that the ECP1 and ECP2 elicitor proteins have a role in virulence of *C. fulvum* (Laugé et al., 1997), but their intrinsic functions are still unknown.

Virulence of strains of *C. fulvum* on tomato plants carrying *Cf*-genes was accompanied by either the loss of the matching *Avr* gene (van Kan et al., 1991) or mutations in the matching *Avr* gene resulting in either truncated proteins (Joosten et al., 1997; Luderer et al., 2002) or single amino acid substitutions (Joosten et al., 1994, 1997). All but one of the identified alleles of *Avr4* fall in the last category, *i.e.* they all contain single base-pair mutations that result in all but one case in single amino acid substitutions (Joosten et al., 1994, 1997). This indicates that the *Avr4* gene is apparently preserved and therefore also its intrinsic function, whereas other *Avrs* are apparently not strictly required for virulence of *C. fulvum*. Some of the mutant *Avr4* alleles still induce a weak hypersensitive response (HR) when transiently expressed using the PVX virus in the tomato genotype *Cf-4*, but the encoded isoforms could not be detected in apoplastic fluid from tomato inoculated with the corresponding strains of *C. fulvum* (Joosten et al., 1997). Most strains of *C. fulvum* virulent on the tomato genotype *Cf-4* contain mutant *Avr4* alleles resulting in single Cys-to-Tyr mutations. Mass analysis indicated that all eight cysteines in AVR4 are involved in disulfide bonding (chapter 2) and that the disulfide bridge pattern of AVR4 (chapter 4) was similar to that of the invertebrate chitin-binding domain (inv ChBD) (Kawabata et al., 1996; Shen and Jacobs-Lorena, 1999; Suetake et al., 2000).

Chitin-binding domains (ChBD) are closely related to plant defense responses. First, production of fungal cell wall degrading enzymes like chitinases is elevated after (fungal) infection (Joosten and de Wit , 1989; Stintzi et al., 1993). Fungal growth is inhibited by basic chitinases, which contain a catalytic domain and a plant ChBD or so-called hevein domain (Mauch et al., 1988; Sela-Buurlage et al., 1993; Neuhaus, 1999). Second, these hevein domains are found as multiple copies in anti-microbial proteins of plants such as wheat germ agglutinin (WGA) (Ciopraga et al., 1999), *Urtica dioica* agglutinin (UDA)

(Broekaert et al., 1989), and the Ac-AMP1/Ac-AMP2 proteins of *Amaranthus caudatus* (Broekaert et al., 1992). Similar to the hevein domain, the inv ChBD is fused with catalytic domains in chitinases of *Arthropoda*, *Chordata*, and *Metazoa* (Shen and Jacobs-Lorena, 1997) and occurs as multiple copies in proteins like peritrophin-44 (Elvin et al., 1996). Peritrophin-44 is an integral protein of the extracellular matrix of the insect gut and it constitutes a large proportion of this matrix (Elvin et al., 1996).

Here we report that AVR4 contains a functional inv ChBD that protects fungi against deleterious effects of plant chitinases. This protection is achieved by binding of AVR4 to chitin present and exposed at the walls of fungi, *e.g.* the walls of *Trichoderma viride* and *Fusarium solani* f.sp. *phaseoli*. *C. fulvum* grown *in vitro* is not sensitive to tomato chitinases, which appears to be due to inaccessibility of chitin in the cell walls. AVR4 is also not produced by *C. fulvum in vitro*, but during infection of tomato AVR4 is produced and chitin is accessible for AVR4 at cell walls of infecting hyphae, which suggests that AVR4 could have a similar function during infection. These data support a defensive virulence function of AVR4, which contrasts to most virulence functions reported for other pathogens, which seems to be offensive, as they suppress host defense responses.

RESULTS

AVR4 Contains an Invertebrate Chitin-Binding Domain

The disulfide bond connectivities of AVR4 were determined by a method known as partial reduction/mass mapping (chapter 4). A query (URL:http://motif.genome.ad.jp) based on the spacing of the cysteine residues and the disulfide bond pattern of AVR4 revealed that the spacing and the disulfide bridges between six of the eight cysteine residues of AVR4, i.e. Cys(1)-Cys(5), Cys(4)-Cys(8), and Cys(6)-Cys(7) (Figure 1), are similar to the spacing and disulfide bond pattern of six of the ten cysteine residues in tachycitin, a member of the inv ChBD family (Kawabata et al., 1996). These six cysteine residues are conserved for the inv ChBD family and the interconnecting disulfide bridges stabilize the fold of the domain (Suetake et al., 2000). The sequence alignment of AVR4 with other members of the inv ChBD family indicated that AVR4 contains the consensus of the domain (Figure 1), *i.e.* five small residues putatively restricting protein conformation (s), three hydrophobic patches (h and a), and two conserved aromatic residues (a) involved in an interaction in the core of the

protein fold. In conclusion, AVR4 contains the characteristic amino acid residues of the inv ChBD required for the fold and putatively the functionality of the domain.

AVR4 Binds Specifically to Chitin

The indication that AVR4 belongs to the inv ChBD family prompted us to test whether the domain was indeed functional. Therefore, AVR4 was incubated with chitin and other insoluble polysaccharides, which are all found in cell walls of various organisms. After incubation, AVR4 remained in solution for most of the polysaccharides except for chitin (both chitin beads and crab shell chitin) (Figure 2A). Boiling of the pellet fraction in 1% SDS effectively disrupted the interaction between AVR4 and chitin. Binding of AVR4 to chitin was (partially) reversible under acidic conditions (data not shown). As control proteins, we used the extracellular proteins ECP1 (van den Ackerveken et al., 1993b) and ECP4 (Laugé et al., 2000) of *C. fulvum*, which both lack an inv ChBD. ECP1 and ECP4 showed no specific

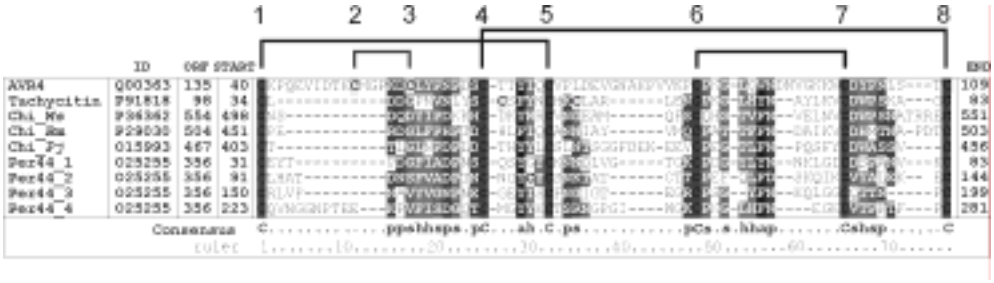

Figure 1. Sequence alignment of the inv ChBD of AVR4 with other family members. The alignment (made in ClustalX; Thompson et al., 1997) and the disulfide bond pattern of AVR4 are shown. The six conserved Cys residues are in red (AVR4 and tachycitin contain additional Cys, yellow). Sequences shown are (*top-to-bottom)*: AVR4 of *Cladosporium fulvum,* tachycitin of *Tachypleus tridentatus* (Japanese horseshoe crab), Chitinase (EC 3.2.1.14) of *Manduca sexta (*Tobacco hawkmoth), *Brugia malayi* (nematode), *Penaeus japonicus* (prawn), and Peritrophin-44 of *Lucilia cuprina* (fly) containing 4 domains. The consensus (80% similar) is given (*bottom*: a, aromatic; h, hydrophobic; p, polar; s, small residues). ID, *ID-code used in the trEMBL database*; ORF, *total number of residues in the ORF*; start/end, *first and last residue belonging to domain*, *respectively*.

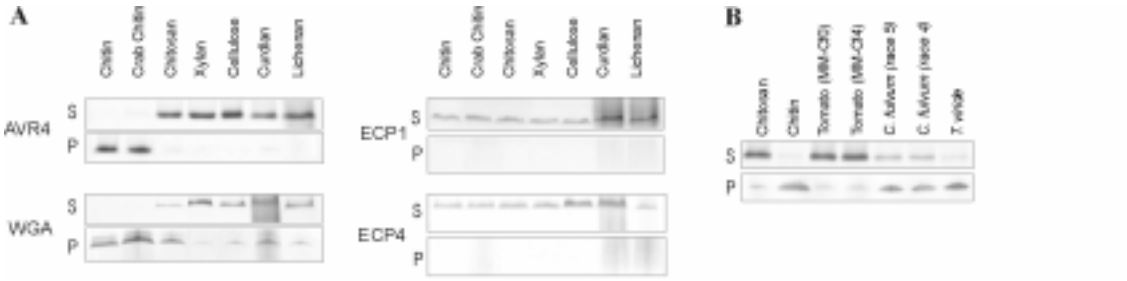

Figure 2. AVR4 binds specifically to crystalline chitin and fungal cell wall fractions. (**A**) Exposure of AVR4, WGA, ECP1 and ECP4 to insoluble polysaccharides. Both AVR4 and WGA bind to chitin. (**B**) Exposure of AVR4 to cell wall fractions of *Cladosporium fulvum* (race 4 and race 5), *Trichoderma viride*, and tomato leaves (cv. MM-Cf0 and MM-Cf4). Chitin and chitosan are included as positive and negative control, respectively. S, supernatant; P, pellet containing the insoluble polysaccharide / cell wall fraction.

affinity for the tested polysaccharides (Figure 2A). As positive control, we used wheat germ agglutinin (WGA), a plant chitin-binding lectin (Bains et al., 1992). WGA binds both to chitin and chitosan (Figure 2A). Together, these data establish that AVR4 is a functional chitin-binding lectin.

During infection of tomato, *C. fulvum* remains confined to the intercellular spaces of leaves (de Wit, 1977). AVR4 released in the apoplast will, therefore, be exposed to both cell walls of *C. fulvum* and tomato. To exclude that AVR4 interacts with polysaccharides present in tomato cell walls, we incubated AVR4 with cell wall fractions isolated from leaves of tomato. In addition, we incubated AVR4 with cell wall fractions obtained from mycelium of two strains of *C. fulvum* and from the soil-borne fungus *Trichoderma viride.* Cell wall material of *T. viride* was included as growth of *T. viride* is effectively inhibited by plant chitinases alone (Mauch et al., 1988). After incubation, AVR4 was hardly detected in the pellet containing tomato cell wall fractions (at best at similar levels as in the chitosan control), whereas AVR4 was predominantly found in the pellet containing the fungal cell wall fractions (Figure 2B). The data suggest that AVR4 has a higher affinity for the fractions of *T. viride* than for those of *C. fulvum*, which could be due to differences in composition of the cell

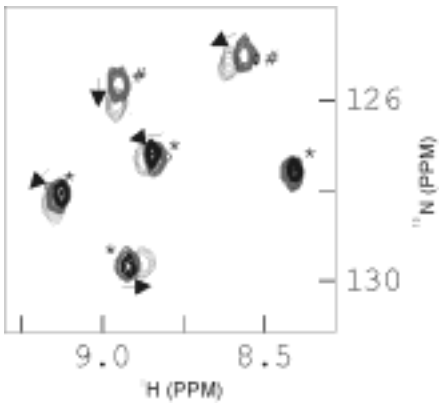

Figure 3. AVR4 interacts with soluble chito-oligomers of three or more residues as determined by nuclear magnetic resonance. The chemical shift resonances (σ) of the backbone amides of AVR4 are affected in the presence of 27 mM $(GlcNAc)_3$ (dark grey, $\Delta\sigma$ indicated by $\rightarrow$), 3.5 mM $(GlcNAc)_6$ (black, increased line with; #; less increased line width, $*$) and without ligand (light grey). Spectra were recorded at a saturated ligand concentration. Lowest depicted contour level is 30% above signal-to-noise intensity.

walls. From these experiments, it is clear that AVR4 binds to a component that is present in fungal cell walls, but absent in plant cell walls. Chitin is the best candidate component as it is abundantly present in fungal cell walls and is absent in plant cell walls (Wessels and Sietsma, 1981).

AVR4 binds to chito-oligomers of three residues or more

Chitin is a biopolymer of *N*-acetyl-D-glucosamine (GlcNAc). We examined whether AVR4 could interact with GlcNAc oligomers of different lengths. NMR was used as technique as subtle conformational changes caused by ligand interactions, are reflected in small shifts of the backbone amide resonances of the protein (Asensio et al., 1995). Indeed, the backbone amide resonances of AVR4 shifted due to the addition of small quantities of $(GlcNAc)_3$ (Figure 3; $\rightarrow$), whereas concentrations of 30 mM of either GlcNAc or $(GlcNAc)_2$ had no effect. Thus, the binding-site of AVR4 seems to facilitate an interaction with three GlcNAc residues (discussed in more extend in chapter 6). The line width of the amide resonances of AVR4 increased substantially in the presence of $(GlcNAc)_6$ as compared to $(GlcNAc)_3$ (Figure 3, #), which indicates a substantial increase of the apparent mass of the complex (whereas the mass is expected to increase with ~6% if one AVR4 molecule binds to one chito-oligomer). We expect that the apparent increased mass of AVR4 is likely due to binding of more than one AVR4 molecule to $(GlcNAc)_6$ (chapter 6). Higher concentrations of

AVR4 (up to 2 mM) in the absence of chito-oligomers gave no changes in the line width (data not shown), which excludes non-specific aggregation of the AVR4 protein under the NMR conditions tested. The spectral overlap between non-complexed and complexed AVR4 was still substantial, which indicates the absence of large conformational differences between AVR4 in complex with either one of the two chito-oligomers.

AVR4 reduces chitinase activity by binding to its substrate

Plant chitinases (PR-3) form an important class of fungal cell wall hydrolyzing enzymes that are actively produced during plant defense responses (Stintzi et al., 1993). We examined whether AVR4 had any affect on the activity of the well-characterized basic chitinase (ChiI) of tobacco (Sela-Buurlage et al., 1993). Chitin azure, for which AVR4 displayed affinity (data not shown), was used as chitinase substrate. To facilitate binding of AVR4 to the substrate, AVR4 was incubated with chitin azure prior to adding ChiI. Increased concentrations of AVR4 effectively reduced chitinase activity, whereas similar concentrations of ECP1 had no effect (Figure 4). Pre-incubation of AVR4 with a three-fold molar excess of $(GlcNAc)_6$ was sufficient to completely block the inhibition of chitinase activity (Figure 4). Chito-oligomers of a length of four or more GlcNAc residues are known to be rapidly degraded by all classes of plant chitinases and have a short half-life time in the presence of chitinases (Brunner et al., 1998). The difference in chitinase activity between the incubations with free AVR4 and AVR4 bound to $(GlcNAc)_6$) indicates that AVR4 has a higher affinity for $(GlcNAc)_6$ than for chitin azure. The interaction between AVR4 and $(GlcNAc)_6$ protected the latter against degradation, but left chitin azure unprotected. Moreover, these results indicate that the chitinase enzyme is not inhibited by AVR4, but rather that AVR4 protects the chitin substrate against degradation.

AVR4 protects sensitive fungi against the deleterious effect of plant chitinases

Growth of *T. viride* is inhibited by plant chitinase (PR-3) alone (Mauch et al., 1988), whereas a combination of plant chitinases and β-1,3-glucanases is required for growth inhibition of *Fusarium solani* f.sp. *phaseoli* (Sela-Buurlage et al., 1993). We examined whether AVR4 could protect growth of these fungi against deleterious effects of basic chitinase (ChiI) alone

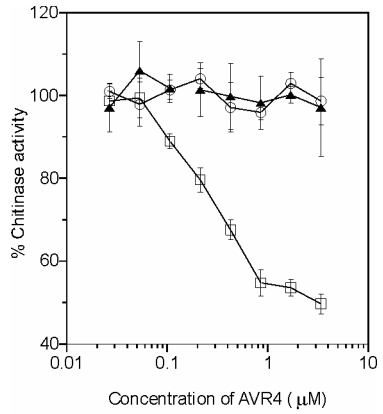

Figure 4. Degradation of chitin azure by basic chitinase of tobacco is inhibited by AVR4. Concentration series of AVR4 (□), ECP1 (○), and AVR4 pre-incubated with a three-fold molar excess of $(GlcNAc)_6$ (▲) were incubated with chitin azure. After 3 hrs of incubation 50 μg of ChiI was added and chitinase activity measured. Bars indicate the standard error between three independent experiments.

or in combination with the basic β-1,3-glucanase (GluI) of tobacco. Increasing concentrations of AVR4 protected germlings of *T. viride* against near lethal concentrations of 0.3 μM ChiI (Figure 5). The protection of *T. viride* against ChiI was specific for AVR4, as similar concentrations of ECP1 did not protect germlings of *T. viride* (data not shown). The growth of germlings of *T. viride* was no affected when AVR4 was added alone (data not shown). Subsequently, we tested the growth of germlings of *F. solani* f.sp. *phaseoli,* which is almost completely inhibited in the presence of both 0.3 μM ChiI and 0.3 μM GluI (Figure 5). AVR4 could also protect this fungus against these deleterious concentrations of these two enzymes. Concentrations of AVR4 of ~ 4 and ~1 μM effectively resulted in 50% protection of growth of *T. viride* and *F. solani* f.sp. *phaseoli*, respectively (Figure 5E).

AVR4 binds to chitin present in cell walls of *T. viride* and *F. solani* f.sp. *phaseoli*

Our findings suggested that *T. viride* and *F. solani f.sp. phaseoli* were possibly protected by binding of AVR4 to their hyphal walls. To examine this possibility, we labeled AVR4 with the fluorescent dye BODIPY-TMR-SE (BDP). Conjugation of BDP to AVR4 did neither affect binding of AVR4 to chitin (data not shown), nor did it affect AVR4-specific induction of the hypersensitive response (HR) in the tomato genotype *Cf-4* (data not shown). In addition, BDP showed no affinity for any polysaccharides when conjugated to a protein (as tested with AVR2-BDP, data not shown). We used WGA labeled with the dye Oregon green (WGA-

OG) as positive control for chitin localization (Benhamou et al., 1990; Wubben, 1996). WGA-OG bound specifically to chitin and chitosan (data not shown) like WGA (Figure 2). Localization of WGA-OG and AVR4-BDP was performed on germinated conidia of both fungi. Both dyes were able to accumulate at the surface of germ tubes and swollen conidia of *T. viride* (swelling indicates the onset of germination) (Figure 6A, 6B). Pretreatment of germlings of *T. viride* with chitinase decreased the accumulation of these dyes substantially (data not shown). From these results, we conclude that AVR4-BDP accumulates on chitin present in hyphal cell walls. Slightly different results were obtained when germlings of *F. solani* f.sp. *phaseoli* were incubated with WGA-OR and AVR-BDP. Both dyes accumulated at the germ tube and the conidium, but the conidium was only stained at the site of protrusion of the germ tube (Figure 6E-6G). Moreover, fluorescence could not be detected over the entire germ tubes of *F. solani* f.sp. *phaseoli* (Figure 6G), which indicates that the chitin layer is partially covered in the process of cell wall formation. Non-germinated conidia of both fungi remained unstained with either dye (Figure 6, UG). In conclusion, the fluorescence data support the idea that binding of AVR4 to chitin embedded in the hyphal wall forms the basis of the protection of both fungi against ChiI.

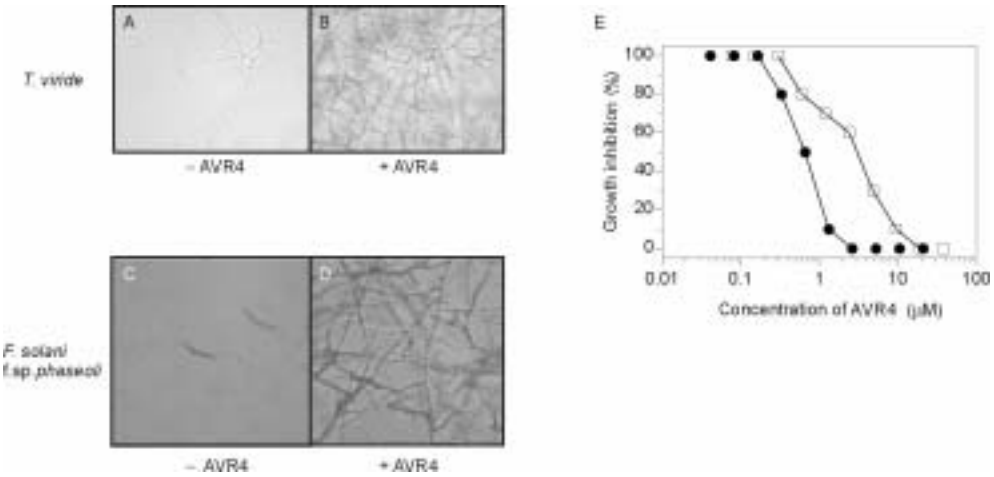

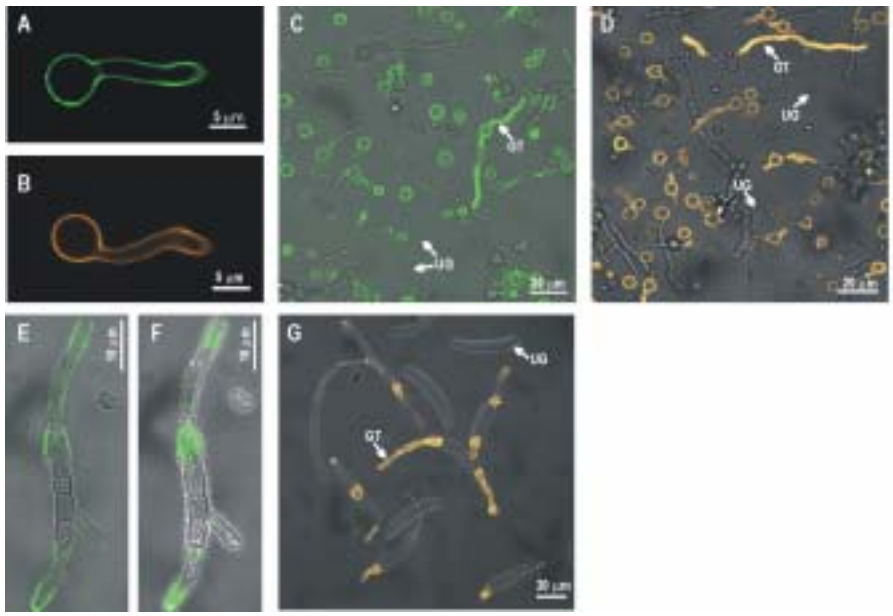

Figure 6. AVR4 accumulates at the surface of hyphal walls of *Trichoderma viride* (**A-D**) and *Fusarium solani* f.sp. *phaseoli* (**E-G**). Fungi were germinated overnight and subsequently incubated with fluorescent AVR4 (AVR4-BDP; **B, D,** and **G**) or WGA (WGA-OR; **A, C, E,** and **F**). (**A, B**) image of one germling of *T. viride,*. (**C, D**) overview of *T. viride,* (**E**) single fluorescent confocal image of a germling of *F. solani* f.sp. *phaseoli,* (**F**) combined fluorescent image of the same germling as in **E**, (**G**) overview of *F. solani* f.sp. *phaseoli*; UG, Non-germinated conidia. germling of *F. solani* f.sp. *phaseoli* as shown in (E).

⟵ **Figure 5.** AVR4 protects fungi against lytic activity of basic chitinase and β-1,3-glucanase of tobacco. Two hrs after the addition of AVR4, either 0.3 μM chitinase (ChiI) alone or both 0.3 μM chitinase and 0.3 μM β-1,3-glucanse (GluI) were added. Fungal growth was, subsequently, scored 24 hrs after adding the enzymes. **(A, B)** *Trichoderma viride* was treated with ChiI, (–/+ 38 μM AVR4) **(C, D)** *Fusarium solani* f.sp. *phaseoli* was treated with ChiI and GluI. (–/+ 6 μM AVR4) (**E**) Effective dose determined for AVR4 in these growth assays with *T. viride* (□) and *F. solani* f.sp. *phaseoli* (●). Enzyme treatments were identical as described for (**A-D**). Shown data are the result of a typical experiment of at least three independent replicates all with comparable results.

Chitin is not accessible in cell walls of *in-vitro* germinated *C. fulvum*

Growth of *in-vitro*-germinated conidia of *C. fulvum* is not inhibited by preparations of tomato chitinases and β-1,3-glucanases (Joosten et al., 1995). We examined whether this could be due to inaccessibility of chitin in cell walls of *in vitro*-germinated conidia of *C. fulvum.* After overnight germination, germlings of *C. fulvum* were incubated with WGA-OG or AVR4-BDP. This resulted in only faint staining of septa in germ tubes and sometimes the

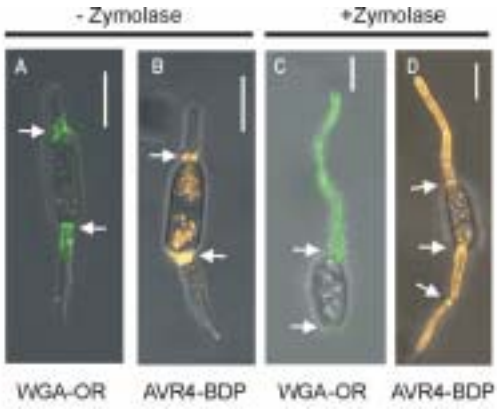

Figure 7. Chitin is not accessible at hyphae of *in vitro*-germinated *Cladosporium fulvum, i.e.* it is only exposed at the onset of germination at the site of protrusion of the germ tube. However, chitin is embedded in the cell wall of the germ tubes as evident from a treatment with zymolase. Arrows indicate septa. AVR4-BDP stained also to some extent vesicular structures inside conidia. Bar=10 μm. (**A, C**) stained with WGA-OR; (**B, D**) stained with AVR4-BDP.

interior of conidial 'ghost' cells stained as well (data not shown), which was independent of the strain of *C. fulvum* we used (races 4 and 5). The
stained conidial cells were termed "ghost" cells as germ tubes were never found at these cells and the cells lacked vesicular structures. When the dye-labeled proteins were added at the onset of germination of the conidia of *C. fulvum* (several strains were tested), staining occurred at the site of protrusion of the germ tube (Figure 7A and 7B*;* →), which raised the question whether chitin is actually present or effectively covered in the cell wall of the germ tubes. The question was answered when germlings of *C. fulvum* were treated with

zymolase, an enzyme preparation that contains both β-1,3-glucanase and protease activity. After this treatment, fluorescence was detected over the entire surface of the germ tubes (Figure 7C and 7D). From these results it can be concluded that chitin is deposited in the cell wall of *in vitro*-grown *C. fulvum,* but that it is only temporarily exposed at the onset of germination and that it is subsequently completely covered by additional cell wall layers as the germ tube elongates.

Chitin is Accessible in the Hyphal Wall of *C. fulvum* during Colonization of Tomato

The *in vitro* experiments might suggest that chitin would also be inaccessible in the hyphal wall of *C. fulvum* hyphae that colonize tomato. For that reason, we inoculated 6-week-old tomato plants (cultivar Moneymaker Cf0, Cf4 and Cf5) with different strains of *C. fulvum* (race 4 and race 5). Five days post inoculation (d.p.i.), epidermal peelings of the lower epidermis of infected tomato leaves exposed to dye-labeled proteins were analyzed. AVR4-BDP accumulated at the runner hyphae of *C. fulvum* present at the exterior of leaves, whereas little or no fluorescence associated with the plant cells (Figure 8A). At 9 d.p.i., tomato leaves were densely covered with runner hyphae of *C. fulvum* of which some had penetrated the leaf through stomata. At this time point, leaves were detached and vacuum-infiltrated with the dye-labeled proteins. Similar to 5 d.p.i., AVR4-BDP accumulated at the surface of runner hyphae (Figure 8B), but in addition also at intercellular hyphae (Figure 8C). Staining of the intercellular hyphae with AVR4-BDP did not differ between strains of *C. fulvum* (race 4 and race 5) infecting susceptible tomato plants. However, AVR2-BDP did not stain the hyphal walls (data not shown), which demonstrates that localization of AVR4-BDP is solely caused by AVR4 and not by the dye. The staining with WGA-OG *in planta* was less effective than with AVR4-BDP, although both dyes accumulated at hyphae of *C. fulvum*. These data indicate that, in contrast to chitin present in the cell wall of *in vitro-grown C. fulvum*, chitin is exposed and accessible to AVR4 in hyphal walls of *C. fulvum* hyphae infecting tomato.

DISCUSSION

AVR4 is a Unique Fungal Representative of the inv ChBD Family

The primary structure of AVR4 contains the consensus of the inv ChBD (Figure 1) (Shen and Jacobs-Lorena, 1999). This domain proved to be functional, as we could precipitate

AVR4 from solution with chitin, but not with chitosan or other polysaccharides abundantly present in cell walls of various organisms (Figure 2A). An extensive search in the genome sequences of *Saccharomyces* genomes of baculoviridae. These ORFs encode single inv ChBDs preceded by a putative signal sequence, but their function is still unknown (IJkel et al., 1999). The absence of the inv ChBD in the public fungal genome databases suggests that a common ancestor of the *Avr4* gene might be absent in fungi. The *Avr4* gene could, therefore, have arisen either independently in *C. fulvum* or by horizontal gene transfer. However, this could not be established by comparing codon-usage or phylogenetic analyses. Only a limited number of genes of *C. fulvum* have been sequenced, which precludes a proper statistical analysis of the codon-usage of the *Avr4* gene. Also a phylogenetic analysis of the domain yielded an unreliable result due to the large number of amino acid substitutions over the relative short length of the inv ChBD in combination with the low number of strictly conserved residues that could define reliable branches.

AVR4 Shields Chitin in Cell Walls of Infecting Hyphae of *C. fulvum,* Thereby Probably Providing Protection Against Chitinases

Growth of *C. fulvum* could not be inhibited *in vitro* by tomato chitinases and β-1,3-glucanases (Joosten et al., 1995). This is possibly due to the fact that chitin is covered by glycan and mannan layers. AVR4 did only bind to cell walls of *in vitro*-grown *C. fulvum* after treatment with zymolase. Zymolase was previously used to reveal chitin in cell walls of *Candida, Histoplasma, Saccharomyces,cerevisiae*, *Neurospora crassa,* and *Schizosaccharomyces pombe*, as well as numerous fungal EST databases using a Hidden-Markov Model (HMM)(Eddy, 1998) of the inv ChBD did not reveal other fungal sequences containing the inv ChBD. In contrast, the inv ChBD is well represented in the genomes of *Drosophila melanogaster* (98 ORFs), *Caenorhabditis elegans* (11 ORFs), and baculoviridae (37 ORFs). The largest group of ORFs that are closely related to AVR4 is found in and *Wangiella* (Brandhorst and Klein, 2000). Our findings indicate that chitin is only temporarily exposed at the protrusion of the germ tube of *C. fulvum,* which appears to relate to septum formation (Cabib et al., 2001). The covered chitin layer in cell walls of *in vitro*-grown *C. fulvum* is in large contrast with the accessibility of chitin for AVR4 in cell walls of infecting hyphae of *C. fulvum*. This difference might be due to different growth conditions, as the composition of fungal cell walls was shown to be affected by different growth conditions (aerial compared to submerged growth) (Wessels, 1997).

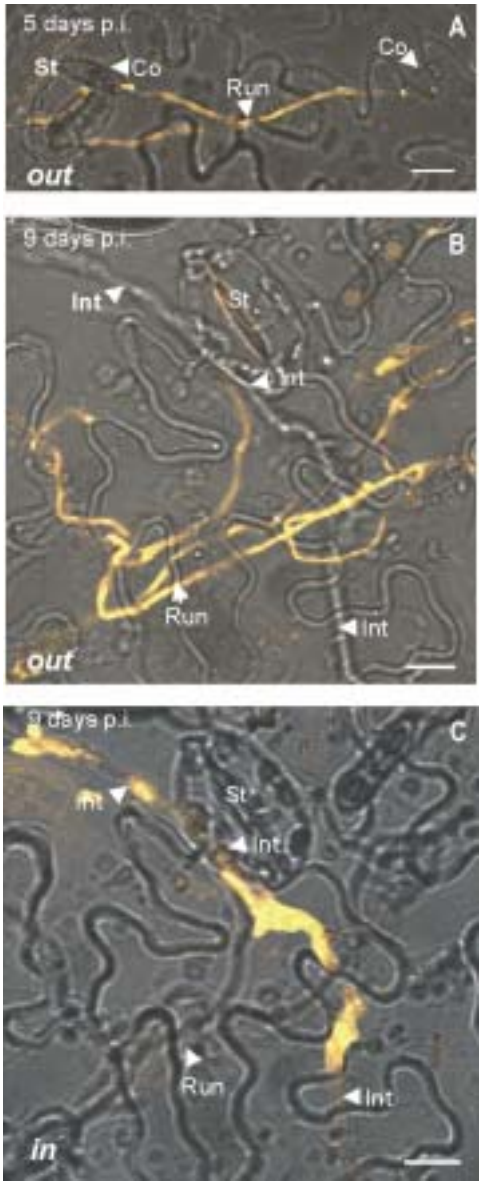

Figure 8. Chitin is accessible for AVR4 at cell walls of invading hyphae of *Cladosporium fulvum* infecting tomato. (**A**) Epidermal peel of a tomato leaf (cv. MM-Cf0) inoculated with race 5 of *C. fulvum.* Runner hyphae of C. fulvum become stained with AVR4. CO, conidia; d.p.i., days post inoculation; Int, intercellular hyphae; Run, runner hyphae; ST, stoma; Bar=20 μm. (**B**) Confocal image of the layer of the epidermal peel taken from a tomato leaf (MM-Cf0) 9 d.p.i. with race 4 (frame shift mutant) of *C. fulvum*. AVR4-BDP was applied by vacuum-infiltration in the leaf. After 4 hrs of incubation the epidermis was peeled. (**C**) Identical epidermal peel as in (B), but confocal image is taken at internal side of the epidermal peel. Incubation with AVR4 lasted 3 hrs at 20°C.

Immunolocalization studies of chitinases and β-1,3-glucanases in *C. fulvum*-infected tomato leaves revealed that these cell wall degrading enzymes accumulate in the vicinity of intercellular hyphae of *C. fulvum* in both compatible and incompatible interactions (Wubben et al., 1992). Furthermore, increased production of cell wall degrading enzymes was reported to occur not only in the incompatible, but also in the compatible interactions (Joosten and de Wit, 1989). Consequently, it seems sensible that intercellular hyphae of *C. fulvum* have acquired some protection against these enzymes by AVR4. Indeed, the penetration of tomato by *C. fulvum* coincides with the initiation of the transcription of the *Avr4* gene (Joosten et al., 1997). Furthermore, AVR4 is found at a lower abundance in apoplastic fluid of colonized tomato leaves as compared to AVR9, whereas the corresponding genes are both highly transcribed in colonized leaves (Joosten et al., 1997). Our findings indicate that release of AVR4 is likely to coincide with binding of AVR4 to chitin in cell walls. The fact that AVR4 can act as a protective agent of chitin present in hyphal walls was demonstrated using the fungi *T. viride* and *F. solani* f.sp. *phaseoli* as models as growth of these fungi is known to be inhibited by chitinases and β-1,3-glucanases *in vitro* (Mauch et al., 1988; Sela-Buurlage et al., 1993). These data are all consistent with AVR4 being an integral cell wall protein of *C. fulvum* that might protect it against deleterious effects of chitinases during colonization of tomato.

Soluble chito-oligomers are non race-specific elicitors of defense responses in a wide range of plant species (Côté and Hahn, 1994; Ebel and Cosio, 1994). The interaction of AVR4 with chitin could potentially reduce the release of chito-oligomers caused by plant chitinases. Furthermore, unbound AVR4 present in the apoplast could also potentially capture part of the released chito-oligomers, as AVR4 binds to soluble chito-oligomers (Figure 3). However, plasma membrane located High-Affinity Binding Sites (HABS) specific for these chito-oligomers have been demonstrated for several plants including tomato (Baureithel et al., 1994; Bradley Day et al., 2001), but their affinity for chito-oligomers appears to be much higher (K_d=20-50 nM) than that of AVR4 (K_d ~5 μM) (H.A. van den Burg, unpublished results). Therefore, AVR4 released in the apoplast cannot compete with the HABS. Thus, AVR4 is not expected to suppress defense responses that are induced by release of chito-oligomers. This suggests that the primary biological function of AVR4 is correlated with its ability to bind to chitin present in the hyphal wall.

All together, the virulence function of AVR4 seems to be quite different from the virulent functions of other bacterial and fungal avirulence factors, as most seem to play an

active role in suppressing plant defense responses rather than in protecting the pathogen against the induced plant defense responses.

Protection of Hyphal Walls Might Be a General Defense Mechanism in Response to Cell Wall-Degrading Enzymes

The implicated biological function for AVR4, i.e. a protective role as an integral cell wall protein reinforcing the cell wall (Elvin et al., 1996), might be a general defense mechanism employed by pathogenic fungi. Plant pathogenic fungi such as *F. solani* f.sp. *phaseoli* and *Nectria haematococca* are sensitive to plant β-1,3-glucanases (PR-2) and chitinases (PR-3), but become insensitive after pre-exposure to these enzymes, which is not due to inactivation of the cell wall degrading enzymes by these fungi (Ludwig and Boller, 1990; Sela-Buurlage, 1996). This would suggest that these fungi respond to the enzymatic activity by modifying their cell walls to protect themselves against the deleterious effects of these enzymes. The molecular basis of this suggested modification is not known yet, but pretreatment with these enzymes might induce genes encoding proteins (functional homologues of AVR4) that protect them against deleterious of these enzymes. The CBP1 protein of the rice pathogenic fungus *Magnaporthe grisea*, which is required for hydrophobic surface sensing and appresorium formation, is the first fungal example of a protein containing the "plant ChBD" (Kamakura et al., 2002). Similarly, an adhesin protein with chitin-binding properties is indispensable for pathogenicity of the dimorphic yeast *Blastomyces dermatitidis* (Brandhorst and Klein, 2000). In contrast to ascomycetes, cell walls of oomycetes do not contain chitin, but mainly β-1,3- and β-1,6-glucans. Strikingly, a family of Glucanase Inhibitor Proteins (GIPs) was shown to exist in the oomycete *Phytophthora sojae* f.sp. *glycines* (and several other *Phytophthora* species), which specifically inhibit plant β-1,3-glucanases (Ham et al., 1997; Rose et al., 2002). The GIP proteins were also found to accumulate on the surface of walls of *Phytophthora* species. These data indicate that some pathogens are able to modify their cell wall composition and architecture after encountering harsh or deleterious environmental conditions. This probably explains why AVR4 is only produced by *C. fulvum* during colonization of tomato where it encounters chitinases in the leaves.

The ability of *Cf-4* tomato plants to recognize AVR4 and to mount an HR seems to represent a counter-attack of tomato to protect itself against *C. fulvum.* The wide introduction of tomato cultivars carrying the introgressed *Cf-4* resistance gene and subsequent selection pressure caused that virulent races of *C. fulvum* advanced in the

population. These strains were found to produce isoforms of AVR4 that are protease sensitive and no longer induce HR on *Cf-4* tomato plants, but still show chitin-binding activity, which clearly indicates that the intrinsic function of AVR4 is retained after loosing HR-inducing activity (van den Burg et al., 2002). However, one strain did no longer produce AVR4 but still appeared to be virulent on tomato. This strain has probably developed an alternative strategy to protect itself against plant chitinases. In conclusion, our findings provide further insight in the way the virulence and avirulence function of AVR4 evolved by co-evolution between *C. fulvum* and tomato.

METHODS

Reagents. AVR4 was produced in the methylotrophic yeast *Pichia pastoris* and purified from culture filtrate (van den Burg et al., 2001). Tobacco basic chitinase (ChiI) (EC 3.2.1.14) and basic β-1,3-glucanase (GluI) (EC 3.2.1.39) were overexpressed in *E. coli* and purified (Jongedijk et al., 1995). ECP1 and ECP4 protein were purified from apoplastic fluid of a compatible interaction between *C. fulvum* and tomato as described by Laugé et al. (2000).

Purification of Cell Wall Material. Crude cell wall material was isolated from tomato plants and two different fungi. Plants were grown in contained environment in the greenhouse to prevent fungal infections. Strains of the fungi *C. fulvum* (race 4 and race 5) and *T. viride* were grown for 3 days in liquid shake cultures containing supplemented B5 medium (van den Ackerveken et al., 1993a). Under these conditions expression of the *Avr4* gene is suppressed (Joosten et al., 1997). Fungal mycelium and leaves of 6-week-old tomato plants (cultivar Moneymaker Cf0 and MM-Cf4) were homogenized in a Warring blender in the presence of 7 parts (v/w) of a solution consisting of 80% (w/w) buffer-saturated phenol (Life technologies)/acetic acid/water (PAW) at a ratio of 2.5/1/1 (v/v/v). After stirring for 18 hrs at room temperature, the homogenate was filtered over a glass filter and the insoluble fraction was collected, resuspended in 5 parts of PAW, and incubated for another 24 hrs. This procedure was repeated two times. By this time most protein had been removed, which was verified by adding 50 μL 10% of ammonium formate and 5 mL acetone to 1 mL filtrate. Absence a precipitate indicates absence of residual proteins. This glycan-enriched cell wall fraction was then rinsed extensively with 70% ethanol and lyophilized before storage. Most glycoproteins were deliberately removed by extraction, as glycoproteins could potentially interfere with specificity of binding.

Polysaccharide Substrate Binding Assay. Binding affinity of AVR4, WGA, ECP1, and ECP4 for various polysaccharides was determined by incubating each of these proteins (at a concentration of 5 μg/ml) with the following insoluble polysaccharides (5 mg): chitin beads (New England Biolabs), crab shell chitin, chitosan, xylan, cellulose, curdlan, and lichenan (all from Sigma). The incubation was performed in 800 μL buffer containing 50 mM Tris·HCl, pH 8, and 150 mM NaCl (Tjoelker et al., 2000). After two hrs of gentle shaking at room temperature, the insoluble fraction was pelleted by centrifugation (3 min, 13000*g*) and the supernatant collected. The insoluble fraction was three times washed with the incubation buffer and subsequently boiled in 200 μL 1% SDS solution. Presence of proteins (AVR4, ECP1, ECP2 or WGA) in both supernatant and pellet was examined by tricine SDS-PAGE gel. Binding affinity of AVR4 for cell wall fractions (5 mg) was performed in a similar manner.

Nuclear magnetic resonance (NMR) experiments. AVR4 was ^{15}N-isotopically enriched for NMR purposes by overexpression of the *Avr4* gene in the methylotrophic yeast *Pichia pastoris* (van den Burg et al., 2001). ^{1}H-^{15}N-heteronuclear single-quantum coherence spectroscopy experiments were performed and calibrated as described (van den Burg et al, 2001). A 1 mM ^{15}N-isotopically labeled AVR4 NMR sample was prepared in a buffer containing 20 mM Acetate-d_4, pH 6, and 150 mM NaCl. To one half of the sample was added a final concentration of chito-oligomer (3.5 mM $(GlcNAc)_3$ or 27.2 mM $(GlcNAc)_6$). Small aliquots of these ligand/^{15}N-AVR4 mixtures were then added to ^{15}N-AVR4 sample. In this way the protein concentration remained constant during the experiment (Asensio et al., 1995). NMR spectra were recorded on a Bruker AMX500 spectrometer.

Chitinase activity assay. Chitin azure suspensions (100 μL start volume, 1 mg/mL; Sigma) were incubated with a dilution series of AVR4, ECP1 or AVR4 preincubated with a three-fold molar excess of $(GlcNAc)_6$ (10 μL was added with a final concentration of 3.5 μM). After 3 hrs of incubation at 37°C on a shaker, 190 μL of a 100 mM sodium acetate buffer pH 5.2 containing 50 μg ChiI was added. The incubation was prolonged for another 10 hrs. Chitinase activity was determined by measuring the A_{550} of the supernatant after the residual insoluble chitin azure had been removed by centrifugation.

Fungal growth assay in the presence of chitinases and β-1,3-glucanases. Fungal growth assays with were performed essentially according to Sela-Buurlage et al. (1993). Conidia ($1x10^4$ conidia/mL) of *Trichoderma viride* and *Fusarium solani* f.sp. *phaseoli* were germinated overnight in liquid media (Czapex-Dox or Potato Dextrose Broth, respectively). The conidial suspensions were dispensed into 96-wells microtiter plates in aliquots of 50 μL, together with 10 μL of a dilution series of AVR4. After for two hrs of incubation, the enzyme

solution was added (40 μL). ChiI and GluI were both applied at a final concentration of 0.3 μM. *T. viride* was only incubated with ChiI, while *F. solani* f.sp. *phaseoli* was incubated with a mixture of both enzymes. Fungal growth was scored after 24 hrs at 22^{o}C.

Localization of AVR4 and WGA with fluorescent dyes. Proteins were labeled with the amine-reactive fluorescent dye BODIPY-TMR-SE (BDP; excitation wavelength (Ex) 543 nm; Molecular Probes) according to the manufacturer's recommendations. The reaction resulted in the labeling of ~0.3-0.5 BDP per protein molecule. Excess dye was separated from the dye-labeled protein by size-exclusion chromatography (P6-DG, Bio-Rad). AVR4-BDP and WGA-Oregon green (WGA-OG; Ex 488 nm, Molecular probes) were applied at concentrations between 0.5 and 2 μM without remarkable differences in staining patterns. Conidia were pregerminated overnight in liquid culture. Enzymatic treatments of germinated conidia lasted for up to 5 hrs. Zymolase (Zymo Research, Orange County, CA) was used at a concentration of 25 μg/mL. After staining for at least 30 min, the germinated conidia were washed two times in standard phosphate buffered-saline and fluorescence was detected with a confocal laser-scanning microscope (CSLM) (Carl Zeiss). For *in planta* fluorescence localization six-week old tomato plants were inoculated with *C. fulvum* (race 4 and race 5). Staining of leaf material was achieved by vacuum-infiltration of the dye into the infected tomato leaves (de Wit and Spikman, 1982) or by incubation of epidermal peelings (Joosten et al., 1997) in standard phosphate-buffered saline (PBS) containing dye-labeled protein. Epidermal peelings were repeatedly washed with PBS prior to the detection of the dye by CSLM. Fluorescent staining was performed at 20^{0}C in dark environments.

REFERENCES

Asensio, J.L., Canada, F.J., Bruix, M., Rodriguez, R.A., and Jimenez, B.J. (1995) Eur. J. Biochem. **230,** 621-633.

Asensio, J.L., Siebert, H.C., von der Lieth, C.W., Laynez, J., Bruix, M., Soedjanaamadja, U.M., Beintema, J.J., Canada, F.J., Gabius, H.J., and Jimenez, B.J. (2000) Proteins **40,** 218-236.

Bains, G., Lee, R.T., Lee, Y.C., and Freire, E. (1992) Biochemistry **31,** 12624-12628.

Bateman, A., Birney, W., Cerruti, L., Durbin, R., Etwiller, L., Eddy, S.R., Griffiths-Jones, S., Howe, K.L., Marshall, M., and Sonnhammer, E.L. (2002) Nuc. Acids Res. **30,** 281-283.

Baureithel, K., Felix, G., and Boller, T. (1994). J. Biol. Chem. **269,** 17931-17938.

Benhamou, N., Joosten, M.H.A.J., and de Wit, P.J.G.M. (1990) Plant Physiol. **92,** 1108-1120.

Bonas, U., and Lahaye, T. (2002) Curr. Opin. Microbiol. **5,** 44-50.

Bradley Day, R., Okada, M., Ito, Y., Tsukada, K., Zaghouani, H., Shibuya, N., and Stacey, G. (2001) **126,** 1162-1173.

Brandhorst, T., and Klein, B. (2000) J. Biol. Chem. **275,** 7925-7934.

Broekaert, W.F., van Parijs, J., Leyns, F., Joos, W., and Peumans, W.J. (1989) Science **245,** 1100-1102.

Broekaert, W.F., Marien, W., Terras, F.R., de Bolle, M.F., Proost, P., van Damme, J., Dillen, L., Claeys, M., Rees, S.B., Vanderleyden, J., and Cammue, B.P.A. (1992) Biochemistry **31,** 4308-4314.

Brunner, F., Stintzi, A., Fritig, B., and Legrand, M. (1998) Plant J. **14,** 225-234.

Cabib, E., Roh, D.-H., Schmidt, M., Crotti, L.B., and Varma, A. (2001) J. Biol. Chem. **276,** 19679-19682.

Casper-Lindley, C., Dahlbeck, D., Clark, E.T., and Staskawicz, B.J. (2002) Proc. Natl. Acad. Sci. USA **99,** 8336-8341.

Ciopraga, J., Gozia, O., Tudor, R., Brezuica, L., and Doyle, R.J. (1999) Biochim. Biophys. Acta **1428,** 424-432.

Côté, F., and Hahn, M.G. (1994). Plant Mol. Biol. **26,** 1379-1411.

Dangl, J.L., and Jones, J.D.G. (2001) Nature **411,** 826-833.

de Nobel, J.G., Klis, F.M., Priem, J., Munnik, T., and van den Ende, H. (1990) Yeast **6,** 491-499.

de Wit, P.J.G.M. (1977) Neth. J. Plant Pathol. **83,** 109-122.

de Wit, P.J.G.M., and Joosten, M.H.A.J. (1999) Curr. Opin. Microbiol **2,** 368-373.

Ebel, J., and Cosio, E.G. (1994). Int. Rev. Cytol. **148,** 1-36.

Eddy, S.R. (1998) Bioinformatics **14,** 755-763.

Elvin, C.M., Vuocolo, T., Pearson, R.D., East, I.J., Riding, G.A., Eisemann, C.H., and Tellam, R.L. (1996) J. Biol. Chem. **271,** 8925-8935.

Guttman, D.S., Vinatzer, B.A., Sarkar, S.F., Ranall, M.V., Kettler, G., and Greenberg, J.T. (2002) Science **295,** 1722-1726.

Ham, K.S., Wu, S.C., Darvill, A.G., and Albersheim, P. (1997) Plant J. **11,** 169-179.

Idnurm, A., and Howlett, B.J. (2001) Mol. Plant Pathol. **2,** 241-255.

IJkel, W.F.J., van Strien, E.A., Heldens, J.G., Broer, R., Zuidema, D., Goldbach, R.W., and Vlak, J.M. (1999) J. Gen. Virol. **80,** 3289-3304.

Jongedijk, E., Tigelaar, H., van Roekel, J.S.C., Bres-Vloemans, S.A., Dekker, I., van den Elzen, P.J.M., Cornelissen, B.J.C., and Melchers, L.S. (1995) Euphytica **85,** 173-180.

Joosten, M.H.A.J., and de Wit, P.J.G.M. (1989) Plant Physiol. **89,** 945-951.

Joosten, M.H.A.J., and de Wit, P.J.G.M. (1999) Annu. Rev. Phytopathol. **37,** 335-367.

Joosten, M.H.A.J., Cozijnsen, T.J., and de Wit, P.J.G.M. (1994) Nature **367,** 384-386.

Joosten, M.H.A.J., Vogelsang, R., Cozijnsen, T.J., Verberne, M.C., and de Wit, P.J.G.M. (1997) Plant Cell **9,** 367-379.

Joosten, M.H.A.J., Verbakel, H.M., Nettekoven, M.E., van Leeuwen, J., Vossen, R.T.M., and de Wit, P.J.G.M. (1995) Physiol. Mol. Plant Pathol. **46,** 45-59.

Kamakura, T., Yamaguchi, S., Saitoh, K.I., Teraoka, T., and Yamaguchi, I. (2002) Mol. Plant-Microbe Interact. **15**, 437-444.

Kawabata, S., Nagayama, R., Hirata, M., Shigenaga, T., Agarwala, K.L., Saito, T., Cho, J., Nakajima, H., Takagi, T., and Iwanaga, S. (1996) J. Biochem. **120,** 1253-1260.

Kim, Y.J., Lin, N.C., and Martin, G.B. (2002) Cell **109,** 589-598.

Kjemtrup, S., Nimchuk, Z., and Dangl, J.L. (2000) Curr. Opin. Microbiol **3,** 73-78.

Laugé, R., and de Wit, P.J.G.M. (1998) Fung. Genet. Biol. **24,** 285-297.

Laugé, R., Goodwin, P.H., de Wit, P.J.G.M., and Joosten, M.H.A.J. (2000) Plant J. **23,** 735-745.

Laugé, R., Joosten, M.H.A.J., van den Ackerveken, G.F.J.M., van den Broek, H.W.J., and de Wit, P.J.G.M. (1997) Mol. Plant-Microbe Interact. **10,** 725-734.

Luderer, R., Takken, F.L., de Wit, P.J.G.M., and Joosten, M.H.A.J. (2002) Mol. Microbiol. **45,** 875-884.

Ludwig, A., and Boller, T. (1990) FEMS Microbiol. Lett. **69,** 61-66.

Mackey, D., Holt, B.F., Wiig, A., and Dangl, J.L. (2002) Cell **108,** 743-754.

Mauch, F., Mauch-Mani, B., and Boller, T. (1988) Plant Physiol. **88,** 936-942.

Neuhaus, J.M. (1999). Plant chitinases (PR-3, PR-4, PR-8, PR-11). *In Pathogenesis-related proteins in plants*, eds S.W. Datta and S. Muthukrishnan (CRC Press) pp. 77-105.

Orbach, M.J., Farrall, L., Sweigard, J.A., Chumley, F.G., and Valent, B. (2000) Plant Cell **12,** 2019-2032.

Rose, J.K.C., Ham, K.S., Darvill, A.G., and Albersheim, P. (2002) Plant Cell **14,** 1329-1345.

Schoffelmeer, E.A.M., Klis, F.M., Sietsma, J.H., and Cornelissen, B.J.C. (1999). Fung. Genet. Biol. **27,** 275-282.

Schultz, J., Milpetz, F., Bork, P., and Ponting, C.P. (1998) Proc. Natl. Acad. Sci. USA **95,** 5857-5864.

Sela-Buurlage, M.B. (1996) *In vitro* sensitivity and tolerance of *Fusarium solani* towards chitinases and β-1,3-glucanases (Thesis: Wageningen Agricultural University), pp. 211.

Sela-Buurlage, M.B., Ponstein, A.S., Bres-Vloemans, S.A., Melchers, L.S., van den Elzen, P.J.M., and Cornelissen, B.J.C. (1993) Plant Physiol. **101,** 857-863.

Shen, Z., and Jacobs-Lorena, M. (1997) J. Biol. Chem. **272,** 28895-28900.

Shen, Z., and Jacobs-Lorena, M. (1999) J. Mol. Evol. **48,** 341-347.

Stintzi, A., Heitz, T., Prasad, V., Wiedemann-Merdinoglu, S., Kauffmann, S., Geoffroy, P., Legrand, M., and Fritig, B. (1993). Biochimie **75,** 687-706.

Suetake, T., Tsuda, S., Kawabata, S., Miura, K., Iwanaga, S., Hikichi, K., Nitta, K., and Kawano, K. (2000) J. Biol. Chem. **275,** 17929-17932.

Thompson, J.D., Gibson, T.J., Plewniak, F., Jeanmougin, F., and Higgins, D.G. (1997) Nucl. Acids Res. **25,** 4876-4882.

Tjoelker, L.W., Gosting, L., Frey, S., Hunter, C.L., Trong, H.L., Steiner, B., Brammer, H., and Gray, P.W. (2000) J. Biol. Chem. **275,** 514-520.

Tormo, J., Lamed, R., Chirino, A.J., Bayer, E.A., Shoham, Y., and Steitz, T.A. (1996) EMBO J. **15,** 5739-5751.

van den Ackerveken, G.F.J.M., Vossen, P., and de Wit, P.J.G.M. (1993a) Plant Physiol. **103,** 91-96.

van den Ackerveken, G.F.J.M., van Kan, J.A.L., Joosten, M.H.A.J., Muisers, J.M., Verbakel, H.M., and de Wit, P.J.G.M. (1993b) Mol. Plant-Microbe Interact. **6,** 210-215.

van den Burg, H.A., de Wit, P.J.G.M., and Vervoort, J. (2001). J. Biomol. NMR **20,** 251-261.

van den Burg, H.A., Westerink, N., Francoijs, K.J., Roth, R., Woestenenk, E., Boeren, S., de Wit, P.J.G.M., Joosten, M.H.A.J., and Vervoort J. (2003) J.Biol. Chem, submitted

van den Hooven, H.W., van den Burg, H.A., Vossen, P., Boeren, S., de Wit, P.J.G.M., and Vervoort, J. (2001) Biochemistry **40,** 3458-3466.

van Kan, J.A.L., van den Ackerveken, G.F.J.M., and de Wit, P.J.G.M. (1991) Mol. Plant-Microbe Interact. **4,** 52-59.

van 't Slot, K.A.E., and Knogge, W. (2002) Crit. Rev. Plant Sci. **21,** 229-271.

Wessels, J.G.H. (1997) Adv. Microbial. Physiol. **38,** 1-45.

Wessels, J.G.H., and Sietsma, J.H. (1981). Fungal cell walls: a survey. *In Plant carbohydrates II, extracellular carbohydrates*, edsW. Tanner and F.A. Loewus (Berlin: Springer-Verlag) pp. 352-394.

Wevelsiep, L., Rüpping, E., and Knogge, W. (1993) Plant Physiol. **101,** 297-301.

White, F.F., Yang, B., and Johnson, L.B. (2000) Curr. Opin. Plant Biol. **3,** 291-298.

Wubben, J.P., Joosten, M.H.A.J., van Kan, J.A.L., and de Wit , P.J.G.M. (1992) Physiol. Mol. Plant Pathol. **41,** 23-32.

Wubben, J.P. (1996) Subcellular localization of fungal ad plant proteins in te *Cladosporium fulvum*-tomato interaction (Thesis: Wageningen Agricultural University), pp. 137.

6

The interaction between the chitin-binding domain of the AVR4 elicitor of *Cladosporium fulvum* and chitin requires three occupied binding subsites

Harrold A. van den Burg, Christian A.E.M. Spronk, Sjef Boeren, Matthew A. Kennedy, Johannes P.C. Visser, Geerten W. Vuister, Pierre J.G.M. de Wit and Jacques Vervoort

ABSTRACT

The two major classes of chitin-binding domains in living organisms, the invertebrate and hevein domain, appear to exemplify convergent evolution as they lack sequence similarities, but they partially share their tertiary structure. The race-specific elicitor AVR4 of the tomato pathogen *Cladosporium fulvum* is the only recognized fungal representative of the invertebrate chitin-binding domain (CBM14). Here, a detailed analysis of the chitin-binding site of AVR4 and its physical properties are provided. AVR4 interacts with chito-oligomers with a minimal degree-of-polymerization of three, while the plant lectins already interact with a single residue of N-acetyl-glucosamine. The thermodynamic properties of binding of AVR4 to chito-oligomers (K_A, ΔH, *and* ΔS) are comparable to those of the plant lectins hevein and *Urtica dioica* Agglutinin (UDA). The non-covalent complex between AVR4 and chito-oligomers could be specifically detected with electrospray ionisation (ESI) mass spectrometry (upper limit in the millimolar range). NMR data obtained for AVR4 indicated that despite common structural motifs between CBM14 (*e.g.* tachycitin) and CBM18 (*e.g.* hevein) different residues seem to be involved in the interaction with chitin.

INTRODUCTION

Recognition of carbohydrates by proteins is of fundamental importance in numerous biological processes, including (self and non-self) cell-cell recognition, cell adhesion, and carbohydrate turnover. Protein domains responsible for this recognition were recently grouped into distinct Carbohydrate-Binding Modules (CBMs), where at least one functional member has been described for each class (1). In carbohydrate-degrading enzymes, the main function of CBMs is to mediate a prolonged and intimate contact between the catalytic domain and insoluble carbohydrate polymers (2,3). Lectins, on the other hand, are by definition carbohydrate-specific binding proteins lacking enzymatic activity that often contain tandem repeats of CBMs. The interaction between CBMs and carbohydrates is often mediated by CH-π interactions causing stacking of the sugar moiety and aromatic amino acid residues in the binding site (4-7). Evidence exists that both the orientation of the aromatic ring (7,8) and hydrogen bonding (9,10) contribute to ligand specificity.

The polysaccharide chitin, a β-1,4-linked polymer of N-acetyl-D-glucosamine (GlcNAc), is a major component of the crustacean shells, the exoskeleton of insects, and the cell wall of fungi, but is absent in plants. Recognition of chitin is predominantly conferred by two CBMs: the hevein domain (hereafter denoted as CBM18) (11), and the invertebrate

chitin-binding domain (CBM14) (12). The CBM18 motif is nearly exclusively found in plants. So far one additional member has been identified in *Streptomyces griseus* (13). Instead, the CBM14 motif is found in the genomes of baculoviridae, invertebrates, and mammals, but CBM14 appears to be absent in plants (12). CBM14 and CBM18 appear to exemplify convergent evolution as the two domains have no clear sequence homologies, but their tertiary structure contains a shared structural motif (14). Moreover, the two domains are similarly arranged in genes and the corresponding genes overlap in their biological function (12). This can be illustrated by lectins containing four in-tandem CBM repeats, e.g. the seed-storage protein wheat germ agglutinin (WGA) (CBM18) is a specific lectin of grasses (*Gramineae*) with four repeats (15), while peritrophin-44 of *Lucilia cuprina* (CBM14) represent a class of cell wall proteins with four repeats found in the gut of insects (16). The overlap in function is most pronounced in chitinases; the plant-specific family-19 chitinolytic domain is strictly fused to the CBM18 module, while in mammals and invertebrates the widespread family-18 chitinolytic domain is fused to the CBM14 module.

The race-specific elicitor AVR4 of the tomato pathogen *Cladosporium fulvum* is the only recognized fungal protein containing a CBM14 (17,18). Strains of *C. fulvum* producing wild-type AVR4 protein (i.e. non-race 4 strains) elicit a defense response in tomato plants carrying the matching *Cf-4* resistance gene (19,20). This specific type of resistance is mostly referred to as the “gene-for-gene” type of resistance. Moreover, *Cf-4* mediated recognition in tomato results in complete resistance against non-race 4 strains of *C. fulvum*. The triggered defense responses include the induction of a hypersensitive response (a type of programmed cell death in plants) and the accumulation of plant pathogenesis-related proteins (PR-proteins) (21,22) including β-1,3-glucanases (PR-2) and chitinases (PR-3, PR-4, PR-8, and PR-11) (23-25). The PR-3 and PR-4 classes of chitinases/chitinase-like proteins contain the family-19 catalytic domain fused to CBM18. Most interestingly, certain plant lectins are processed from PR-4 precursors from which an inactive chitinolytic domain is cleaved off (15,26). Well-studied examples are hevein of *Hevea brasilliensis* and *Urtica dioica* agglutinin (UDA). The latter contains two CBM18 repeats.

Fungal growth is inhibited by PR-3/PR-4 chitinases (27-29), but also by lectins of the PR-4 class (30-32). Presently, an extensive list of transgenic plants overexpressing chitinases has been generated, which all appear less susceptible for a large number of plant pathogenic fungi (33). The fungus *C. fulvum* is when grown *in vitro*, however, reported to be insensitive to a mixture of tomato chitinases and β-1,3-glucanases (34). Recent studies have demonstrated that AVR4 can protect the fungi *Trichoderma viride* and *Fusarium solani* f.sp.

phaseoli against anti-fungal activity of PR-3 chitinases (18). The protective effect is most probably due to accumulation of AVR4 at chitin present in the fungal cell wall, thereby protecting these fungi against the deleterious effects of chitinases.

To better understand the role of AVR4 during infection, we examined the binding properties of AVR4 to chitin using soluble chito-oligomers. This system allows a close comparison between AVR4 and CBM18 lectins (e.g. hevein, prohevein, UDA, and WGA). For the CBM18 lectins, the use of chito-oligomers has provided a detailed description of the chitin-binding site. In CBM18 lectins, the binding site is composed of three binding subsites (a subsite is defined as all amino acids that interact with one sugar residue). Subsite +1 is formed by the residues S18, W23, and Y30, while W21 is involved in subsite +2 and +3 (10,35-41). More importantly, CBM18 lectins already interact with GlcNAc. Here we report that AVR4 only interacts with chito-oligomers with a minimal degree-of-polymerization (DP) of three. Using NMR, we identified several residues in AVR4, which are important for the interaction. These residues are indeed positioned in the structural motif shared by CBM14 and CBM18, but they appear to highlight differences in binding rather than similarities as compared to the binding-site in CBM18 (14).

Materials and Methods

Materials. AVR4 was produced in culture by the methylotrophic yeast *Pichia pastoris* and purified from culture fluids (42). AVR9 was obtained by solid-phase synthesis followed by oxidative-folding (43,44). Ribonuclease A was obtained from Sigma. Chito-oligomers (*N*-acetyl-D-glucosamine (GlcNAc), *N-N'*-diacetylchitobiose (chitobiose), *N,N',N''*-triacetylchitotriose etc.) were purchased from Seikagaku (Tokyo). All solvents and chemicals used were of the highest grade available. Concentrations of AVR4 were determined spectrophotometrically using a molar extinction coefficient of 1.50×10^4 M^{-1} cm^{-1} at 280 nm.

Isothermal Titration Calorimetry (ITC). ITC measurements were performed at 25°C following standard procedures using a MCS Microcal titration calorimeter (45). The reaction cell (with a volume of ~1.35 mL) containing the AVR4 protein sample was continuously stirred while successive aliquots of ligand solution were added (final volume of the additions was 250 μL). Ligand and protein were dissolved in the same buffer. The AVR4 concentration in the cell was in the range of 90-360 μM depending on DP of the chito-oligomer added (see supplementary data). The chito-oligomer concentrations used were 23 mM, 20 mM, 3.2 mM, and 2.0 mM for a DP=3, 4, 5, and 6, respectively. The integrated heat effects after correction for heat of dilution were analyzed using standard software provided by Microcal Inc. The

cumulative heat effect (Q) during the titration process for a simple set of binding sites is given by the following equations:

$$Q = M_t V_o n \upsilon \Delta H \quad \text{(a)}$$

where M_t is the macromolecule concentration in the calorimetric cell, characterized by the volume (V_o), n the number of binding sites with a binding enthalpy of ΔH, and υ the fractional saturation of the binding sites, which can be related to the apparent association constant (K_A) and to the total ligand concentration (L_T).

$$K_A = \upsilon / [(1-\upsilon)L_T] \quad \text{(b)}$$

$$L_T = L_f + M_t n \upsilon \quad \text{(c)}$$

where L_f is the concentration of free ligand. Other thermodynamic parameters were calculated using the standard thermodynamic equation

$$-RT \ln K_A = \Delta G = \Delta H - T\Delta S \quad \text{(d)}$$

Tryptophan fluorescence quenching. Fluorescence measurements were performed with a Varian Cary Eclipse thermostated at 293 K. The excitation wavelength was 295 nm with an excitation slit of 2.5 nm. Emission intensities were collected over the wavelength range of 315-400 nm with an emission slit of 5 nm. Spectra were the average of 3 scans and corrected for the effect of dilution, buffer and chito-oligomer additions. Quantitative binding experiments were performed in a volume of 3 mL to which aliquots of a ligand solution (5-30 μl) were added under continuous stirring. AVR4 was dissolved at a protein concentration of 3.6 μM in 20 mM potassium phosphate buffer pH 7.0 containing 50 mM sodium chloride. Chito-oligomers were dissolved in the same buffer at a concentration of 38 mM, 30 mM, 16 mM, and 2.0 mM for a DP=3, 4, 5, and 6, respectively. The maximum change in volume due to the ligand additions was less than 5%. The fluorescence quenching at full saturation of binding (F_∞) was estimated by plotting $1/(F_0-F)$ versus 1/[S], and extrapolating to the y-axis, where F_0 is the fluorescence intensity of AVR4 without ligand and F is the fluorescence intensity of AV4 at a chito-oligomer concentration [S]. Association constants (K_A) were estimated using two methods: the fluorescence quenching titration equivalent of the Hill Plot

(*i.e.* Log (F_0–F/F–F_∞) versus log [S] (46), and Scatchard plot analysis (*i.e.* υ/L_f versus υ) (47).

Size-exclusion chromatography. pH-dependent size-exclusion chromatography was performed at 20^{0}C using a Superdex-75 (HR 10/30; Amersham) column operated at a flow rate of 0.5 ml/min. The apparent molecular mass (Mw) of the oligomeric/complexed state of AVR4 (25 μM in 50 μL injection volume) was estimated from a standard curve produced at different pH values (5.0, 7.0 and 8.6) in buffer containing 50 mM potassium phosphate and 150 mM potassium chloride. Standard curves were obtained by plotting the log molecular mass of protein standards (aprotinin, insulin, ubiquitin, Ribonuclease A, serum albumin (all bovine), horse myoglobin, chicken albumin, and blue dextran) versus $K_{av.}$ The K_{av} is defined as

$$K_{av} = (V_E - V_V) / (V_B - V_v) \qquad \text{(e)}$$

where V_E is the elution volume, V_V is the void volume, and V_B is the bed volume of the column matrix.

Mass spectrometry. ESI-MS was performed with a Q-Tof *Ultima* Global mass spectrometer (Waters Corporation, MS Technologies Centre, England). The standard buffer used to detect non-covalent complexes was 10 mM ammonium acetate / acetic acid (pH range 5.0-8.6). The sample infusion flow rate was 10 μl/min. Instrument settings were: Capillary potential–3 kV, Cone voltage–100 V, Desolvation gas flow rate–150 L/h, Source temperature–90 ^{o}C, Radio Frequency 1 (RF1)–225 kHz, and the MALDI strip was positioned at 3600 units resulting in an elevated intermediate pressure of 4.35 mbar. The instrument was operated under standard ESI conditions. Calibration of the TOF analyzer was performed with a CsI solution of 2 mg/mL in isopropanol/water (50:50, v/v) over the mass range 800-7100 Da.

Nuclear magnetic resonance spectroscopy. ^{13}C/^{15}N-labelled NMR samples of AVR4 typically contained 1.5 mM protein in 20 mM acetate-d_4 and 50 mM sodium chloride at pH 4.6. Isotopic labeling and purification of AVR4 was performed as described previously (42). All NMR samples were prepared in a H_2O/D_2O 95/5 (v/v) mixture and contained trace amounts of sodium azide as a preservative. All NMR spectra were acquired at 25 ^{0}C on Varian *Inova* 500, 600, or 800 MHz, and Bruker AMX500 spectrometers. Triple and double-resonance hetero-nuclear NMR experiments performed to obtain backbone and side-chain assignments of AVR4 included 3D HNCA, HN(CO)CA, HNCACB, CBCA(CO)NH, (H)CCH-

TOCSY and HC(C)H-TOCSY (Protein pack, Varian Inc.). The assignment was performed using the standard assignment procedures based on triple and double resonance NMR spectra: First, ^{15}N HSQC spectra were used to obtain a set of ^{1}H-^{15}N resonance frequencies. Sequential assignment was then performed using these shift-pairs in combination with HNCA, HN(CO)CA, HNCACB, and CBCA(CO)NH spectra. Assignment of the non-aromatic side chain resonances were obtained by means of (H)CCH-TOCSY and HC(C)H-TOCSY spectra. A ^{15}N-NOESY-HSQC (48) spectrum was used for NOE assignments of the backbone HN and tryptophan side chain H$^{\varepsilon 1}$ protons. All data processing and analysis was done using the programs NMRPipe (49) and XEASY (50), respectively. The chemical shifts of tachycitin were retrieved from BioMagResBank (51).

NMR titration experiments. Binding of chito-oligomers of different DP to AVR4 was monitored by recording ^{1}H-^{15}N-HSQC spectra of a series of samples at five different temperatures. The temperature in the NMR tube was carefully calibrated by referencing the water resonance to Sodium 2,2-dimethyl-2-silapentane-5-sulfonate (DSS). The protein concentration was kept constant throughout the titration (1 mM), while the ligand concentration was increased in successive steps, as described previously (36). The buffer used for the titration contained 20 mM Acetate-d_4 and 150 mM NaCl at pH 6. Final concentrations of the ligand were: 50mM GlcNAc, 35 mM $(GlcNAc)_2$, 27.2 mM $(GlcNAc)_3$, and 3.5 mM $(GlcNAc)_6$. The association constants (K_a) were estimated using a NMR derivative of the Scatchard plot,

$$(\Delta/\Delta_o)/[L_f] = -K_a n + K_a(\Delta/\Delta o) \qquad (f)$$

where $\Delta=\delta_{observed}-\delta_{free}$ and $\Delta_o=\delta_{saturated}-\delta_{free}$. Thermodynamic parameters (ΔH and ΔS) were estimated from a van 't Hoff plot based on a set of K_as obtained from a set of backbone resonances.

RESULTS AND DISCUSSION

Ligand binding studies. In previous studies, the binding specificity of AVR4 for insoluble polysaccharides was studied in detail using affinity precipitation (18). From these studies, it was concluded that AVR4 specifically binds to chitin and not to other polysaccharides. Polysaccharides tested were chitin, cellulose, xylan, curdlan (β-1,3-glucan), lichenan, and chitosan (deacytelated chitin).

Calorimetric titrations. Isothermal titration calorimetry (ITC) was used to determine the affinity of AVR4 for linear chito-oligomers with increasing degrees-of-polymerization (DP). The ITC experiments show that AVR4 only interacts with chito-oligomers when the DP ≥ 3 (Figure1, Table 1). No heat-of-binding was measured when AVR4 was titrated with 50 mM N-acetyl-D-glucosamine (GlcNAc) or 50 mM $(GlcNAc)_2$. This result indicates that AVR4 contains at least three binding subsites. Moreover, these three subsites need apparently to be occupied by the ligand in order to achieve binding. These findings sharply contrast with CBM18 lectins also contain three binding subsites in the binding site, but they already interact with a single GlcNac residue (10,47,52).

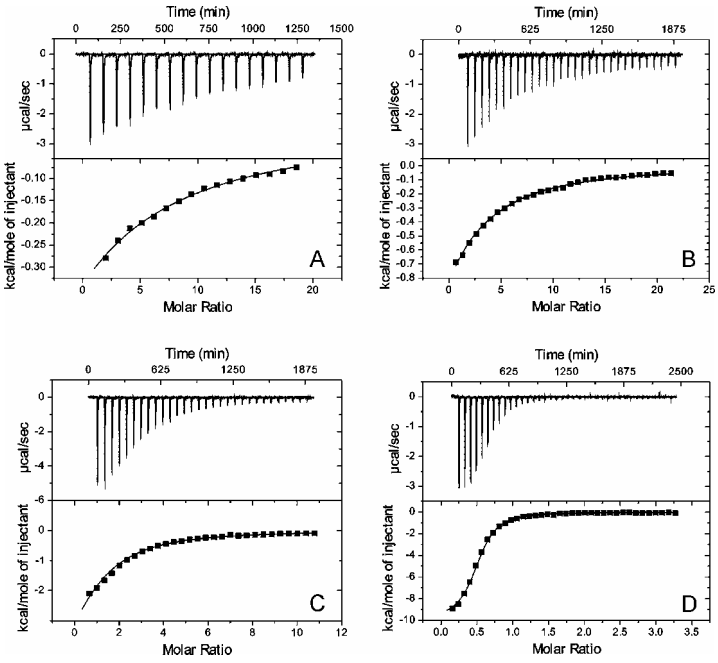

Figure 1. Isothermal titration of AVR4 (*upper panel*) with chito-oligomers of different degree-of-polymerization (DP) at 25°C, plus the integrated heat released by the binding event (*lower panel*) of the same titration. Concentration of AVR4 in the cell was (A) 350 μM, (B) 180 μM, (C)120 μM, and (D)100 μM. The concentration of the chito-oligomers in the syringe was in order of increasing DP: (A) 23 mM, DP=3; (B) 20 mM, DP=4; (C) 3.2 mM, DP=5; and (D) 2.0 mM, DP=6. The shown data are the result of a typical experiment of at least three independent replicates.

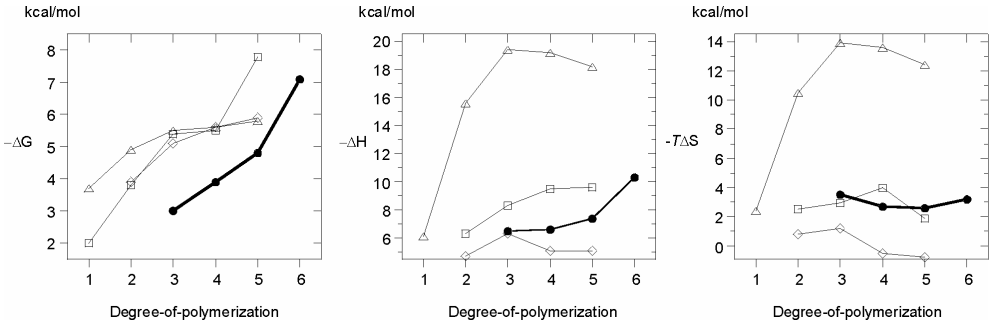

Figure 2. Comparison of the thermodynamic parameters (A) ΔG, (B) ΔH, (C) $-T\Delta S$ of binding for chito-oligomers with increasing degree-of-polymerization (DP) to AVR4 (●), WGA (Δ; taken from (52)), UDA (◊; taken from (47)), and hevein (□; taken from (10)).

A similar sign and order of magnitude was obtained for the thermodynamic parameters (ΔG, ΔH, and ΔS) for the interaction between AVR4 and chito-oligomers as was previously reported for the plant chitin-binding lectins hevein (10,36), prohevein (38), and UDA (47) (only WGA deviates(52)) (Figure 2). Small negative ΔH and ΔS values were found for each of these lectin-sugar interactions, as is the case for AVR4. Thus, in general, the interaction between lectins and chito-oligomers appears to be enthalpically driven. For this sign and size of ΔH, hydrogen bonds, CH-π interactions, and van-der-Waals forces appear to be the most important factors contributing to the stabilization of the complex (7,53-55). However, the conclusion that the lectin-sugar interaction is enthalpically driven may only be valid for soluble ligands, as binding events to crystalline polysaccharides have been reported to be entropically driven as well (56).

The binding-saturation curves for chito-oligomers with a DP=3–5 were fitted assuming a one-binding site model (Fig 1). The binding-saturation curve for $(GlcNAc)_6$ deviated from a 1:1 stoichiometry. However, a model with two independent binding sites at the sugar ligand accurately described the binding event between AVR4 and $(GlcNAc)_6$. This second binding site could not be shown for $(GlcNAc)_5$, which agrees with a three-binding subsite model for AVR4. Another striking feature for $(GlcNAc)_6$ is the substantially increased association constant (K_A), which is ~45 times higher than the K_A observed for $(GlcNAc)_5$ and ~200 times higher than the K_A observed for $(GlcNAc)_4$. This increased K_A can be ascribed to the more negative value of ΔH, as ΔS becomes also more negative (thus opposes binding)

when the DP increases from 5 to 6. The increased ΔH for a $(GlcNAc)_6$ could possibly be explained by allosteric interactions that occur between two AVR4 molecules when they bind $(GlcNAc)_6$. This will result in an increased solvent buried area, thereby contributing to ΔH. The existence of a protein-protein interaction was also noted when examining the pH-dependency of the binding event. The number of binding sites (Table 2) appeared to be pH-dependent with an apparent pK_A of ~4. A possible explanation could be that an Asp or Glu residue becomes protonated at acid pH. This residue could form an essential interaction at the protein-protein interface.

The three binding subsite model also fits the more negative entropy found in the case of $(GlcNAc)_6$ as compared to $(GlcNAc)_5$. In the case of $(GlcNAc)_6$, most translations and rotations of the sugar chain become restrained upon complexation with the second AVR4 molecule, while this flexibility partially remains for $(GlcNAc)_4$ and $(GlcNAc)_5$. This explains the increased ΔS for the latter two ligands as compared to $(GlcNAc)_3$ (thereby contributing to the increased K_A). Similar studies with hevein (10) also revealed a sharp increase in K_A (~45 times) when the DP increased from 4 to 5, but in this case ΔS was more favorable (Fig 2). The less negative (thus more favorable) ΔS was explained by demonstrating that several hevein-$(GlcNAc)_5$ complexes coexisted involving complexes having a 1:1 and 1:2 stoichiometry, respectively.

The cost of restraining translations and rotations of the GlcNAc chains has been given as one explanation for the “enthalpy-entropy” compensation in lectin-sugar interactions resulting in K_d’s in the micro- to millimolar range (57). AVR4 complies with this rule (Fig 3). Notably, the binding energetics of AVR4 clusters with those reported for hevein and UDA, but not with those of WGA. Structures of hevein (10) and UDA (40) in complex with $(GlcNAc)_3$ revealed that these lectins contained a surface-exposed binding site, while the binding site of WGA (35) is completely solvent-buried at the interface of the WGA dimer. The more solvent-buried binding site of WGA is reflected in a three-fold increased ΔH, but it is also compensated by a more negative ΔS, so that for WGA ΔG does not differ from ΔG obtained for the other plant chitin-binding lectins (Fig 2). In conclusion, our analysis indicates that the binding site of AVR4 is most likely solvent-exposed.

Table 1 Thermodynamics of AVR4 Binding to chito-oligomers using Isothermal Titration Calorimetry

DP[a]	$K_A \times 10^{-3}$ M^{-1}	ΔG Kcal mol^{-1}	ΔH Kcal mol^{-1}	$T\Delta S$ Kcal mol^{-1}	ΔS cal $mol^{-1}K^{-1}$	n[b]
1			ND[c]			
2			ND			
3	0.16±0.006	–3.0±0.02	–6.5±0.18	–3.5±0.20	-11.8±0.67	1.00
4	0.76±0.021	–3.9±0.02	–6.6±0.11	–2.7±0.13	-8.8±0.44	1.00
5	3.60±0.34	–4.8±0.06	–7.4±0.13	–2.6±0.19	-8.7±0.64	1.00
6	160±6.2	–7.1±0.05	–10.3±0.12	–3.2±0.17	-10.7±0.57	0.50

[a] DP, degree-of-polymerization; [b] fixed value; [c] ND, no binding detected; Buffer used was 50 mM potassium phosphate, 150 mM sodium chloride pH 7.0. The average result of at least three independent experiments is shown.

Table 2 Thermodynamics of AVR4 Binding to $(GlcNAc)_6$ over a pH range using Isothermal Titration Calorimetry

pH	$K_A \times 10^{-3}$ M^{-1}	ΔG Kcal mol^{-1}	ΔH Kcal mol^{-1}	$T\Delta S$ Kcal mol^{-1}	ΔS cal $mol^{-1}K^{-1}$	n
3.4[a]	74±7.2	–6.6±0.06	–8.8±0.20	–2.2±0.26	–7.4±0.87	1.05±0.03
4.4	104±8.3	–6.8±0.05	–10.3±0.04	–3.5±0.09	–11.7±0.30	0.65±0.04
5.3	121±11	–6.9±0.05	–10.4±0.05	–3.5±0.10	–11.7±0.34	0.73±0.03
5.9[b]	149±13	-7.1±0.05	–10.0±0.05	–2.9±0.10	–9.7±0.34	0.62±0.03
6.9	155±11	–7.1±0.05	–10.3±0.03	–3.2±0.08	–10.7±0.27	0.54±0.04
7.9	136±8.5	–7.00±0.05	–9.3±0.04	–2.3±0.09	–7.7±0..30	0.63±0.02

[a] in 50 mM potassium acetate buffer, 150 mM sodium chloride; [b] in 50 mM potassium phosphate buffer, 150 mM sodium chloride; The average result of at least three independent experiments is shown.

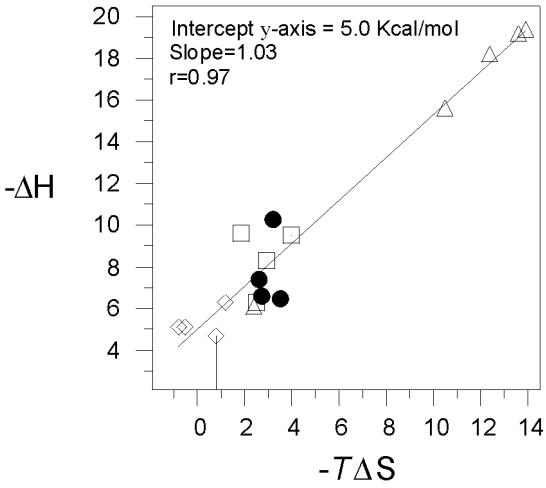

Figure 3. Enthalpy-entropy compensation for the interaction between chito-oligomers of different degree-of-polymerization and chitin-binding lectins: AVR4 (●), WGA (Δ; taken from (52), UDA (◊; taken from (47), and hevein (□; taken from (10).

Tryptophan fluorescence quenching. Surface-exposed tryptophans are often involved in protein-carbohydrate interactions forming CH-π interactions (7). Trp fluorescence quenching (46) can, therefore, be employed to study the possible involvement of tryptophans in the interaction. When chito-oligomers of DP ≥ 3 were added to AVR4, Trp fluorescence was significantly quenched, which was associated by a small blue shift from 354 nm to 348 nm (Fig 4). As expected, the addition of GlcNAc or $(GlcNac)_2$ (up to 50 mM) did not give any blue shift or quenching of the fluorescence (Table 3). The blue shift indicates that one of the Trp residues becomes more solvent-buried upon complexation, which is most likely W71 as the corresponding residue in tachycitin is also solvent-exposed (14). In analogy with the structure of tachycitin (14), the second Trp residue in AVR4, W63, is expected to be involved in a hydrophobic interaction in the core of the protein with another aromatic residue, Y38 (14). This interaction appears to be highly conserved, as all members of the CBM14 family contain these two aromatic amino acid residues (chapter 5).

Regardless of the DP, the maximum Trp fluorescence quenching was always near 50% at full saturation of binding (F_∞) (Table 3). Thus, the DP did not influence the maximum fluorescence quenching (F_∞), from which we conclude that no additional amino acid residues become involved in the interaction when chito-oligomers bind of a DP > 3. This finding corroborates the proposed three subsite model for AVR4. A different situation was previously observed for hevein (10), *i.e.* its binding site appeared to involve more interactions for $(GlcNAc)_4$ and $(GlcNAc)_5$. In addition, our data for $(GlcNAc)_6$ indicate that

both Trp residues are distant from the protein-protein interface between the two AVR4 molecules bound to the same ligand.

The fluorescence quenching experiments were used independently from the ITC data to determine K_A values for the interaction between AVR4 and chito-oligomers (Table 3). Estimates for the K_A were obtained from Scatchard (Fig 4B) and Hill plot analyses (Fig 5). The K_A values obtained were in good agreement with the K_A values obtained by ITC. The slopes obtained for the Hill plots approached unity for the different chito-oligomers, including $(GlcNAc)_6$. However, the Scatchard plot was clearly curved for $(GlcNAc)_6$, while for chito-oligomers with a DP=3, 4 or 5 a perfect linear regression was obtained, as expected for a single binding event (Fig 4B). The former confirms the presence of two-binding sites for $(GlcNAc)_6$. Moreover, the curved Scatchard plot indicates positive cooperativety for the second binding event, which is partially reflected in the enhanced negative ΔH for $(GlcNAc)_6$. Our initial assumption that the two binding sites were independent seems, therefore, incorrect. However, a data analysis with two dependent binding sites for DP=6 did not further improvement the fit of the ITC data. In conclusion, the fluorescence experiments strongly suggest the existence of a protein-protein interface between the AVR4 molecules when bound to $(GlcNAc)_6$.

Trp fluorescence quenching experiments were also reported previously for peritrophin-44 (16). In this case, Trp fluorescence quenching was ~16% at full saturation for $(GlcNAc)_3$; peritrophin-44 contains only one Trp residue in one of the four CBM14 repeats. On the other hand, similar binding experiments with UDA and WGA (both CBM18) resulted in enhanced fluorescence intensity in the presence of chito-oligomers–up to 27% for UDA (47) and ~36% for WGA (46). The increased fluorescence intensity for CBM18 as compared to fluorescence quenching for CBM14 implies that the aromatic residues in the two complexes may have different orientations in relation to the chito-oligomer.

Analytical size-exclusion chromatography. To exclude that non-specific aggregation of AVR4 occurred under any of the tested conditions, we performed analytical size-exclusion chromatography. AVR4 eluted from the column as a monomer at acidic to neutral pH (Table 4), whereas at pH 8.6 higher order complexes were observed (the estimated pI of AVR4 is 8.6). The formation of higher order complexes (dimer, trimer, etc.) proved to be reversible as the equilibrium shifted to monomer when the pH was decreased again. The monomer of AVR4 eluted at an apparent molecular mass (Mw) of 10.3 kDa at pH 7.0 (Table 4), which is 8% higher than the Mw as determined by MALDI-TOF mass spectrometry. This supports that AVR4 behaves like a globular protein on the column. Subsequently, the column

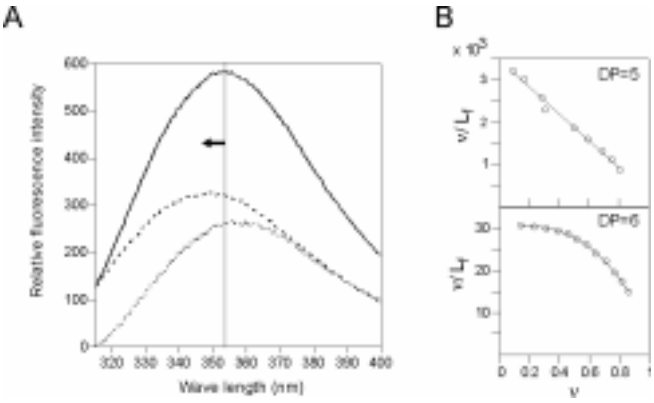

Figure 4. Tryptophan fluorescence spectra of AVR4 in the presence of $(GlcNAc)_5$ and $(GlcNAc)_6$ (A) Emission spectrum of AVR4 (3.6 μM) without (—) and with 77 μM of DP=6 (full saturation; ––––), as well as the difference spectrum (----). Maximum fluorescence quenching was 50% for $(GlcNAc)_6$. (B) Scatchard plot of the fluorescence quenching obtained for $(GlcNAc)_5$ and $(GlcNAc)_6$. A single binding event is observed for $(GlcNAc)_5$ (linear regression with an intercept at *y*-axis at ν=1.0), while for DP=6 positive cooperativety between two binding sites is observed. Experiments with $(GlcNAc)_3$ and $(GlcNAc)_4$ showed also a single binding event (not shown). L_f, concentration of free ligand; ν, fraction of occupied binding sites.

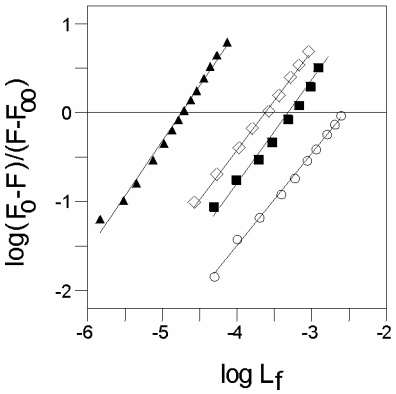

Figure 5. Hill plot obtained for the tryptophan fluorescent quenching titration experiments of AVR4 in the presence of chito-oligomers with increasing degree-of-polymerization (DP): 3 (○), 4 (■), 5 (◊), and 6 (▲).

was equilibrated with concentrations of either 35 mM $(GlcNAc)_5$ or 25 mM $(GlcNAc)_6$. Under these conditions, the apparent Mw of AVR4 increased significantly. When the column was equilibrated with $(GlcNAc)_5$, a protein complex eluted at an apparent Mw corresponding to the Mw of AVR4 plus one bound $(GlcNAc)_5$ molecule. However, in the case of $(GlcNAc)_6$, a protein complex eluted at an apparent Mw 60% higher than to be expected for AVR4 alone. This led us to conclude that equilibrium exists on the column between one and two AVR4 molecules bound to one $(GlcNAc)_6$. This equilibrium originates most likely form the relative slow nature of size-exclusion chromatography. Similar experiments with 35 mM GlcNAc or 35 mM $(GlcNac)_2$ caused no shift in the elution time of AVR4 as compared to the buffer-equilibrated column. Increased concentrations of the chito-oligomers could not be used as they increased the column pressure above threshold.

Table 3 Association constants of AVR4 binding to chito-oligomers determined by tryptophan fluorescence quenching

DP[a]	$K_A \times 10^{-3}$ (M^{-1}) *from* Hill Plot[b]	$K_A \times 10^{-3}$ (M^{-1}) *from* Scatchard[c]	Maximum % quenching of *F*	**n**
1		ND[d]		
2		ND		
3	0.35	0.21	50	1
4	1.1	1.1	52	1
5	4.2	3.5	52	1
6	110	6.1 and 42[e]	50	2

[a] DP, degree-of-polymerization; [b] intercept *x*-axis of log $(F\text{-}F_0) / (F_\infty\text{-}F)$ vs. log L_f, [c] Scatchard plot of v / L_f versus v; [d] ND, no binding detected; [e] apparent K_A values estimated from the upper and lower segment of the Scatchard plot. Buffer used was 20 mM potassium phosphate, 50 mM sodium chloride pH 7.0.

Mass Spectrometry. Electrospray ionization mass spectrometry (ESI-MS) is increasingly used for the direct detection of non-covalent complexes over an extended range of K_D values from 10^{-6} to 10^{-14} M (58,59). Despite the K_D (K_A^{-1}) values in the order of 10^{-2}-10^{-6} M for the chito-oligomers, we investigated whether we could detect specific non-covalent complexes between AVR4 and chito-oligomers using ESI-MS. Care was taken to optimize the instrument settings, such as source temperature, cone potential, and desolvation gas flow rate, which have all been reported to influence the detection of non-covalent complexes (60,61). Instrument settings in this study were optimized using the mass peak of the tetramer of yeast alcohol dehydrogenase (ADH) in 10 mM ammonium acetate at pH 7.0. Subsequently, ESI MS was performed on a sample of 20 μM AVR4 in the presence of 20 μM $(GlcNAc)_6$ (both dissolved in 10 mM ammonium acetate at pH 7) (Fig 6). Under these conditions, the mass spectrum showed a distribution of charge states ranging from 3+ to 8+, with the dominance of the 6+ charge state. Further analysis of this mass spectrum revealed three distinct entities: AVR4, $(GlcNAc)_6$ and the non-covalent complex between AVR4 and $(GlcNAc)_6$ (with a 1:1 stoichiometry). A primary concern for the detection of complexes with ESI-MS is the specificity of the observed complex. First of all, the observed 1:1 stoichiometry of the complex in the gas-phase is regarded as a good indicator of specificity of non-covalent complexes (58). A survey over the pH 3.5-8.5 (using 10 mM ammonium acetate as buffer) gave the highest mass peak intensity for the complex

Table 4 Analytical size-exclusion chromatography of AVR4 in the presence of chito-oligomers

	Apparent Mw (kDa)	Calculated Mw (kDa)	Stoichiometry[a]
AVR4	10.3	9.551	1.08
AVR4+$(GlcNAc)_5$	11.7		1.10
AVR4+$(GlcNAc)_6$	16.7		1.55
$(GlcNAc)_5$[b]	2.5	1.050	
$(GlcNAc)_6$	2.5	1.243	

[a] Apparent MW of the Complex / Calculated MW of the monomer complex [AVR4]= 25 μM; [b] 50 μl chito-oligomer (25 μM) loaded. All experiments are the average of two injections

at neutral pH; higher order “hybrid” assemblies were not observed over the pH range tested. The ITC data had already indicated that the interaction weakens towards acidic pH (Table 2). Increased concentrations of AVR4 caused only a reduction of the relative mass peak intensity of those peaks that corresponded with the 1:1 complex (as expected). On the other hand, a five times surplus of ligand (100 μM) compared to protein (tested with a DP=5 and DP=6) resulted in non-specific aggregates containing two, three or even four chito-oligomers per single AVR4 molecule. However, all conditions tested (including variations of the instrument settings) did not result in mass peaks that would correspond with a complex containing two AVR4 molecules and one $(GlcNAc)_6$ molecule. The gas phase itself is already known to affect any complexes possibly explaining the absence of the 1:2 complex.

Next, we compared the relative peak intensities for the AVR4-$(GlcNAc)_n$ complex (5+ charge state) using ligands with increasing DP (Fig 6B). The relative intensity of the mass peak corresponding to the non-covalent complex was found to correlate with the DP, *i.e.* peak intensities increased with the DP. No complex was observed for GlcNAc or $(GlcNac)_2$. Thus, these findings seem to reflect the K_d values as determined with ITC and fluorescence quenching. As control experiments, two other proteins were examined in parallel: AVR9 of *C. fulvum* (3.3 kDa) and Ribonuclease A (13.5 kDa). These control proteins were chosen because they lack a carbohydrate-binding module, have a basic pI and contain disulfide bonds. Mass peaks corresponding to protein-ligand complexes were observed for both AVR9 and Ribonuclease A. However, the relative peak intensity of the mass peaks corresponding to a complex was always low (5%<) and appeared to be independent of the DP for a DP=3-6 (Fig 6B). Therefore, we conclude that the observed interactions between AVR4 and chito-oligomers with a DP=4-6 with ESI MS are specific, but care should be taken when detecting complexes with K_D > 1 mM (as for the interaction between AVR4 and $(GlcNAc)_3$).

Nuclear magnetic resonance. The ^{1}H, ^{13}C, ^{15}N backbone and side chain resonances of AVR4 were assigned using common NMR protocols. In general, the backbone amides were well-resolved and well-dispersed in the ^{15}N-HSQC spectrum, indicative of a folded protein (42). Of the 72 expected amide cross-peaks in the ^{15}N-HSQC, the peaks C57, G68 and C72 could not be assigned, presumably due to unfavorable chemical exchange processes. Further, determination of the solution structure of AVR4 was severely impaired by the presence of 14 prolines and extreme overlap of side chain ^{1}H and ^{13}C resonances.

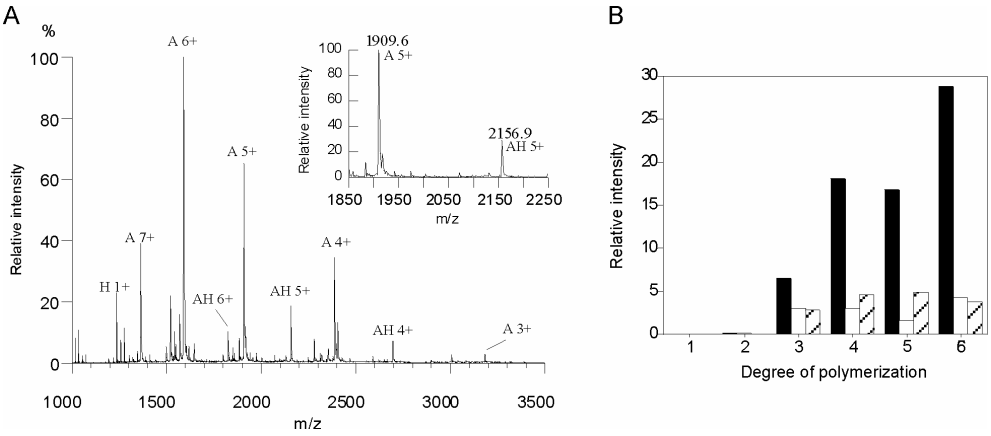

Figure 6. (A) ESI mass spectrum of AVR4 in the presence of $(GlcNAc)_6$ (both at 20 μM). Numbers denote the charge state of the ions. The insert shows an enlargement of m/z 1850-2150 Da showing the most dominant mass peaks corresponding to the non-covalent complex and AVR4 (5+ charge state for both) within this mass range. (B) Relative intensities of the mass peaks corresponding to the non-covalent complex of AVR4 (black bars), AVR9 (white bars), and Ribonuclease A (hatched bars)(all at 20 μM). The relative intensity of the mass peak corresponding to a complex was normalized to the mass peak corresponding to the protein alone with a similar charge. Complexes were not observed for DP=1 and 2 for any of the proteins. Instrument settings were identical in (A) and (B). All experiments were performed in 10 mM ammonium acetate at pH 7. A–Avr4; H–$(GlcNAc)_6$, AH–non-covalent complex with a 1:1 stoichiometry.

We obtained, however, information about the secondary structure of AVR4. Firstly, the NOE patterns in the ^{15}N-NOESY-HSQC spectrum clearly indicated an α-helix (62) for the residues 14-22. ^{13}Cα chemical shift index (CSI) analysis (63) confirmed the α-helical character of this stretch of residues (Fig 7A). Notably, these residues represent a sequence insertion in AVR4, which is connected to the "consensus" of the protein through an additional disulfide bond, C21-C28. Secondly, the Hα chemical shifts of the residues 25-46 and 58-80 follow closely the Hα shifts of the corresponding residues in tachycitin (Fig 8). In addition, all but one (the first conserved Cys) of the conserved residues forming the consensus of CBM14 are amongst these residues. Together, these data indicate that the residue 25-46 and 58-80

adapt a similar fold in AVR4 as the corresponding residues in tachycitin. Thirdly, a ribbon diagram of tachycitin is shown in Figure 10B. Tachycitin contains two anti-parallel β-sheets and these may as well be present in AVR4 as we observed strong dαN(i+1) NOE contacts in combination with long stretches of β-sheet propensity in the $^{13}C\alpha$ CSI plot. Finally, the six Cys residues conserved for CBM14 have a similar disulfide bond pattern in AVR4 and tachycitin (17). In conclusion, we propose that AVR4 adapts a similar fold as tachycitin, except for one additional α-helix comprising the residues 14-22.

NMR studies of the AVR4-chito-oligomer complex. Residues involved in the interaction between AVR4 and chitin were identified from changes in chemical shifts of the HN resonances of AVR4 induced by adding chito-oligomers. When aliquots of $(GlcNAc)_3$ were added to AVR4, a concentration dependent change in chemical shift (Fig 9) was observed for a set of HN resonances in the HSQC spectra without substantial line broadening. Adding GlcNAc or $(GlcNAc)_2$ did not induce such changes in the spectrum. The continuous change in chemical shift is characteristic for fast exchange on the NMR time scale (64). The concentration-dependent chemical shift changes allowed us to estimate K_A values using the NMR-derivative of the Scatchard plot. We analyzed the HN resonances of D73 and Y74 in this way; these two resonances exhibited the largest changes in chemical shift upon complexation (Fig 7B). The obtained K_A values were 188 and 184 M^{-1} (at 298 K) for D73 and Y74, respectively. These numbers are in close agreement with the ITC and fluorescence quenching data. Subsequently, the temperature dependency of the K_A was used to estimate the ΔH and the ΔS from a van 't Hoff plot (using the average K_A obtained D73 and Y74), *i.e.* $-R$ ln (K_A) versus $1/T$ (Fig 7C). The slope of the linear relationship corresponded with to a ΔH^o_{vH} of –7.78 Kcal/mol, which gives a ΔS of –15.7 cal mol^{-1} K^{-1}. Although these numbers are in the same order as the ITC data, they should be regarded as qualitative rather than quantitative since the derivation of thermodynamic parameters from a van 't Hoff plot assumes that ΔH^o is independent of the heat capacity ΔC_p ($=\delta\Delta H / \delta T$). A small, but negative contribution of ΔC_p to ΔH^o_{cal} is generally observed for lectin-sugar interactions, which is not included in ΔH^o_{vH} (55,65,66)

When AVR4 was titrated with $(GlcNAc)_6$, two separate phenomena were observed. Line broadening occurred for a subset of the HN resonances in the HSQC at low concentrations of ligand, while at increased concentrations (> 0.5 mM) almost all HN resonances showed increased line widths. The former set of resonances strongly overlapped with those that showed large shifts for $(GlcNAc)_3$, which indicates that the

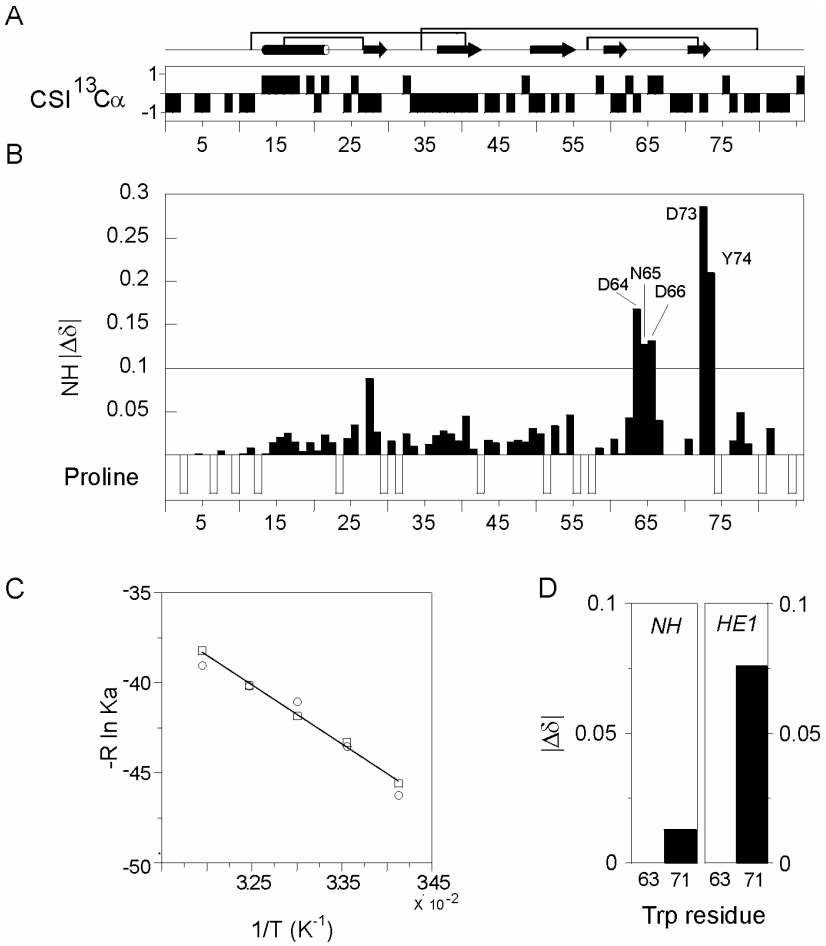

Figure 7. (A) Schematic diagram of the secondary structure elements of AVR4 including the disulfide bond pattern. The positions of the β-strands were based on the sequence alignment with tachycitin. Disulfide bonds were taken from (17). (B) Induced changes in the amide (HN) chemical shifts in AVR4 (1 mM) upon binding $(GlcNAc)_3$ (27.3 mM). Black bars, amide resonances that shift upon complexation; open bars, Proline residues in the primary structure of AVR4. (C) Van 't Hoff plot for the dissociation constant of the complex between AVR4 and $(GlcNAc)_3$. Binding constants were derived from the HN chemical shifts of the residues Y74 (□) and D73 (○). (D) Chemical shift changes of the HN and side-chain (Hε1) resonances of W63 (N/HN=122.8 / 8.57 ppm, Nε/Hε=127.09 / 10.50 ppm) and W71 (N/HN =111.5/6.55, Nε/Hε=127.7/9.758 ppm) upon complexation with $(GlcNAc)_3$.

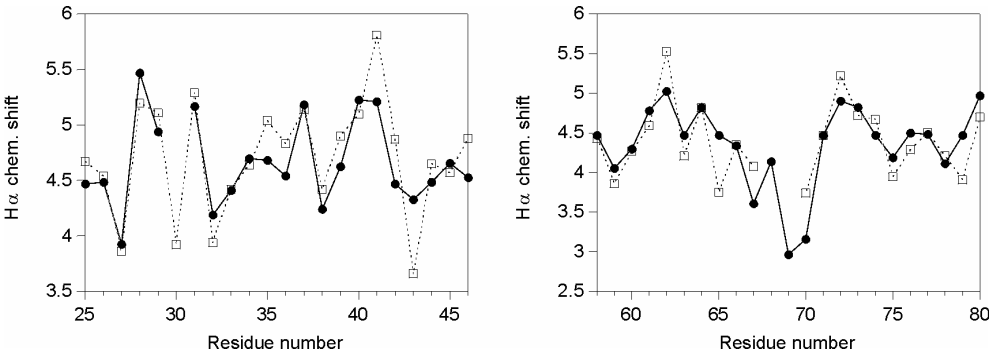

Figure 8. Comparison of Hα-proton chemical shifts of AVR4 and tachycitin. Hα-chemical shifts (ppm) are shown for AVR4 (●, solid line), and for tachycitin (□, dashed line). The data for tachycitin were retrieved from BioMagResBank (ID:4290). The residues of tachycitin are aligned with AVR4 and the numbers refer to the residue numbering in AVR4. A broken line in the case of tachycitin indicates interruptions in the alignment. The residue 30 is not assigned for AVR4

exchange rate in equilibrium between AVR4 and $(GlcNAc)_6$ is moderate to slow on the NMR scale. Lowering the temperature further increased the line widths without generating slow exchange conditions. Raising the temperature did not result in the fast exchange regime for the interaction between AVR4 and $(GlcNAc)_6$. Therefore, we could not use the same approach to estimate the K_A as we had previously used for $(GlcNAc)_3$. The fact that the entire spectrum was affected by line broadening at increasing concentrations of $(GlcNAc)_6$, suggests an increased rotational correlation time τ_c for higher concentrations of $(GlcNAc)_6$. As the τ_c reflects the apparent size of AVR4 in complex, this increased τ_c indicates the occurrence of higher order complexes between AVR4 and $(GlcNAc)_6$, most likely a complex with 2:1 protein-ligand stoichiometry.

Residues in AVR involved in the interaction. Studies with CBM18 lectins have shown that backbone HN and Hα resonances can be used as selective markers for residues involved in ligand-binding; these resonances showed shifts exceeding 0.1 ppm at the end point of the ligand titrations (10,36,37,39). Shifts <0.1 ppm were mostly due to reorientation of aromatic side chains influencing other residues as well. Large conformational changes were never reported to occur for any of the CBM18 lectins as a result of complexation. Figure 10B shows for hevein the changes in HN chemical shift as induced by $(GlcNAc)_3$ (10)

Figure 9. Temperature study on the change in HN chemical shift (δ) of residue D73 in AVR4 (1.0 mM) as a function of the concentration of $(GlcNAc)_3$. The sample contained 20 mM sodium acetate, 150 mM NaCl pH 6.0. Temperature was increased in steps of 5 degrees from 293 K to 313 K (K_A=260, 188, 139, 126, 110 M^{-1}, respectively).

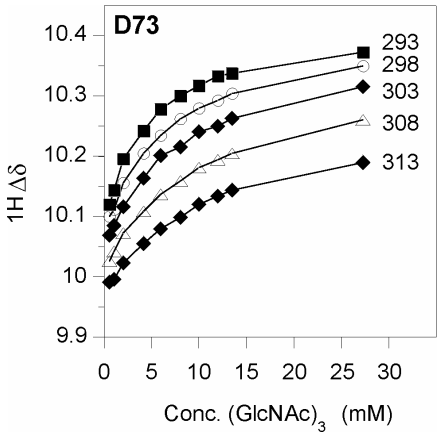

superimposed on the ribbon structure of hevein. These data indicate that four residues form the core of the chitin-binding site in hevein. Subsite +1 is formed by S19, W23, and Y30, while W21 is involved in subsite +2 and subsite +3. Comparable data were reported for UDA (37,40), prohevein (39) and WGA (38).

A similar analysis of the NMR titration of AVR4 with $(GlcNAc)_3$ indicated that the residues N64, D65, N66, D73, and Y74 are important in AVR for binding to chito-oligomers (Fig 7B). From sequence comparison, it is, however, evident that none of the foregoing five residues is conserved between the two ChBD motifs (Fig 10A). Nevertheless, these five residues are clearly located in the predicted chitin-binding site of tachycitin (14).

The residues N64 and N66 would structurally align with S19 (subsite +1) and W21 (subsite +2) in hevein, respectively. A strong indication for a conserved role of N64 in CBM14 comes from the high degree of conservation of this residue (90% similarity; mostly Asn, Asp, and less often Ser). On the other hand, N66 is not conserved in CBM14. Noteworthy, tachycitin contains an aromatic residue at the position corresponding to W21, and tachycitin is for this fact a rather unique member of the CBM14 family.

The role of W71 in the binding-site of AVR4 is more elusive. W71 would structurally align with W23 in hevein, which is an important residue in subsite +1 of the CBM18 lectins. W71 in AVR4 is rather unique as most other CBM14 members do not contain an aromatic residue at this position. The titration with $(GlcNAc)_3$ revealed, nevertheless, that the side chain of W71 experienced a large shift upon complexation, while the backbone HN chemical shift was to some extent affected (Fig 7D). Likewise, low concentrations of $(GlcNAc)_6$ were

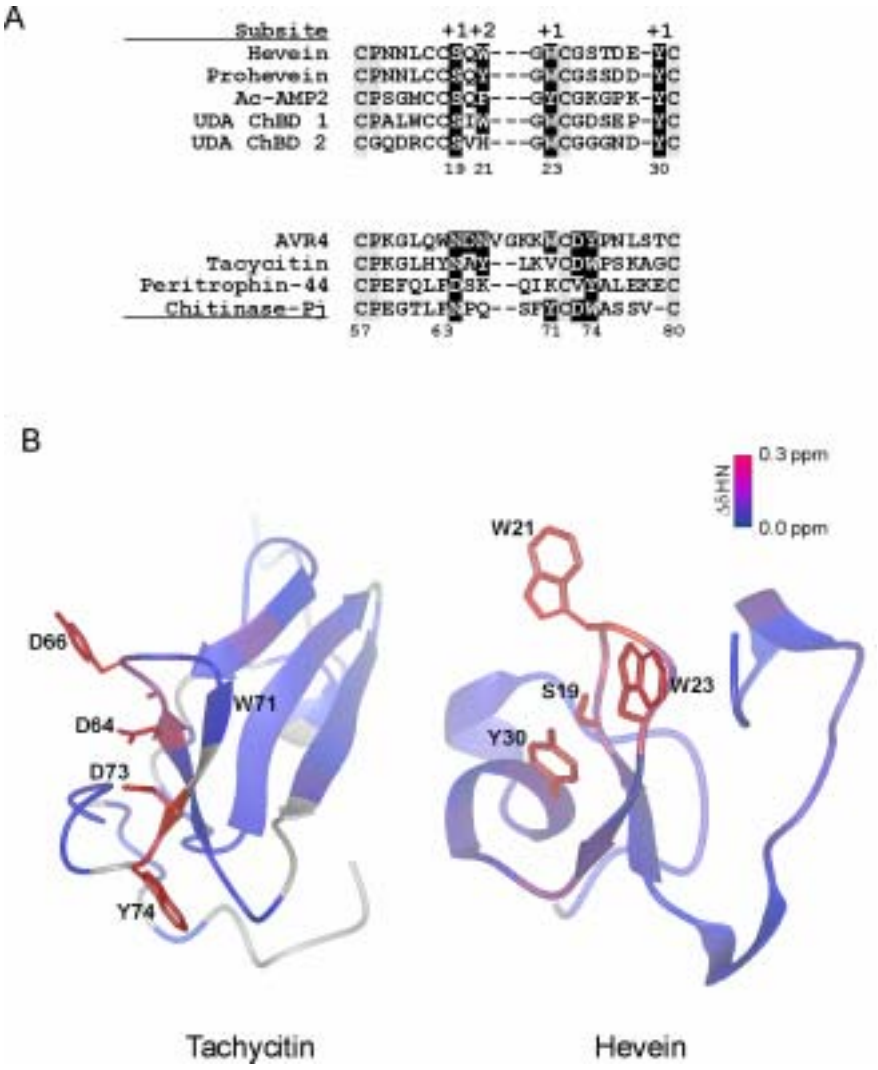

Figure 10. (**A**) Sequence alignment of proteins containing CBM18 (*top*) or CBM14 (*bottom*) chitin-binding domain, respectively. Residues in black indicate residues important for binding (**B**) Ribbon model of the three-dimensional structure of CBM14 (*e.g.* tachycitin) and CBM18 (*e.g.* hevein) (10). The side chains are shown for those residues that are important for the ligand-interaction (the side chains of tachycitin are shown for the corresponding residues in AVR4). The blue to red color scheme is based on the degree of chemical shift changes as obtained for AVR4 (Fig 7B) and for hevein (10).

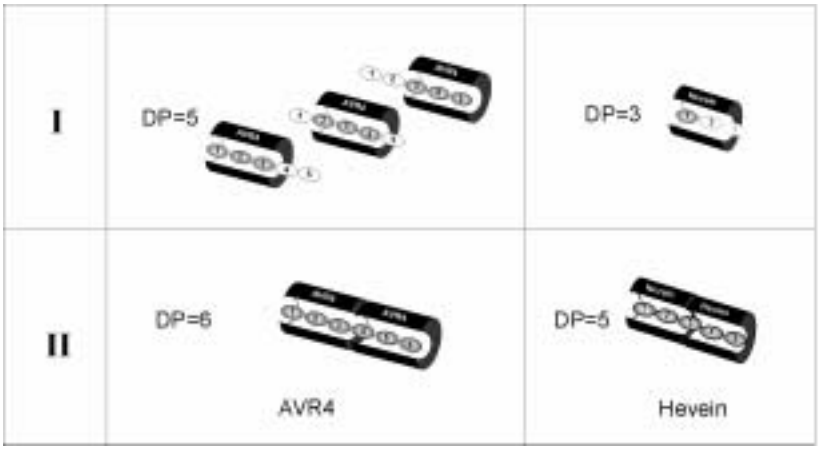

Figure 11. Schematic representation of the different characteristics of the CBM14 and CBM18 chitin-binding domains (*e.g.* AVR4 and hevein, respectively). (I) AVR4 interact with a ligand with a DP of three or more, while hevein already interacts with N-acetyl-D-glucosamine. (II) A second binding site becomes available for AVR4 when the DP of the ligand is six. For hevein the DP may be five to obtain the second binding site. For AVR4, the second binding event is, however, accompanied by positive cooperativety, while for hevein several complexes with 1:1 and 1:2 stoichiometry coexisted, which would not support positive cooperativety for hevein.

enough to cause significant line broadening of the side chain of W71. From this we conclude that for AVR4 W71 appears to contribute to the interaction, but we expect this to be a rather unique feature for AVR4. These data also indicate that W71 would indeed become less solvent exposed upon binding as indicated by the fluorescence experiments. In addition, the NMR data also confirm that W63 is not directly involved in binding, as both the backbone amide and the side chain of W63 were not substantially affected by varying concentrations of $(GlcNAc)_3$ (Fig 7D) or low concentrations of $(GlcNAc)_6$ (data not shown).

The D73 and Y74 HN resonances experienced the largest changes in chemical shift, but both residues lack an equivalent residue in hevein or any of the CBM18 lectins. Both D73 and Y74 show a high degree of conservation in CBM14 (as based on the 233 sequences in the seed of CBM14 family in the Pfam database). Interestingly, both residues

are located at the opposite site of the protein as compared to W21 in hevein (Fig 10B). This indicates that the chitin-binding site in AVR4 is more extended compared to that of the CBM18 lectins. In turn, this would also explain why AVR4 only interact with chito-oligomers when a DP ≥ 3, while for CBM18 the subsite +1 provides enough contacts to stabilize an interaction with GlcNAc (Fig 11).

References

1. Coutinho, P. M., and Henrissat, B. (1999) in *Recent Advances in Carbohydrate Bioengineering* (Gilbert, H. J., Davies, B., Henrissat, B., and Svensson, B., eds), pp. 3-12, The Royal Society of Chemistry, Cambridge
2. Bolam, D. N., Ciruela, A., McQueen-Mason, S., Simpson, P., Williamson, M. P., Rixon, J. E., Boraston, A., Hazlewood, G. P., and Gilbert, H. J. (1998) *Biochem. J.* **331,** 775-781.
3. Brunner, F., Stintzi, A., Fritig, B., and Legrand, M. (1998) *Plant J.* **14,** 225-234
4. Tormo, J., Lamed, R., Chirino, A. J., Morag, E., Bayer, E. A., Shoham, Y., and Steitz, T. A. (1996) *EMBO J.* **15,** 5739-5751
5. Szabó, L., Jamal, S., Xie, H., Charnock, S. J., Bolam, D. N., Gilbert, H. J., and Davies, G. J. (2001) *J. Biol. Chem.* **276,** 49061-49065.
6. Czjzek, M., Bolam, D. N., Mosbah, A., Allouch, J., Fontes, C. M., Ferreira, L. M., Bornet, O., Zamboni, V., Darbon, H., Smith, N. L., Black, G. W., Henrissat, B., and Gilbert, H. J. (2001) *J. Biol. Chem.* **276,** 48580-48587
7. Muraki, M. (2002) *Prot. Pept. Lett.* **9,** 195-209
8. Simpson, P. J., Xie, H., Bolam, D. N., Gilbert, H. J., and Williamson, M. P. (2000) *J. Biol. Chem.* **275,** 41137-41142.
9. Xie, H., Bolam, D. N., Nagy, T., Szabó, L., Cooper, A., Simpson, P. J., Lakey, J. H., Williamson, M. P., and Gilbert, H. J. (2001) *Biochemistry* **40,** 5700-5707.
10. Asensio, J. L., Canada, F. J., Siebert, H. C., Laynez, J., Poveda, A., Nieto, P. M., Soedjanaamadja, U. M., Gabius, H. J., and Jiménez, B. J. (2000) *Chem. Biol.* **7,** 529-543
11. Beintema, J. J. (1994) *FEBS Lett.* **350,** 159-163
12. Shen, Z., and Jacobs-Lorena, M. (1999) *J. Mol. Evol.* **48,** 341-347
13. Ohno, T., Armand, S., Hata, T., Nikaidou, N., Henrissat, B., Mitsutomi, M., and Watanabe, T. (1996) *J. Bacteriol.* **178,** 5065-5070
14. Suetake, T., Tsuda, S., Kawabata, S., Miura, K., Iwanaga, S., Hikichi, K., Nitta, K., and Kawano, K. (2000) *J. Biol. Chem.* **275,** 17929-17932
15. Chrispeels, M. J., and Raikhel, N. V. (1991) *Plant Cell* **3,** 1-9

16. Elvin, C. M., Vuocolo, T., Pearson, R. D., East, I. J., Riding, G. A., Eisemann, C. H., and Tellam, R. L. (1996) *J. Biol. Chem.* **271,** 8925-8935
17. van den Burg, H. A., Westerink, N., Francoijs, K.-J., Roth, R., Woestenenk, E., Boeren, S., de Wit, P. J. G. M., Joosten, M. H. A. J., and Vervoort, J. (2003) submitted
18. van den Burg, H. A., Harrison, S., Joosten, M. H. A. J., de Wit, P. J. G. M., and Vervoort, J. (2003) submitted
19. Joosten, M. H. A. J., Cozijnsen, T. J., and de Wit, P. J. G. M. (1994) *Nature* **367,** 384-386
20. Joosten, M. H. A. J., Vogelsang, R., Cozijnsen, T. J., Verberne, M. C., and de Wit, P. J. G. M. (1997) *Plant Cell* **9,** 367-379
21. Stintzi, A., Heitz, T., Prasad, V., Wiedemann-Merdinoglu, S., Kauffmann, S., Geoffroy, P., Legrand, M., and Fritig, B. (1993) *Biochimie* **75,** 687-706
22. Neuhaus, J. M. (1999) in *Pathogenesis-related proteins in plants* (Datta, S. W., and Muthukrishnan, S., eds), pp. 77-105, CRC Press
23. Joosten, M. H. A. J., and de Wit, P. J. G. M. (1989) *Plant Physiol.* **89,** 945-951
24. Joosten, M. H. A. J., and de Wit, P. J. G. M. (1999) *Annu. Rev. Phytopathol.* **37,** 335-367
25. Cai, X., Takken, F. L., Joosten, M. H. A. J., and de Wit , P. J. G. M. (2001) *Mol. Plant Pathol.* **2,** 77-86
26. Passarinho, P., and de Vries, S. C. (2002) in *Arabidopsis book* (Sommerville, C. R., and Meyerowitz, E. M., eds), pp. 25, http://www.aspb.org/publications/arabidopsis, American Society of Plant Biologists, Rockville, MD
27. Sela-Buurlage, M. B., Ponstein, A. S., Bres-Vloemans, S. A., Melchers, L. S., van den Elzen, P. J. M., and Cornelissen, B. J. C. (1993) *Plant Physiol.* **101,** 857-863
28. Ponstein, A. S., Bres-Vloemans, S. A., Sela-Buurlage, M. B., van den Elzen, P. J. M., Melchers, L. S., and Cornelissen, B. J. C. (1994) *Plant Physiol.* **104,** 109-118
29. Melchers, L. S., Apotheker-De Groot, M., van der Knaap, J. A., Ponstein, A. S., Sela-Buurlage, M. B., Bol, J., F., Cornelissen, B. J. C., van den Elzen, P. J. M., and Linthorst, H. J. M. (1994) *Plant J.* **5,** 469-480
30. Broekaert, W. F., van Parijs, J., Leyns, F., Joos, W., and Peumans, W. J. (1989) *Science* **245,** 1100-1102
31. Van Parijs, J., Broekaert, W. F., Goldstein, I. J., and Peumans, W. J. (1991) *Planta* **183,** 258-264
32. Heusing, J. E., Murdock, L. L., and Shade, R. E. (1991) *Phytochemistry* **30,** 3565-3568
33. Punja, Z. K. (2001) *Can. J. Plant Pathol.* **23,** 216–235
34. Joosten, M. H. A. J., Verbakel, H. M., Nettekoven, M. E., van Leeuwen, J., Vossen, R. T. M., and de Wit, P. J. G. M. (1995) *Physiol. Mol. Plant Pathol.* **46,** 45-59
35. Wright, C. S. (1990) *J. Mol. Biol.* **215,** 635-651
36. Asensio, J. L., Cañada, F. J., Bruix, M., Rodriguez, R. A., and Jiménez, B. J. (1995) *Eur. J. Biochem.* **230,** 621-633
37. Hom, K., Gochin, M., Peumans, W. J., and Shine, N. (1995) *FEBS Lett.* **361,** 157-61

38. Asensio, J. L., Siebert, H. C., von der Lieth, C. W., Laynez, J., Bruix, M., Soedjanaamadja, U. M., Beintema, J. J., Cañada, F. J., Gabius, H. J., and Jiménez, B. J. (2000) *Proteins* **40,** 218-236
39. Espinosa, J. F., Asensio, J. L., Garcia, J. L., Laynez, J., Bruix, M., Wright, C., Siebert, H. C., Gabius, H. J., Cañada, F. J., and Jiménez, B. J. (2000) *Eur. J. Biochem.* **267,** 3965-3978
40. Harata, K., and Muraki, M. (2000) *J. Mol. Biol.* **297,** 673-681
41. Saul, F. A., Rovira, P., Boulot, G., Damme, E. J., Peumans, W. J., Truffa-Bachi, P., and Bentley, G. A. (2000) *Struct. Fold. Des.* **8,** 593-603
42. van den Burg, H. A., de Wit, P. J. G. M., and Vervoort, J. (2001) *J. Biomol. NMR* **20,** 251-261
43. Mahé, E., Vossen, P., van den Hooven, H. W., Le-Nguyen, D., Vervoort, J., and de Wit, P. J. G. M. (1998) *J. Pept. Res.* **52,** 482-494
44. van den Hooven, H. W., Appelman, A. W. J., Zey, T., de Wit, P. J. G. M., and Vervoort, J. (1999) *Eur. J. Biochem.* **264,** 9-18
45. Wiseman, T., Williston, S., Brandts, J. F., and Lin, L. N. (1989) *Anal. Biochem.* **179,** 131-137
46. Privat, J. P., Delmotte, F., Mialonier, G., Bouchard, P., and Monsigny, M. (1974) *Eur. J. Biochem.* **47,** 5-14
47. Lee, R. T., Gabius, H. J., and Lee, Y. C. (1998) *Glyconjugate J.* **15,** 649-655
48. Marion, D., Driscoll, P. C., Kay, L. E., Wingfield, P. T., Bax, A., Gronenborn, A. M., and Clore, G. M. (1989) *Biochemistry* **28,** 6150-6156
49. Delaglio, F., Grzesiek, S., Vuister, G. W., Zhu, G., Pfeifer, J., and Bax, A. (1995) *J. Biomol. NMR* **6,** 277-293
50. Bartels, C., Xia, T. H., Billeter, M., Guntert, P., and Wüthrich, K. (1995) *J. Biomol. NMR* **6,** 1-10
51. BioMagResbank, URL:http://www.bmrb.wisc.edu
52. Bains, G., Lee, R. T., Lee, Y. C., and Freire, E. (1992) *Biochemistry* **31,** 12624-12628
53. Kronis, K. A., and Carver, J. P. (1985) *Biochemistry* **24,** 826-833
54. Kronis, K. A., and Carver, J. P. (1985) *Biochemistry* **24,** 834-840
55. Garcia-Hernández, E., Zubillaga, R. A., Rojo-Domínguez, A., Rodrígues-Romero, A., and Hernández-Arana, A. (1997) *Proteins* **29,** 467-477
56. Creagh, A. L., Ong, E., Jervis, E., Kilburn, D. G., and Haynes, C. A. (1996) *Proc. Natl. Acad. Sci. USA* **93,** 12229-12234.
57. Searle, M. S., and Williams, D. H. (1992) *J. Am. Chem. Soc.* **114,** 10690-10697
58. Loo, J. A. (1997) *Mass Spectrom. Rev.* **16,** 1-23
59. Nesatyy, V. J. (2001) *J. Mass Spectrom.* **36,** 950-959
60. Chen, Y.-L., Campbell, J. M., Collings, B. A., Konermann, L., and Douglas, D. J. (1998) *Rapid Comm. Mass Spectrom.* **12,** 1003-1010
61. Tahallah, N., Pinkse, M., Maier, C. S., and Heck, A. J. R. (2001) *Rapid Comm. Mass Spectrom.* **15,** 596-601
62. Wüthrich, K. (1986) *NMR of Proteins and Nucleic Acids*, Wiley, New York

63. Wishart, D. S., and Sykes, B. D. (1994) *J. Biomol. NMR* **4,** 171-180

64. Lian, Y., and Roberts, G. C. K. (1993) *NMR of Marcomolecules*, Oxford University Press, Oxford

65. Chaires, J. B. (1997) *Biophys. Chem.* **64,** 15-23

66. Horn, J. R., Russell, D., Lewis, E. A., and Murphy, K. P. (2001) *Biochemistry* **40,** 1774-1778

7

General discussion

GENERAL DISCUSSION

Several independent observations question whether the paradigm of the “gene-for-gene model” can be translated into a protein-for-protein model where resistance gene products (R) and pathogen avirulence gene products (Avr) would physically interact, which subsequently mounts a plant defense response that ultimately leads to host resistance. First, a physical interaction between R-proteins and Avr proteins has only been demonstrated for two R/Avr protein pairs, Pto/AvrPto(B) (Kim et al., 2002; Tang et al., 1996) and Pita/AvrPita (Jia et al., 2000) despite vast efforts to prove direct interactions for many other R/Avr protein pairs. Secondly, the R protein RPM1 recognizes two unrelated AVR proteins, AvrRpm1 and AvrB (Ritter and Dangl, 1995). The recent identification of second plant component, RIN4, might represent the missing link. RIN4 appears to physically interact with both AvrRrpm1 and AvrB, and both AVR effector proteins cause hyperphosphorylation of RIN4 independent of RPM1 (Mackey et al., 2002). Importantly, RIN4 also interacts with the R protein RPM1. Recently, a third effector protein, AvrRpt2, has also been shown to interact with RIN4. AvrRpt2, however, seems to cause elimination of RIN4 (Axtell and Staskawicz, 2003; Mackey et al., 2003). Intriguingly, Rpt2-mediated resistance depends on RIN4 elimination rather than the presence of the AvrRpt2 protein itself. Finally, the requirement of Prf in Pto/AvrPto(B)-mediated resistance is puzzling. Prf interacts with Pto in a yeast two-hybrid interaction, and contains a Leucine-Rich Repeat (LRR) domain. LRRs are widely regarded as motifs defining specificity in protein-protein interactions. It has, therefore, been argued that Prf could represent the R protein rather than Pto.

Each of these findings would also be consistent with a model where pathogen perception of the pathogen’s Avr proteins by R proteins occurs indirectly through the action of an Avr protein on a second plant protein rather than by a physically interaction with the Avr protein. This concept was introduced as the ‘guard hypothesis’ (van der Biezen and Jones, 1998; Dangl and Jones, 2001; Schneider, 2002; van der Hoorn et al., 2002). Complying with this concept, RIN4 would act as a negative regulator of plant defense responses. The guard model proposes that effector proteins manipulate host targets in order to enhance pathogen virulence by suppression of basal defense responses as suggested for RIN4. Manipulation of RIN4 is, subsequently, sensed by R proteins that then orchestrate an array of defense responses including HR.

In recent years, it has been demonstrated that numerous bacterial Avr proteins belong to the type-III effector proteins and contribute to virulence including

avrRpm1–required for full virulence of *Pseudomonas syringae* pv. *maculicola* (Ritter and Dangl, 1995)-, AvrPphF–an inhibitor of HR in bean (Tsiamis et al., 2000), AvrPto-an enhancer of virulence of *Pseudomonas syringae* pv. *tomato* on tomato plants lacking Pto (Chang et al., 2000), AvrPtoB–an inhibitor of HR in tomato and *Nicotiana benthamiana* (Abramovitch et al., 2003; Kim et al., 2002). Thus, the pattern emerges that bacterial pathogens actively secrete proteins that contribute to virulence.

One could imagine that fungal elicitor proteins also manipulate host targets and that they contribute in this way to virulence. The consequence would be that R protein-mediated resistance might also perceived be by the action of a fungal elicitor on a target protein. Circumstantial evidence would indeed support the indirect perception of at least two fungal AVR elicitors, *e.g.* AVR-Pita of *Magnaporthe grisea* (Jia et al., 2000) and AVR2 of *Cladosporium fulvum* (Luderer et al., 2002). AVR-Pita is a putative metalloprotease and artificial point mutations introduced in the protease consensus sequence resulted in a loss-of-recognition of the mutated fungi when infecting the host (including a natural strain with an allele encoding a null mutation due to the loss of an essential amino acid residue in the catalytic site) (Jia et al., 2000). This implies that Pita-mediated resistance requires activity of AVR-Pita and would support a role for a specific target protein that is processed by AVR-Pita. The tomato protein Rcr3 is required for Cf-2-mediated resistance against fungal isolates carrying the *Avr2* gene. Rcr3 is an extracellular cysteine endoprotease with homology to the papain subclass of proteases (Dixon et al., 2000; Krüger et al., 2002). The *L. pimpenelifolum* allele of *Rcr3* suppresses, independent of AVR2, a Cf-2–dependent autonecrosis in *L. esculentum* plants conditioned by the Rcr3 *L. esculentum* allele, which suggests a role for Cf-2 as Rcr3 guard (Krüger et al., 2002). It will be most interesting to investigate the role of AVR2 in this putative protein complex. Is there physical interaction between AVR2 and Rcr3, and if so, does AVR2 inhibit Rcr3 irreversibly or does it regulate Rcr3 levels? And furthermore, how is the action of AVR2 on Rcr3 related to Cf-2-mediated resistance?

A direct interaction could also not be demonstrated between AVR9 and Cf-9 despite vast efforts by several groups (Luderer et al., 2001). However, an AVR9-specific High-Affinity Binding Site (HABS) resides in plasma membrane and microsomal fractions of *Solanaceous* plants (Kooman-Gersmann et al., 1996). The presence of the HABS was independent of the presence of the *Cf-9* resistance gene. Supportive evidence for a guardee role of the HABS is given by the correlation found between the necrosis-inducing activity and the dissociation constant (K_D) of the HABS-AVR9 complex for a set of artificial AVR9

mutants in which single amino acid mutations were introduced leading to decreased, neutral or increased necrosis-inducing activity (Kooman-Gersmann et al., 1998).

Data presented in **Chapter 3** might give us some further clues for the function of AVR9. First, the disulfide bond pattern of AVR9 complies with the cystine knot motif. The cystine knot family contains at least 25 plant trypsin inhibitors (*e.g.* CMTI-I–a squash family of serine protease inhibitors), thirteen toxins or channel blockers (*e.g.* ω-CgTx–a high-affinity binding neurotoxin that binds to N-type voltage-gated Ca^{2+} channels), and several closely related cyclic cystine knots (*e.g.* Circulin A, Kalata B1) (Craik et al., 2001; Pallaghy et al., 1994). From both the 3D structure and cysteine spacing, it is evident that AVR9 deviates from the cyclic cystine knot peptides. As for the toxins and ion channel blockers, they lack a short loop spanning between Cys12 and Cys16, which is present in AVR9 and also in protease inhibitors. The absence of this loop causes slight differences in the 3D structure of the toxins as compared to the protease inhibitors (Craik et al., 2001), which would support that AVR9 does not act as such a type of ion channel blocker. In addition, a role as inhibitor of essential ion channels is less likely for AVR9 as host cells will become seriously stressed by inhibition of these ion channels. Nevertheless, two cyclic-nucleotide gated-ion channels, HML1 and *Dnd*, were recently shown to be an essential signaling components for HR in *Arabidopsis* (Balague et al., 2003; Clough et al., 2000). Such a channel could be redundant under normal growth conditions, while inhibition could favor fungal infection. Thus, the AVR9-specific HABS might represent such a type of ion channel, although an AVR9-specific HABS has not been identified in *Arabidopsis.* The NMR data obtained for AVR9 support structural homology with potato carboxypeptidase inhibitor (CPI). However, AVR9 and artificially produced chimeras of AVR9-CPI did not show any carboxypeptidase inhibiting activities (Van den Hooven, pers. comm.). This observation, however, provides only answers for CPI, while plants contain a plethora of additional proteases and protease inhibitors.

Continuing along the line of the guard hypothesis, AVR9 might negatively influence plant cell signaling in some way. In addition, the AVR9-specific HABS seems to be localized in the plasma membrane (Van der Hoorn et al., 2001). These two features can be consistent with a function for AVR9 as protease inhibitor as there is growing evidence that subtilisin-like serine carboxypeptidase proteases are involved in intracellular signaling in plants. The system is best studied in yeast for the Kex1p and Kex2p proteases that cooperatively excise signaling peptides from their inactive precursors, *e.g.* α-mating pheromone, and K1 killer toxin (Dmochowska et al., 1987; Fuller et al., 1989). Kex2p is a membrane-bound

endoprotease that specifically cleaves at the carboxyl terminus between pairs of basic amino acids. This type of protease could very well be a target for the AVR9 peptide. After the action of Kex2p, the subtilisin-like serine carboxypeptidase Kex1p selectively trims off the flanking amino acids from the C-terminus. In tomato at least 15 subtilisin-like proteases have been identified (Meichtry et al., 1999). For example, the tomato peptide systemin (18 amino acid) is processed from its inactive precursor prosystemin (200 amino acid) in response to wounding by a subtilisin endoprotease (a physical interaction between the two has also been demonstrated) (Pearce et al., 1991). Another subtilisin-like protease, BRS1, has been shown to regulate brassinosteroid signaling in *Arabidopsis* upstream of the LRR receptor-like kinase (LRK) BRI1 (a brassinosteroid receptor), (Li et al., 2001). Intriguingly, the putative receptor of systemin, SR160, seems to be the tomato orthologue of BRI1 (Montoya et al., 2002; Scheer and Ryan, 2002). The prevailing model for BRS1 function is that it activates a brassinosteroid binding protein by cleavage, which subsequently complexes the ligand. Only this ligand-binding protein complex is perceived by BRI1 and BAK1 (both LRR receptor-like kinases) (Li et al., 2002; Nam and Li, 2002). Other subtilisin-like serine proteases include the tomato PR-protein P69, which is strongly induced after infection of tomato by various pathogens and is involved in processing of LRP (an extracellular LRR containing protein) (Jorda et al., 1999), and SDD1 from *Arabidopsis,* which functions in stomatal guard cell development (Berger and Altmann, 2000). Thus, several lines of evidence indicate an important role for proteases in processing extracellular signaling ligands like polypeptides and hormones. In conclusion, fungal elicitors with protease-inhibiting activities are not necessarily involved in protection of other fungal proteins against degradation, but rather they could inflict intracellular signaling of the host plant as a part of the host response to a pathogen infection.

AVR4 seems to hold a different function. The **chapters 4-6** provide evidence that AVR4 contains a functional invertebrate chitin-binding domain (inv ChBD). Six cysteine residues forming three disulfide bonds are conserved in the consensus of the inv ChBD (**Chapter 4**). NMR data obtained for AVR4 indicated that the secondary structure of AVR4 is closely related to that of tachycitin for which the 3D structure was solved (**Chapter 6**). We predicted that this novel motif in AVR4 reflects the biological function of AVR4. Accordingly, AVR4 provided protection to fungi against plant chitinases (**chapter 5**). Chitinases can be directly involved in defense of plants against chitin-containing intruders like fungi. In addition, AVR4 was found to localize at cell walls of *C. fulvum* after the fungus has penetrated the tomato leaf through the stomata. By analogy, the 34-kDa glycoprotein elicitor CBEL of the

oomycete *Phytophthora parasitica* var. *nicotianae* contains two cellulose-binding domains (oomycetes lack chitin in their cell wall) (Gaulin et al., 2002). CBEL appeared to be involved in cell wall depositions and treatments of tobacco cultivars with CBEL resulted in protection of these plants against subsequent infection by an otherwise virulent race of *P. parasitica* var. *nicotianae*.

In contrast to AVR9, an AVR4-specific HABS identified in microsomal fractions of tomato appeared to originate from some undesired fungal infections of tomato contaminating the fractions (Westerink et al., 2002). Most of all, the AVR4-specific binding site was heat and proteinase K resistant, which could signify the involvement of a highly glycosylated protein or certain polysaccharides. The identification of chitin-binding motif in AVR4 might explain these observations (**Chapter 4-6**). However, an AVR4-specific cross-linked molecule was identified in microsomal fractions as a distinct band migrating at ~75kDa after SDS-PAGE (Westerink et al., 2002). The positive cooperativety found for AVR4 binding to larger chitin oligomers (**chapter 6**) would support that multiple AVR4 molecules might have been cross-linked while bound to chitin fragments, but a laddering signal should have been observed in such instance. Alternatively, another abundant cell wall protein that exhibits chitin affinity could have been cross-linked to AVR4 as well.

The dissociation constants (K_D) found for the AVR4-specific binding site varied in the subnanomolar range (0.07-0.26 nM) (Westerink et al., 2002). The K_Ds obtained for AVR4 binding to chitin oligomers of increasing length (from three up to six GlcNac residues) decreased from the mM to the low μM range (**chapter 6**). We expect that the K_D will further decrease when AVR4 interacts with crystalline chitin because the substantial negative contribution of the entropy term will reduce for the more ridged substrate chitin (Creagh et al., 1996). In addition, an additional contribution from positive cooperativety is anticipated when an AVR4 molecule becomes involved in two protein-protein interactions while bound to chitin. Whether this will account for a K_D in the subnanomolar range is not clear. Therefore, other factors could still contribute to the AVR4-specific binding site. The proposed passive defense function of AVR4 would require a K_D of less than 0.1 μM, as Km values of chitin-substrates for chitinases are in the upper μM region. As proposed in **chapter 5**, AVR4 could act as an integral cell wall protein embedded in the extracellular matrix, but additional localization studies are certainly required to further support this. It is, nevertheless, reasonable to expect that AVR4 will be present in excess at the growing hyphal tip during infection. The exposed hyphal tip is exclusively associated with protein secretion. The vast majority of the ChBD-containing plant chitinases, on the other hand, is stored in the plant

vacuole awaiting secretion in response to any general stress (amongst them the most anti-fungal chitinases; (Brunner et al., 1998). Although the concentrations of plant chitinases increase during a defense response, they might not be nearly as high to compete with the AVR4 concentrations near the hyphal tip. Accordingly, the IC_{50} values of AVR4 observed in growth assays of the fungi for *T. viride* and *F. solani* f.sp. *phaseoli* in the presence of chitinases were of a similar order than those reported for anti-microbial proteins and (chapter 5) and competed perfectly with lytic activity presented by the chitinases.

The missing link between Cf-4 mediated resistance and AVR4 might be the guardee. An indication for a possible guardee of Cf-4 comes from sequence information of invertebrate and mammalian chitinases. chitinases in invertebrates and mammals contain often the family-18 chitinolytic domain fused to an inv ChBD. A similar fusion between two functionally related domains is frequently observed in enzymes and proteins involved in cell signaling. From a functional point of view, the presence of a carbohydrate-binding module in enzymes hydrolyzing polysaccharides often contributes to an increased activity for insoluble polysaccharides. The “Stone-of-Rosetta” principle provides an interesting link in that it predicts that, when two protein motifs are encoded by two different genes in one organism, but they can be in another organism as fusion-protein, that these two proteins then potentially interact with one another (Marcotte et al., 1999). This implies that AVR4 potentially interacts with family-18 chitinases, but not necessarily with family-19 chitinases. Similarly, the hevein domain might have affinity for the family-19 chitinases. Family-18 chitinases of fungal origin are cell wall-bound and involved in cell wall morphogenesis. A member of the family-18 chitinases could, possibly, represent the protein that was found to cross-link to AVR4 (Westerink et al., 2002). In plants, a chitinase-like receptor kinase, CHRK1, has been reported to contain an extracellular family-18 catalytic chitinase domain that is inactive due to a substitution of an essential amino acid (Kim et al., 2000). CHRK1 expression was strongly induced after infection by a fungal pathogen and tobacco mosaic virus, but not by chitin oligomers. This observation might indicate that chitin oligomers are no longer the ligand for this receptor-like kinase, rather we suspect that chitin-binding domains could have a role as ligand (as argued above). Constitutive expression CHRK1 at low levels could be detected in leaf tissue, but whether that would be enough for a role as Cf-4-guardee is not clear. Moreover, AVR4 is also recognized when an initial trigger for CHRK1 expression is absent. Foremost, it would be intriguing to see whether AVR4 indeed physically interacts with different chitinases in the presence and absence of substrate, and if this interaction forms the basis of Cf-4 mediated resistance.

To cut a long story short, the holy grail of intracellular plant defense signaling appears to be a gene with a domain organization like Sp22D, a secreted multidomain serine protease with a possible role in insect immunity (Danielli et al., 2000; Gorman et al., 2000). In addition to the C-terminal proteolytic domain, Spd22 contains two CBM14 domains, a mucin-like domain, two low density lipoprotein receptor class A domains, a two scavenger receptor cystine rich domains (SRCR). Each of these domains is separately reported to be involved in intracellular signaling and each of these domains would even be a sensible target for inhibitors in the form of AVR elicitors.

REFERENCES

Abramovitch, R.B., Kim, Y.J., Chen, S., Dickman, M.B., and Martin, G.B. (2003) *EMBO J **22***, 60-69.

Axtell, M.J., and Staskawicz, B.J. (2003) *Cell **112***, 369-377.

Balague, C., Lin, B., Alcon, C., Flottes, G., Malmstrom, S., Kohler, C., Neuhaus, G., Pelletier, G., Gaymard, F., and Roby, D. (2003) *Plant Cell **15***, 365-379.

Berger, D., and Altmann, T. (2000) *Genes Dev **14***, 1119-1131.

Brunner, F., Stintzi, A., Fritig, B., and Legrand, M. (1998) *Plant J **14***, 225-234.

Chang, J.H., Rathjen, J.P., Bernal, A.J., Staskawicz, B.J., and Michelmore, R.W. (2000) *Mol Plant-Microbe Interact **13***, 568-571.

Clough, S.J., Fengler, K.A., Yu, I.C., Lippok, B., Smith, R.K.J., and Bent, A.F. (2000) *Proc Natl Acad Sci USA **97***, 9323-9328.

Craik, D.J., Daly, N.L., and Waine, C. (2001) *Toxican **39***, 43-60.

Creagh, A.L., Ong, E., Jervis, E., Kilburn, D.G., and Haynes, C.A. (1996) *Proc Natl Acad Sci USA **93***, 12229-12234.

Dangl, J.L., and Jones, J.D.G. (2001) *Nature **411***, 826-833.

Danielli, A., Loukeris, T.G., Lagueux, M., Muller, H.M., Richman, A., and Kafatos, F.C. (2000) *Proc Natl Acad Sci USA **97***, 7136-7141.

Dixon, M.S., Golstein, C., Thomas, C.M., Van der Biezen, E.A., and Jones, J.D.G. (2000) *Proc Natl Acad Sci USA **97***, 8807-8814.

Dmochowska, A., Dignard, D., Henning, D., Thomas, D.Y., and Bussey, H. (1987) *Cell **50***, 573-584.

Fuller, R.S., Brake, A.J., and Thorner, J. (1989) *Science **246***, 482-486.

Gaulin, E., Jauneau, A., Villala, F., Esquerre-Tugaye, M.T., and Bottin, A. (2002) *J Cell Sci **115***, 4565-4575.

Gorman, M.J., Andreeva, O.V., and Paskewitz, S.M. (2000) *Gene **251***, 9-17.

Jia, Y., McAdams, S.A., Bryan, G.T., Hershey, H.P., and Valent, B. (2000) *EMBO J* ***19***, 4004-4014.

Jorda, L., A., C., Conejero, V., and Vera, P. (1999) *J Biol Chem* ***274***, 2360-2365.

Kim, Y.J., Lin, N.C., and Martin, G.B. (2002) *Cell* ***109***, 589-98.

Kim, Y.S., Lee, Y.H., Yoon, G.M., Cho, H.S., Park, S.-W., Suh, M.C., Choi, D., Ha, H.J., Liu, J.R., and Pai, H.-S. (2000) *Plant Physiol* ***123***, 1162-1173.

Kooman-Gersmann, M., Vogelsang, R., Vossen, P., van den Hooven, H.W., Mahe, E., Honee, G., and de Wit, P.J.G.M. (1998) *Plant Physiol* ***117***, 609-618.

Krüger, J., Thomas, C.M., Golstein, C., Dixon, M.S., Smoker, M., Tang, S., Mulder, L., and Jones, J.D.G. (2002) *Science* ***296***, 744-747.

Li, J., Lease, K.A., Tax, F.E., and Walker, J.C. (2001) *Proc Natl Acad Sci USA* ***98***, 5916-5921.

Li, J., Wen, J., Lease, K.A., Doke, J.T., Tax, F.E., and Walker, J.C. (2002) *Cell* ***110***, 213-222.

Luderer, R., Rivas, S., Nurnberger, T., Mattei, B., van den Hooven, H.W., van der Hoorn, R.A.L., Romeis, T., Wehrfritz, J.M., Blume, B., Nennstiel, D., Zuidema, D., Vervoort, J., De Lorenzo, G., Jones, J.D.G., de Wit, P.J.G.M., and Joosten, M.H.A.J. (2001) *Mol Plant-Microbe Interact* ***14***, 867-876.

Luderer, R., Takken, F.L., de Wit, P.J.G.M., and Joosten, M.H.A.J. (2002) *Mol Microbiol* ***45***, 875-884.

Mackey, D., Belkhadir, Y., Alonso, J.M., Ecker, J.R., and Dangl, J.L. (2003) *Cell* ***112***, 379-389.

Mackey, D., Holt, B.F., Wiig, A., and Dangl, J.L. (2002) *Cell* ***108***, 743-754.

Marcotte, E., Pellegrini, M., Ng, H.L., Rice, D.W., Yeates, T.O., and Eisenberg, D. (1999). *Science* ***285***, 751-753.

Meichtry, J., Amrhein, N., and Schaller, A. (1999) *Plant Mol Biol* ***39***, 749-760.

Montoya, T., Nomura, T., Farrar, K., Kaneta, T., Yokota, T., and Bishop, G.J. (2002) *Plant Cell* ***14***, 3163-3176.

Nam, K.H., and Li, J. (2002) *Cell* ***110***, 203-212.

Pallaghy, P.K., Nielsen, K.J., Craik, D.J., and Norton, R.S. (1994) *Protein Sci* ***3***, 1833-1839.

Pearce, G., Strydom, D., Johnson, S., and Ryan, C.A. (1991) *Science* ***253***, 895-898.

Ritter, C., and Dangl, J.L. (1995) *Mol Plant-Microbe Interact* ***8***, 444-453.

Scheer, J.M., and Ryan, C.A. (2002) *Proc Natl Acad Sci USA* ***99***, 9585-9590.

Schneider, D.S. (2002) *Cell* ***109***, 537-540.

Tang, X., Frederick, R.D., Zhou, J., Halterman, D.A., Jia, Y., and Martin, G.B. (1996) *Science* ***274***, 2060-2063.

Tsiamis, G., Mansfield, J.W., Hockenhull, R., Jackson, R.W., Sesma, A., Athanassopoulos, E., Bennett, M.A., Stevens, C., Vivian, A., Taylor, J.D., and Murillo, J. (2000) *EMBO J* ***19***, 3204-3214.

van der Biezen, E.A., and Jones, J.D.G. (1998) *Trends Biochem Sci* ***23***, 454-456.

van der Hoorn, R.A.L., de Wit , P.J.G.M., and Joosten, M.H.A.J. (2002) *Trends Plant Sci* ***7***, 67-71.

Van der Hoorn, R.A.L., Van der Ploeg, A., de Wit , P.J.G.M., and Joosten, M.H.A.J. (2001).] *Mol Plant-Microbe Interact* ***14***, 412-415.

Westerink, N., Roth, R., van den Burg, H.A., de Wit , P.J.G.M., and Joosten, M.H.A.J. (2002). *Mol Plant-Microbe Interact* ***15***, 1219-1227.

Summary

Recognition of the extracellular race-specific elicitor proteins AVR4 and AVR9 produced by the pathogenic fungus *Cladosporium fulvum* is mediated by the tomato resistance genes *Cf-4* and *Cf-9*, respectively. Recognition of these elicitors triggers host defense responses resulting in full resistance against the fungus. So far, intrinsic functions have not been identified for these two race-specific elicitors and all other characterized proteineous elicitors of *C. fulvum*. A short overview of the present state of the knowledge on the role of elicitor proteins in virulence is given in the introduction (chapter 1). In this thesis, we provide details on the molecular structure of both AVR4 and AVR9. Based on the protein structure homologies, known protein motifs were identified in both proteins. Subsequently, we analyzed whether these structural homologies could be translated into functional homologies based on bioassays.

To this purpose, the disulfide bonds of AVR4 and AVR9 were elucidated. The chosen approach relied on the reducing agent tris-(2-carboxyethyl)-phosphine (TCEP), which allowed partial reduction of disulfide bonds at acidic pH. After partial reduction, the thiol groups of newly formed cysteines were modified in order to prevent disulfide bond shuffling. The disulfide bond pattern was identified following two different approaches. For AVR9 (chapter 3), the newly formed thiols were blocked by *N*-ethylmaleimide (NEM) and 4-vinylpyridine (VP). The resulting modified cysteines are compatible with standard protein sequencing protocols making use of the Edman degradation. For AVR4 (chapter 4), partial reduction was achieved by cyanylation of the sulfhydryl groups with 1-cyano-4-diethylamino-pyridinium (CDAP). This modification facilitated specific base-induced cleavage of the peptide bond yielding peptide fragments that could easily be identified by mass spectrometry.

The disulfide bonds in the mature AVR9 protein involve Cys2–Cys16, Cys6–Cys19, and Cys12–Cys26, respectively. Cysteine spacing and the disulfide bond pattern of AVR9 are identical to those found in cystine-knotted inhibitor peptides. The cystine knot motif is best described by a “ring” formed by two disulfide bonds and their connecting amino acid residues, which is penetrated by a third disulfide bond. NMR data confirm that AVR9 is structurally most related to the cystine-knotted carboxypeptidase inhibitor (CPI). However, although structurally related to CPI, AVR9 does not show any carboxypeptidase inhibiting activity. Yet, AVR9 could still very well inhibit other plant proteases.

Sequence homology revealed that AVR4 contains the invertebrate chitin-binding domain (inv ChBD) (chapter 5). This motif was previously reported to occur in most eukaryotic kingdoms except in plants and fungi. Six cysteine residues are conserved in the inv ChBD, which are interconnected by three disulfide bonds in mature AVR4: Cys11-Cys41, Cys35-Cys80, and Cys57–Cys72. AVR4 contains one additional disulfide bond, Cys21–Cys27 (chapter 4). Tachycitin is the only inv ChBD protein for which the disulfide bond pattern and 3D structure have been reported; the conserved cysteines in tachycitin show an identical disulfide bond pattern to that found in AVR4. Interestingly, AVR4 is the only fungal representative of the inv ChBD family found so far.

It could be proven experimentally that AVR4 indeed binds specifically to chitin, but not to other related polysaccharides such as chitosan (chapter 5). Fluorescently labeled AVR4 localizes at chitin present in cell walls of *Trichoderma viride* and *Fusarium solani* f.sp. *phaseoli*. AVR4 can protect these fungi against the deleterious effect of class I plant chitinases (family-19 catalytic domain). Chitin in cell walls of *in vitro*-grown *C. fulvum* is not accessible and the fungus does not produce AVR4 under these conditions. However, chitin appeared accessible for AVR4 in cell walls of *C. fulvum* growing in the intercellular space of tomato where AVR4 is abundantly secreted by the fungus (chapter 5). These results suggest that AVR4 might contribute to the virulence of *C. fulvum* as it can protect the fungus during infection of tomato against constitutive and induced tomato chitinases.

Independent disruption of the three conserved disulfide bonds resulted in protease sensitive isoforms of AVR4. Many strains of *C. fulvum* virulent on *Cf-4* tomato circumvent recognition by single Cys-to-Tyr mutations in the AVR4 protein. However, the identified amino acid mutations only involve two of the three conserved disulfide bonds. Disruption of any of the four disulfide bonds in AVR4 did not result in a complete loss of chitin-binding, although Cys57–Cys72 might contribute to chitin-binding activity. These results indicate that in naturally occurring mutant alleles of *avr4,* the intrinsic function of AVR4 (chitin-binding ability) remained. Thus, races 4 of *C. fulvum* circumvent recognition mediated by the *Cf-4* resistance gene without losing the correlated virulence function of AVR4.

The two main classes of chitin-binding domains, the invertebrate (CBM14) and the plant ChBD (CBM18), appear to exemplify convergent evolution. The thermodynamic properties (K_A, ΔH, *and* ΔS) of AVR4 binding to chito-oligomers with a degree-of-polymerization (DP) of 1 to 6 were compared to those of the plant lectins hevein and *Urtica dioica* agglutinin (UDA) (chapter 6). AVR4 only interacts with oligomers with DP≥3, while the plant lectins interact with the monomer N-acetyl-glucosamine (GlcNAc). The non-covalent

complex between AVR4 and chito-oligomers could specifically be detected with ESI MS (upper limit in the millimolar range). NMR data indicated that the chitin-binding site has a topology similar to that of tachycitin a well-characterized representative of the CBM14 type of ChBD proteins, but that different amino acid residues within the motif are important for the interaction with chito-oligomers.

Thus the expression pattern (both timing and local concentration), affinity and localization of AVR4 support a role as an integral cell wall protein forming a protective barrier against plant chitinases.

In conclusion, our studies have proved that structural studies of AVR proteins do not only reveal structural homologies with other proteins (AVR9) present in structural databases, but also functional homologies, as has been proven for AVR4. In the future close collaborations between molecular biologists and structural biologist are required to accelerate progress in functional genomics and proteomics.

Samenvatting

In dit proefschrift staat onderzoek beschreven naar de resistentie van tomaat tegen een ziekteverwekker van tomaat, de schimmel *Cladosporium fulvum*. Sommige tomatenplanten herkennen deze schimmel doordat zij resistentiegenen bezitten. Deze herkenning van de schimmel blijkt specifiek gestimuleerd te worden door kleine eiwitten, die worden uitgescheiden door de schimmel. Deze schimmeleiwitten worden avirulentiefactoren (AVR) genoemd. De herkenning van avirulentiefactoren gebeurt op basis van een één-op-één relatie tussen avirulentiefactor en resistentiegen, bijvoorbeeld AVR4 versus *Cf-4*.

Tot op heden is weinig bekend over de functie van avirulentiefactoren voor de schimmel. Het is bekend dat ze specifiek aangemaakt worden tijdens de infectie van tomaat. Verder is gebleken dat tomatenresistenties doorbroken worden door middel van mutaties in de genen coderend voor avirulentiefactoren. Deze mutaties leiden vaak tot de volledige afwezigheid van het AVR eiwitproduct, waardoor herkenning van de schimmel niet meer mogelijk is en de tomaat geïnfecteerd raakt. Het specifieke doel van dit onderzoek was om structurele verwantschappen aan te tonen tussen avirulentiefactoren en andere eiwitten, waarvan de functie reeds bekend is. In dit proefschrift staan dan ook mogelijke functies beschreven voor zowel AVR4 als AVR9. Een volledig begrip van AVR4 en AVR9 is van groot belang, omdat beide eiwitten veelvuldig gebruikt worden in studies naar de onderliggende mechanismen van plantenresistentie.

Een noodzakelijke voorwaarde voor structuuronderzoek aan eiwitten is het in voldoende mate in bezit hebben van het eiwit. Hoofdstuk 2 beschrijft de grootschalige productie van AVR4 met de gistsoort *Pichia pastoris* en een nieuwe zuiveringsmethode voor AVR4. De keuze voor *Pichia* is gebaseerd op de mogelijkheid dat deze gist op de eenvoudige koolstofbron methanol kan groeien terwijl *Pichia* tegelijkertijd grote hoeveelheden aan lichaamsvreemde eiwitten kan produceren. De optimalisatie van *Pichia* fermentaties heeft geleid tot een nieuwe methode voor isotoopverrijking van eiwitten. *Pichia* kan ‘magnetische’, isotoop-verrijkte eiwitten produceren door aan de voedingsstoffen (het groeimedium) voor *Pichia* stoffen toe te voegen, die ‘magnetische’ eigenschappen hebben. De gemerkte eiwitten kunnen vervolgens met bijvoorbeeld kernspinresonantie (NMR) bestudeerd worden. Kernspinresonantie levert unieke informatie op over de driedimensionale structuur van eiwitten. De hoofdstukken 3 en 6 beschrijven resultaten verkregen met deze techniek voor AVR4 en AVR9.

Voor de driedimensionale structuur van eiwitten zijn zwavelbruggen zeer typerend. In de hoofdstukken 3 en 4 zijn methodes ontwikkeld voor de bepaling van zwavelbruggen in respectivelijk AVR9 en AVR4. De opheldering van deze zwavelbruggen heeft geleid tot de herkenning van een structurele verwantschap met potato carboxypeptidase inhibitor en tachycitin, respectievelijk. Kernspinresonantie bevestigde deze structurele verwantschappen. Nader onderzoek toonde echter aan dat AVR9 niet de enzymactiviteit van het enzym carboxypeptidase kan remmen; dit is een bekende functie van potato carboxypeptidase inhibitor.

Van tachycitin is bekend dat het chitine bindt dankzij een motief in het eiwit dat specifiek is voor ongewervelde dieren (invertebraten). Chitine is een type suikerketen dat voorkomt in de celwand van schimmels, maar niet in de celwand van planten. Verder komt chitine voor in het pantser van ongewervelde dieren zoals krab. De overeenkomsten tussen AVR4 en tachycitin suggereren dat AVR4 ook chitine zou kunnen binden. Proeven in hoofdstuk 5 laten inderdaad zien dat AVR4 uniek aan chitine bindt en niet aan andere suikerketens. Verder blijkt dat natuurlijk voorkomende mutaties in het *Avr4* gen geen negatief effect hebben op de chitine-binding, terwijl dezelfde mutaties wel de herkenning van de schimmel door tomaat blijken te voorkomen. Dit zou betekenen dat de functie van AVR4 voor de schimmel behouden is, terwijl resistentie doorbroken is.

Het belangrijkste resultaat van dit proefschrift is dat AVR4 schimmels blijkt te beschermen tegen chitinases van planten. Chitinases zijn enzymen, die de schimmelcelwand afbreken Tevens maken chitinases een belangrijk onderdeel uit van de resistentiereactie van planten. De schimmel *C. fulvum* lijkt ongevoelig te zijn voor chitinases. Resultaten in hoofdstuk 5 ondersteunen dat AVR4 een beschermende laag kan vormen op de celwand van de schimmel tijdens de infectie van tomaat. Dit zou dan ook de ‘echte’ functie van AVR4 zijn voor de schimmel.

In hoofdstuk 6 is in groot detail gekeken naar de interactie tussen chitine en AVR4. De reden is dat planten ook een chitine-bindend motief hebben. Dit motief komt onder andere voor in chitinases. Het blijkt dat AVR4 op een andere manier chitine bindt dan is beschreven voor het planten chitine-bindend motief. Dit verschil in binding kan een basis vormen voor verder onderzoek om te begrijpen waarom AVR4 de afbraak van de schimmelcelwand kan blokkeren.

Tenslotte, in hoofdstuk 7 worden de bevindingen van dit onderzoek bediscussieerd in het licht van de herkenning van de avirulentiefactor in tomaat. De gevonden structuur-

functie relaties kunnen nieuw onderzoek inleiden naar eiwitten die mogelijk betrokken zijn bij plantenresistentie.

Dankwoord

Hier begint volgens goed gebruik voor vele lezers het proefschrift. Voor mij is het de slotsom van 6 jaar hard werken. De resultaten zouden niet bereikt zonder de hulp van velen. Ik wil dan ook iedereen bedanken voor zijn/haar hulp tijdens deze jaren. Een aantal mensen wil ik graag expliciet noemen.

Allereerst, Pa en Ma. Ik waardeer enorm dat Arjan en ik een wereld konden verkennen die jullie niet kenden, maar die wij zelf uitzochten. Jullie hebben ons altijd bewust op pad gestuurd voorbij die bekende horizon… uiteraard wel met een veel te zware rugzak en een pond snoep, die ik snel bezuurde. Dit proefschrift zou er niet gekomen zijn zonder het meegekregen stukje karakter.
Arjan, we hebben nauwelijks bij elkaar in de buurt gewoond in de afgelopen tien jaar. Voor ons beide geldt letterlijk en figuurlijk dat we altijd aan het vliegen zijn. Ik vond het jammer toen je verhuisde naar Frankrijk, maar ik ben altijd weer blij verrast door de gastvrijheid van Laetitia en jou tijdens één van mijn bliksembezoeken.

Mijn (co-) promotoren Pierre de Wit en Jacques Vervoort wil ik bedanken voor de inzet en het enthousiasme in al zijn vormen. Jacques, de ruimte en de aanmoedigingen die je mij gaf voor mijn eigen weg gaven mij het vertrouwen met iets goeds bezig te zijn. Elk bereikt resultaat kwam tot stand door dat grenzeloze vertrouwen. Pierre, ik was niet altijd in je zicht, maar je was zeker altijd betrokken. Bedankt voor de tomeloze inzet in mijn laatste fase, ‘het schrijven’. Mijn krabbels gingen vaak heen en weer, en waarschijnlijk ben ik nu beter gewapend voor een volgende keer ‘schrijven’.

Het resultaat zou er zeker ook niet zijn zonder een aantal super waardevolle samenwerkingen. Ten eerste, de prettige samenwerking en goede vriendschap met Henno van den Hooven, mijn kamergenoot bij Biochemie in de eerste twee jaar. Onze samenwerking heeft tot een paar mooie en belangrijke resultaten geleid in dit proefschrift. Chris Spronk, ik ging altijd met veel plezier naar Nijmegen. Eerst nog boemelend, daarna gemotoriseerd. Ik waardeer enorm de tijd die je vrij maakte voor mij en dat eiwit met de bijbehorende rare spectra. Je plek bij hoofdstuk 6 is dan ook zeker op zijn plaats. Misschien zal het werk allemaal nog eens leiden tot die enige echte structuur. Dat zou toch moeten lukken met een vrieskist vol gelabeld eiwit. Sjef Boeren, ook jij verdient een grote pluim.

Vaak was je er even om te helpen met die korte discussies, het ‘wat-en-hoe’, gewoon de kleine dingen. Je hebt het wagenpark goed voor elkaar en dat heeft me vaak geholpen. Stuart Harrison (Syngenta-Mogen), together we achieved some very significant results regarding AVR4 (described in chapter 5). These results are for me the crown on the work described in this thesis. I would like to express my sincere thanks for that fact. Matthew Kennedy, Hans Vissers, en Mike van Oosterhout (Waters, MS technologies) wil ik graag bedanken voor de mogelijkheid om metingen te verrichten in Almere. Fred van den End wil ik graag bedanken voor de hulp bij het in elkaar zetten van de *Pichia*-fermentor.

Mijn paranimfen:
Supervriend Sander Borgsteede, je blijkt al jaren een garantie voor verrassingen: snookeren in de achtertuin, vele lekke banden met de fiets, slapen in de glades, kanoën op alligators – laten we dat maar niet meer doen als verstandige jongens, maar wanneer gaan we weer? O ja, er ligt nog een stapel kwartjes op je te wachten.
Corien Struijk, je wist me vaak op ontnuchterende wijze te wijzen op alles voorbij het OIO-schap. Iets dat ik nog wel eens vergat..., maar dan tegelijkertijd moedigde je me ook aan om door te gaan.

Niet te vergeten, alle (ex-)‘Clados’ (Bas, Camiel, Frank, John, Maarten, Marco, Matthieu, Nienke, Paul, Rianne, Renier, Ronelle, Susane) bedankt voor al die dingen waar jullie me weer eens ‘kort’ mee hielpen en natuurlijk de gastvrijheid op ‘Fyto’. Nienke, onze samenwerking kwam uiteindelijk op verrassende manier tot stand en ik heb het zeker als positief ervaren. Uiteraard alle collega’s op Biochemie bedankt, met name Marco, Kees-Jan, Jean-Louis, Lars, Marjon, Eyke, Yves, Niek, Jan-Willem, Caroline, en Laura.

Belangrijk onderdeel voor een succesvol OIO: de thuisbasis. Hoe kan het ook anders: huize ‘de afronding’ met al haar bewoners in de loop van de tijd. Diane, Karin, Huybert, Martijn, Karlijne, Renate, Lot, Clythe en buurman Bert bedankt voor de ontspannen sfeer, peptalk en gezellige tijd.

Bianca, bedankt voor je engelengeduld. We komen er samen wel. Nu is het tijd om leuke dingen te doen!

Harrold

List of Publications

Visser, A.J.W.G., van den Berg, P.A.W., Visser, N.V., van Hoek, A., van den Burg, H.A., Parsonage, D., and Claiborne, A. (1998). Time-resolved fluorescence of Flavin Adenine Dinucleotide in wild-type and mutant NADH Peroxidase. Elucidation of quenching sites and discovery of a new fluoresecence depolarization mechanism, *J. Phys. Chem. B* ***102***, 10431-10439.

van den Burg, H.A., de Wit, P.J.G.M., and Vervoort, J. (2001). Efficient C-13/N-15 double labeling of the avirulence protein AVR4 in a methanol-utilizing strain (Mut^+) of *Pichia pastoris*, *J Biomol NMR* ***20***, 251-261.

van den Hooven, H.W., van den Burg, H.A., Vossen, P., Boeren, S., de Wit, P.J.G.M., and Vervoort, J. (2001). Disulfide bond structure of the AVR9 elicitor of the fungal tomato pathogen *Cladosporium fulvum*: Evidence for a cystine knot, *Biochemistry* ***40***, 3458-3466.

de Wit, P.J.G.M., Brandtwagt, B.F., van den Burg, H.A., Cai, X., van der Hoorn, R.A.L., de Jong, C.F., van Klooster, J., de Kock, M.J.D., Kruijt, M., Lindhout, W.H., Luderer, R., Takken, F.L., Westerink, N., Vervoort, J., and Joosten, M.H.A.J. (2002). The molecular basis of co-evolution between *Cladosporium fulvum* and tomato, *Antonie Van Leeuwenhoek* ***81***, 409-412.

Rivas, S., Mucyn, T., van den Burg, H.A., Vervoort, J., and Jones, J.D.G. (2002). An ~400 kDa membrane-associated complex that contains one molecule of the resistance protein Cf-4, *Plant J* ***29***, 783-796.

van den Burg, H.A., de Wit, P.J.G.M., Vervoort, J. (2002) (inventors), US patent application

Westerink, N., Roth, R., van den Burg, H.A., de Wit , P.J.G.M., and Joosten, M.H.A.J. (2002). The AVR4 elicitor protein of *Cladosporium fulvum* binds to fungal components with high affinity, *Mol Plant-Microbe Interact* ***15***, 1219-1227

van den Burg, H.A., Harrison, S., Joosten, M.H.A.J., de Wit, P.J.G.M., and Vervoort, J. (2003). Avirulence factor AVR4 of the tomato pathogen *Cladosporium fulvum* is a chitin-binding lectin that protects fungi against plant chitinases, *submitted*.

van den Burg, H.A., Westerink, N., Francoijs, K.-J., Roth, R., Woestenenk, E., Boeren, S., de Wit, P.J.G.M., Joosten, M.H.A.J., and Vervoort, J. (2003). Natural disulfide bond disrupted mutants of AVR4 of the tomato pathogen *Cladosporium fulvum* are sensitive to proteolysis, thereby, circumventing *Cf-4* mediated resistance, *Journal of Biological Chemistry (published on-line)*

van den Burg, H.A. Spronk, CA.E.M., Boeren, S., Kennedy, M.A. Visser, J.P.C., Vuister, G.W., de Wit, P.J.G.M., and Vervoort, J. (2003) the AVR4 elicitor of *Cladosporium fulvum* and chitin requires three occupied binding subsites, *in preparation.*

van 't Slot, K.A.E., van den Burg, H.A., Kloks, C.P.A.M., Hilbers, C.W., Knogge, W., and Papavoine, C.H.M. (2003) Solution structure of the fungal plant disease resistance-triggering protein NIP1 shows a novel beta-sheet fold, *in preparation.*

.

Curriculum Vitae

Harrold Alfred van den Burg werd geboren op 28 maart 1974 te Kampen. In 1992 werd het VWO diploma aan het Almere College te Kampen behaald. In hetzelfde jaar begon hij met de studie Moleculaire Wetenschappen aan de Landbouwuniversiteit te Wageningen (de huidige Wageningen Universiteit), waar hij in september 1997 het doctoraaldiploma met lof behaalde. Tijdens de doctoraalfase deed hij een onderzoekstage bij Prof. dr. Al Claiborne (Wake Forest University, Winston-Salem, NC) en volgde hij afstudeerprojecten bij de leerstoelgroepen Biochemie en Fytopathology. Van september 1997 tot mei 2002 was hij als onderzoeker in opleiding (oio) verbonden aan de leerstoelgroepen Biochemie en Fytopathology onder supervisie van Dr. ir. J. Vervoort en Prof. dr. ir. P. J. G. M. de Wit. Dit door NWO gefinancierde onderzoek van CW-SLW resulteerde in dit proefschrift. In oktober 2002 kreeg hij een ‘Marie Curie’ fellowship (EU) toegekend, waarna hij als post-doctoraal onderzoeker begon bij Prof. dr. J. Jones aan het Sainsbury Laboratory in Norwich (Verenigd Koninkrijk). In zijn huidige betrekking onderzoekt hij in moleculair detail de herkenning door planten van plantenziekteverwerkers.